Australian Regolith Geoscientists Association

Fourth Australian Regolith Geoscientists Association Conference

Proceedings

Thredbo, NSW
7-11th February 2016

Editor: Matilda Thomas

Australian Government
Geoscience Australia

CSIRO

Contents

page number

About ARGA ... 3

How to join ARGA ... 3

What is regolith? ... 4

2016 conference program ... 5

Oral presentation abstracts (see program for individual abstract page numbers)... 9

Poster presentation abstracts ... 75

Field guide abstract ... 94

Authors list ... 98

Cover image credits (from clockwise from top left): Helen Dulfer, Matilda Thomas, Cameron Mitchell, Dan Clark.

This publication is available online at: http://regolith.org.au/publications.html

ISBN 978-1-925297-03-4

Australian Regolith Geoscientists Association

The Australian Regolith Geoscientists Association Inc. (ARGA) is a not-for-profit learned association of regolith practitioners throughout Australia. The Association was set up to to provide a mechanism through which people interested in regolith science could keep in touch and share their experiences via newsletters, email, the internet and an annual conference.

The objects of the association are to further the study of regolith geoscience and allied disciplines by:

a. Facilitating the exchange of information among members of the association, and, in general, all those interested in regolith science;
b. Stimulating interest in regolith geoscience;
c. Encouraging the practical applications of regolith geoscience research.

How to join ARGA

All those having an interest in the objectives of the Association are eligible to become members. All who have attended a Biennial Conference of the Association become members for the next four years. Alternatively, you can join the Society by contacting the Secretary, explaining your interest and paying $1 per year.

ARGA 2014-2016 Committee

President: Vanessa Wong
Past President: David Gray
Secretary: Stephanie McLennan
Treasurer: John Keeling
Conference Organiser: Matilda Thomas
Student Representative: Margie Sweeney
Ian Roach (website manager)
Jon Clarke
Nathan Reid
Martin Smith

Website: http://regolith.org.au

Regolith is "The entire unconsolidated or secondarily recemented cover that overlies coherent bedrock, that has been formed by weathering, erosion, transport and/or deposition of older material. The regolith thus includes fractured and weathered basement rocks, saprolites, soils, organic accumulations, volcanic material, glacial deposits, colluvium, alluvium, evaporitic sediments, aeolian deposits and groundwater." (Eggleton 2001*). Or, regolith is everything between fresh rock and fresh air!

*Eggleton R.A. ed. 2001. The Regolith Glossary: surficial geology, soils and landscapes. Cooperative Research Centre for Landscape Environments and Mineral Exploration (CRC LEME).

4th ARGA

Conference Program

Thredbo 7th-11th February 2016

Sunday 7th February 2016 – PRE-Conference Field trip
8am Canberra depart =>Cooma – Monaro – arrive Thredbo ~5pm for check in. **From 6pm: Icebreaker and BBQ:** Out the front of the Thredbo Alpine Hotel (near river)

Program

Monday 8th February – Townsend conference room, Thredbo Alpine Hotel			
8.45am	**Registration**		
Chair: Matilda Thomas			
9.05	Vanessa Wong	Welcome and opening	Page
9.15	**Keynote:** John Gallant	Digital Elevation Models and Terrain Analysis	9
9.50	Pauline English	Ancient origins of some major Australian salt lakes: geomorphic and regolith implications	10
10.10	Brad Pillans	Quartz-dominated Cenozoic gravels in SE Australia: Where did all the quartz come from?	15
10.30 am	**Morning tea**		
Chair: John Keeling			
11.05	Alie Cowood	An objective and repeatable method for the construction of Hydrogeological Landscape Units	17
11.25	Ian Roach	Cover Characterisation and Shallow Basement Mapping using Airborne Electromagnetic Data: examples from the Southern Thomson Project	21
11.45	Matilda Thomas	Comprehensive new public datasets helping to understand cover and mineral potential in the Stavely Region, western Victoria.	27
12.05	Patrice de Caritat	Recognition of geochemical footprints of mineral systems at the regional to continental scales	33
12.30 pm	**Lunch**		
Chair: Brad Pillans			
1.40	Vanessa Wong	A preliminary investigation in to pedogenic effects on rare earth element concentrations in Victorian soils	34
2.00	Nadir de Souza Kovacs	Regolith-landforms of the Balanggarra area, north Kimberley	38
2.20	Andrew McPherson	Tectonic Geomorphology in Australia: Earthquakes and more…	40
2.40	Carsten Laukamp	Regional to district scale mineral footprints in the Capricorn Orogen interpreted from ASTER, soil geochemical and radiometric data	48
3.00 pm	**Afternoon Tea**		
Chair: Leah Moore			
3.30	Tony Eggleton	About anatase	50
3.50	Ken McQueen	Landscape evolution of the Clarence River catchment: Weird rivers and wild ideas	51
4.10	Georgina Gordon	Regolith Modelling – The Bulldog Shale	56
4.30	Carmen Krapf	Silcretes of the NE Eyre Peninsula and their association with the underlying bedrock	57
4.50	Slide Show	Regolith slide show (& short field trip briefing)	
5pm	Day 1 close	Drinks and/or dinner somewhere near TBA	

Tuesday 9th February: Mid Conference Field trip
Thredbo Alpine Resort 8.30am, Kosciusko chair, circ lake lookout, picnic lunch and return to base of chair for afternoon bus tour. Bring hat, raincoat, backpack for lunch, camera, etc (4.30pm afternoon tea at Wild Brumby Distillery and café) ***N.B. CONFERENCE DINNER** at CASCADES RESTAURANT@ Thredbo Alpine Hotel: **6.30pm***

Wednesday 10th February – Townsend conference room, Thredbo Alpine Hotel			
Chair: Lisa Worrall			*page*
9.15 am	**Keynote:** Jon Clarke	Regolith and the Selection of Landing Sites for Crewed Missions to Mars	59
9.50	Steve Hobbs	Multi-agent gully processes: Evidence from the MVP, Australia and Noachis Terra, Mars	63
10.10	Stephanie McLennan	Paleodrainage evolution and neotectonism in the western Murray Basin, southeast Australia	66
10.30 am	**Morning Tea**		
Chair: Ken McQueen			
11.10	Graham Taylor	The Trouble with Silcrete	68
11.30	John Keeling	Provenance of zircon in Miocene strandline heavy mineral deposits, south western Murray Basin - implications for paleo-coastal reconstructions	70
11.50	Lisa Worrall	Exploring for Heavy Minerals on Cape York Peninsula, Queensland, Australia	73
12.10	Vanessa Wong	Identifying sources of acidity and acid sulfate soil characterisation in the Anglesea River catchment	74
12.30 pm	**Lunch**		
Chair: Vanessa Wong			
1.35	Judges	Best Student Presentation: The Keith Scott Memorial Award	
1.40	AGM	Drinks and board elections	
2.40	Poster session	Adjacent to tea room	84-102
3pm pm	**Afternoon Tea**		
Chair: Carmen Krapf			
3.30	Discussion: Future directions for regolith science		
4.30	Awards	Best Presentation: GA book prize, final comments	
4.45 pm	Day 3 close	End of proceedings.	

Thursday 11th February: POST-Conference Field trip
Leave Thredbo Alpine Hotel 8am – drive to Charlotte Pass walk to Blue Lake, hiking trip return = ~9km sunscreen, wind and waterproof gear mandatory.

Digital Elevation Models and Terrain Analysis

John Gallant

CSIRO Land and Water, GPO Box 1666, Canberra ACT 2601

Geomorphology describes the interactions between materials, processes, shape and history, and the shape component is the domain of geomorphometry or terrain analysis. Products of terrain analysis include maps of slope steepness, flow accumulation, catchment boundaries, surface curvature, exposure to solar radiation and landform classifications.

Digital Elevation Models (DEMs) are the raw material for geomorphometry: the elevation of the land surface, in varying levels of detail and quality, from which useful information about land surface shape is derived. The quality of the result is always linked to the quality and nature of the underlying DEM: finer spatial resolutions resolve smaller features enabling more detailed shape measurements but vertical precision, random noise and measurement artefacts also play a role.

DEMs from airborne laser scanning (ALS) or lidar are generally the highest quality and most expensive source of elevation data; airborne photogrammetry also provides high quality elevation data but lacks the ability of lidar to measure ground heights under vegetation cover. For coverage of larger areas, space-borne radar is the current technology of choice. NASA's Shuttle Radar Topographic Mission (SRTM) collected elevation data over most of the earth's surface at a horizontal resolution of about 30 m with vertical accuracy better than 10 m in most areas, and is now available for free download. The German TanDEM-X mission has more recently collected data to create WorldDEM, a global DEM of about 10 m resolution with vertical accuracy of about 2 m and with less noise than SRTM, but this is not a free product.

In Australia, we have processed the SRTM data to remove artefacts including striping, offsets due to trees and noise to produce DEMs suitable for routine terrain analysis work (Gallant *et al*, 2011). We have also produced a suite of derived terrain attributes including most of the commonly used shape properties relevant to geomorphology, hydrology and ecology (Gallant and Austin, 2015). One product of particular relevance to regolith geoscience is MrVBF, the multi-resolution valley bottom flatness index (Gallant and Dowling, 2003). This index identifies regions that are low and flat compared to their surroundings, at a range of scales, depicting areas that are likely to be sediment deposits. The MrVBF index shows areas of sediment accumulation ranging in scale from small hillslope hollows to large sedimentary basins and has been used for soil and regolith mapping, flood modelling and groundwater studies.

At the other extreme of the steepness spectrum are cliffs. These features can also be detected from DEMs but considerable care is needed to discriminate between steep slopes and cliffs. In most landscapes a slope threshold of well over 100%, or 45 degrees, is needed to reliably identify cliffs, which translates to a minimum detectable cliff height of several times horizontal resolution of the DEM.

References

GALLANT J.C., DOWLING T.I., READ A.M., WILSON N, TICKLE P.K. AND INSKEEP C. 2011. 1 second SRTM-derived Digital Elevation Models User Guide. Geoscience Australia www.ga.gov.au/topographic-mapping/digital-elevation-data.html

GALLANT J.C. AND DOWLING T.I. 2003. A multi-resolution index of valley bottom flatness for mapping depositional areas. *Water Resources Research* **39(12)**, 1347-1360.

GALLANT J.C. AND AUSTIN J.M. 2015. Derivation of terrain covariates for digital soil mapping in Australia. *Soil Research* **53(8)**, 895-906.

Ancient origins of some major Australian salt lakes: geomorphic and regolith implications

Pauline English[1]

[1]Geoscience Australia, GPO Box 378, Canberra ACT 2601

The benchmark work of Bowler (1981, 1986) established the importance of climatic setting and hydrologic processes to the evolution of Australia's salt lakes (Figure 1), particularly with respect to their geomorphology and evaporite mineralogy. Regional-scale reconstruction of palaeovalleys in the Australian arid zone (English *et al.* 2012, 2013a, 2013b, 2015; Bell *et al*. 2012) has extended our appreciation of the distribution and systematics of salt lake evolution. In addition, recent work on the prospectivity of Australia's salt lakes for potash and other economic evaporites (Mernagh *et al.* 2013) has emphasised their importance as regolith elements. This recent work has also highlighted the previously unrecognised role of diapirs of ancient salts in salt lake evolution within inland parts of the continent.

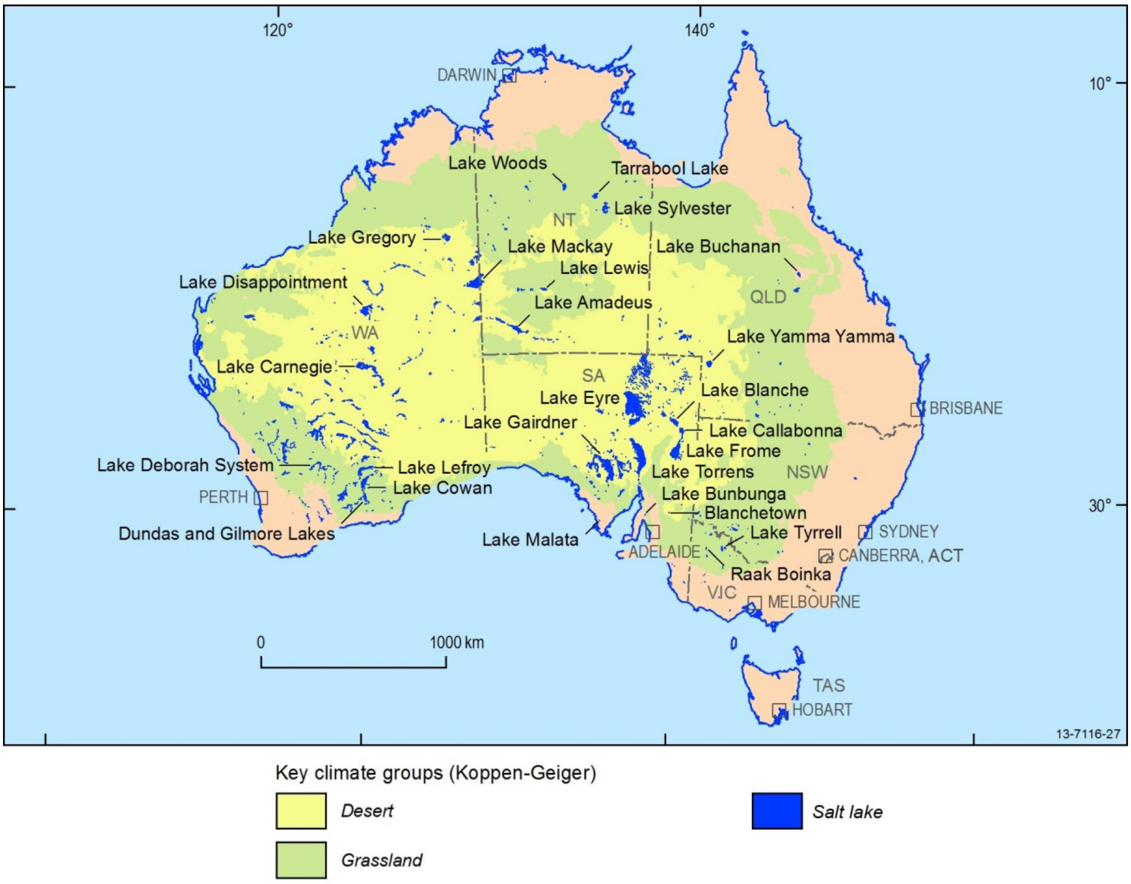

Figure 1: Distribution of selected major Australian salt lakes; not all of the approximately 1,200 salt lakes are shown. The arid (desert) and semi-arid (grassland or semi-desert) zones are based on the Köppen-Geiger climate classification: http://www.bom.gov.au/iwk/climate_zones/

Ancient evaporite units make up a significant component of the Proterozoic-Palaeozoic stratigraphy of some of Australia's major sedimentary basins, for example, the Amadeus, Officer and Canning basins. Cenozoic structural deformation involving these ancient evaporites, in the form of salt diapirs and salt domes, has resulted in their intrusion to shallow crustal levels and resultant distortion of the surface and near surface environments. This halotectonic deformation, by tangential compressive stress, is distinct from other forms of modern tectonism, and is a unique type of tectonic geomorphology. Both ductile (folding) and brittle (faulting) disruption have been observed. The interplay between neotectonic deformation and surface processes has shaped the topography and drainage patterns of extensive parts of arid Australia and directly contributed to salt lake formation and the subsequent evolution of these settings.

Palaeovalley reconstruction

Regional-scale palaeovalley mapping in desert lands of Western Australia, South Australia and the Northern Territory was completed by Geoscience Australia in 2012 (English *et al*. 2012). The aims were to elucidate the distribution and characteristics of buried palaeovalleys and their potential groundwater resources. The Multi-resolution Valley Bottom Flatness (MrVBF) index (Gallant and Dowling, 2003), applied to 9-second Shuttle Radar Topography Mission (SRTM) DEM data, was utilised along with geological datasets to map broad-scale palaeovalley networks, mostly buried or partly obscured by dunefields (Bell *et al*. 2012). Irregular topographic features and incoherent drainage patterns were disclosed in the vicinity of some major salt lakes, including Lake Disappointment (WA) and Lake Mackay (WA-NT border). The locations of such anomalies, coupled with complementary geologic information, indicate that these particular sites were intruded by large salt diapirs during the Late Cenozoic.

Lake Disappointment

There has been considerable conjecture regarding indefinite palaeovalley watersheds and drainage diversions at Lake Disappointment, reviewed by Magee (2009). It is uncertain whether the topographic depression containing Lake Disappointment connected with palaeorivers flowing westward to the Indian Ocean via Savory Creek, or southward to Lake Carnegie and the Throssell Palaeovalley, or northward through the Rudall Uplands to the Percival Palaeovalley either via a north-eastward conduit to Lake Winifred or northward via the Rudall River to Lake Dora. Figure 2 shows Lake Disappointment with its haphazard centripetal drainage system.

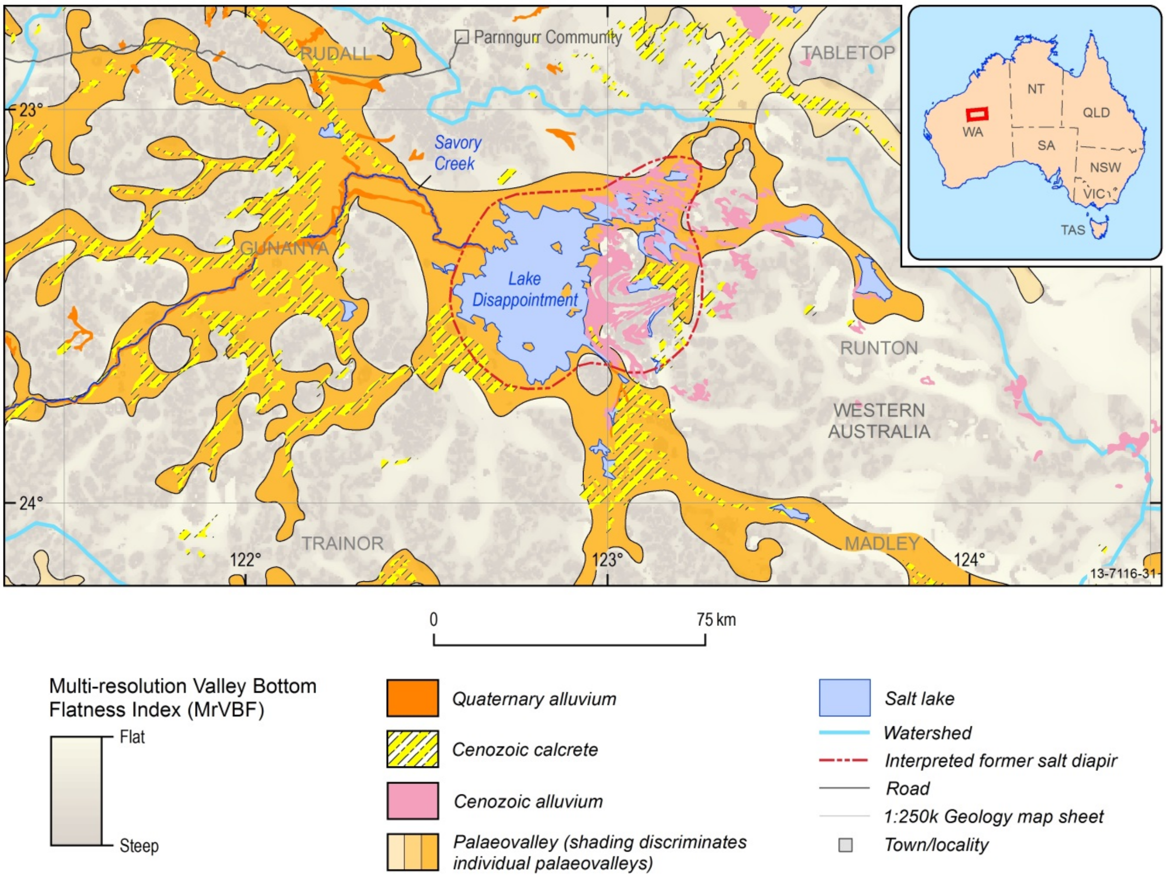

Figure 2: Lake Disappointment, northern Officer Basin, WA, and interpreted centripetal palaeovalley drainage network overlain on the MrVBF Index image. Highly deformed outcrops of Proterozoic sedimentary rock immediately east of Lake Disappointment are portrayed by Cenozoic alluvial deposits (pink polygons) between tight sandstone folds. The deformation supports an interpretation of halotectonism underpinning the evolution of Lake Disappointment and of the associated haphazard endorheic drainage pattern. Savory Creek, west of Lake Disappointment, is the only named creek in the area. The Rudall Uplands of exposed crystalline bedrock make up the main drainage divide north of Lake Disappointment. 1:250 000 scale mapsheet extents and names are shown: http://www.ga.gov.au/cedda/maps/279?ms=250000

The proximity of tightly folded Proterozoic sedimentary rocks in the form of "cauliflower structures" adjacent to the large circular salt lake, along with the distinctive endorheic drainage pattern, support an interpretation of halotectonism. Following a long period of diapiric ascent and associated deformation of overlying rock units, it is postulated that a large salt body rose to the landscape surface whereupon it dissolved and created a hydrologically-closed depression in which the modern Lake Disappointment evolved.

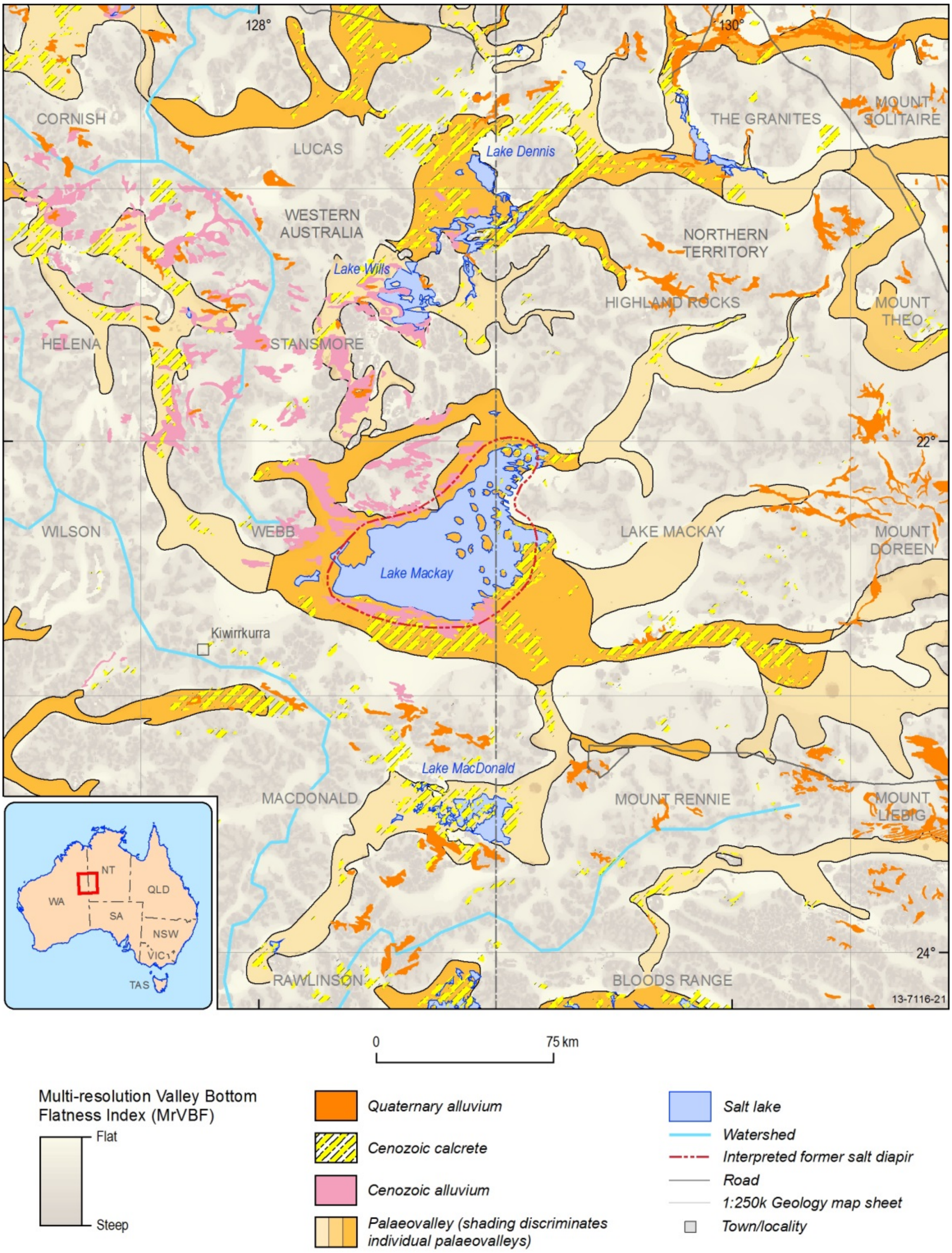

Figure 3: Lake Mackay and Lake MacDonald in the Great Sandy Desert on the NT-WA border. The MrVBF Index image and selected surficial geologic units depict disorganised endorheic drainage patterns and no connections with coastward-flowing rivers or palaeorivers. 1:250 000 scale mapsheet extents and names are shown: http://www.ga.gov.au/cedda/maps/279?ms=250000

Lake Mackay and other halotectonic salt lakes

Lake Mackay lies in the western part of the Amadeus Basin of which the basal sequence is the Proterozoic Bitter Springs Formation comprising limestones, dolomites and evaporites. The Bitter Springs Formation outcrops sparsely near Lake Mackay and may occur at shallow depth elsewhere beneath dunes of the Great Sandy Desert.

The topographic depression of Lake Mackay is seen in the MrVBF Index image, Figure 3; its connectivity with surrounding regional palaeovalleys is not straightforward. This large salt lake does not unequivocally relate to any particular through-flowing palaeovalley or palaeoriver course, but rather to disaggregated internal-drainage. Palaeovalley reconstruction supports an interpretation of Lake Mackay as a legacy of an ancient evaporite basin composed of Bitter Springs Formation which rose to the landscape surface to dissolve and create a hydrologically-closed depression. Collapse of the salt structure and further dissolution of ancient evaporite salts would have created a shallow void in which the Quaternary salt lake evolved as the water table became exposed through subsidence. Salt accumulations in the brine pool would have continued to be concentrated under arid climatic conditions. Centripetal drainage would have developed around the newly-formed depression to contribute surface waters and salts to the underlying evolving groundwater body.

Lake MacDonald south of Lake Mackay, Figure 3, displays comparable criteria to indicate a halotectonic origin: (a) an anomalous palaeovalley pattern disconnected from other major palaeovalley systems; and, (b) outcrops of deformed Proterozoic Bitter Springs Formation surrounding the salt lake. Other salt lakes that may have their origins in various ancient evaporitic units include: Lake Hopkins, Lake Neale, Lake Amadeus, Karinga lakes, Lake Cobb, Lake Newell and salt lakes in the Baker Palaeovalley, eastern WA.

Halotectonism as a regolith and geomorphic process

The proposition that Lake Disappointment, Lake Mackay, Lake MacDonald, and potentially many other salt lakes in Australia's major basins evolved at locations where former diapirs of ancient evaporites penetrated the landscape surface in the Late Cenozoic, may account for the apparent absence of major palaeo-shorelines in the landscape surrounding these lakes. Bowler (1986) described palaeo-shorelines for terminal lakes that, in response to the onset of arid climatic conditions, have evolved from large rounded surface water lakes to contracted shallow lakes to dry playas, leaving palimpsest concentric imprints of sequential former shorelines. In comparison, lakes Disappointment and Mackay, and other salt lakes that are disconnected from major drainages and that lie within basins containing ancient evaporite units, appear to have formed in large, shallow crater-like depressions without evidence for substantial antecedent perennial lake phases foreshadowing more recent to contemporary responses to aridity. Whether palaeo-shorelines have evolved in such settings is predicated by the timing of salt diapir intersection with the landscape and the duration of subsequent catchment evolution under changing climatic conditions.

In a halotectonic scenario, salt lake development would be delayed until such time as the diapir became exposed, or close to exhumation, and began to collapse and dissolve. Subsequent subsidence of a shallow depression would foster salt accumulation in the brine pool through evaporative concentration under arid (tacitly, Late Quaternary) climatic conditions. Topographic lowering would proceed through deflation of salts and lakebed sediments, further exposing the lakebed and water table to evaporation, and promoting expansion of the salt lake surface area.

The fact that ancient salts originating from Proterozoic-Palaeozoic coastal-estuarine settings ultimately emerge in the Late Cenozoic landscape from great depths to evolve in Quaternary salt lakes raises questions about the hydrochemistry of the salts and brines in these 'halotectonic scenarios'. Whether such salts and evaporite mineral assemblages differ from those salt lakes whose chemical signatures are largely meteoric or, at most, reflect the geochemistry of their immediate catchments, should be investigated.

Halotectonism that has promoted formation of some major Australian salt lakes may justifiably expand our definition of regolith (Eggleton 2001) to include the term "intrusion" or "diapirism" along with more prevalent processes of weathering, erosion, and alluvial and aeolian activity that dominate regolith formation across Australia.

Acknowledgements

This paper is published with the permission of the CEO, Geoscience Australia. David Champion, John Magee, Ian Roach and Matilda Thomas are thanked for their contributions and reviews.

References

BELL J.G., KILGOUR P.L., ENGLISH P.M., WOODGATE M.F., LEWIS S.J. AND WISCHUSEN J.D.H. COMPILERS 2012. *WASANT Palaeovalley Map - Distribution of Palaeovalleys in Arid and Semi-arid WA-SA-NT*, 1:4 500 000 scale. Geoscientific thematic map (Geocat No 73980): Geoscience Australia, Canberra.

BOWLER J.M. 1981. Australian salt lakes: a palaeohydrological approach. *Hydrobiologia* **82**, 431-444.

BOWLER J.M. 1986. Spatial variability and hydrologic evolution of Australian lake basins: analogues for Pleistocene hydrologic change and evaporite formation. *Palaeogeography, Palaeoclimatology, Palaeoecology* **54**, 21-41.

EGGLETON R.A. ed. 2001. The Regolith Glossary: surficial geology, soils and landscapes. Cooperative Research Centre for Landscape Environments and Mineral Exploration, 144 pp.

ENGLISH P. LEWIS S. BELL J. WISCHUSEN J. WOODGATE M. BASTRAKOV E. MACPHAIL M. AND KILGOUR P. 2012. *Water for Australia's arid zone – identifying and assessing Australia's palaeovalley groundwater resources: summary report. Waterlines Report,* National Water Commission, Canberra.

ENGLISH P.M., MAGEE J.W. AND CLARKE J.D.A. 2013a. *Review of Australian Continental Salt Lakes*. Chapter 2 *In*: Mernagh T. ed. *A review of Australian salt lakes and assessment of their potential for strategic resources.* Record 2013/39. Geoscience Australia: Canberra, pp. 25-90.

ENGLISH P., CARR L., COSTELLOE M., ROACH I., HOLZSCHUH J. 2013b. *Precompetitive geophysical data by Geoscience Australia: Uncovering onshore basins in Western Australia*. Western Australian Basins Symposium (WABS) Abstract & Poster, August 2013, Perth, WA.

ENGLISH P. BASTRAKOV E. BELL J. KILGOUR P. STEWART G. AND WOLTMANN M. 2015. *Paterson Province Investigation for the Palaeovalley Groundwater Project*. Geoscience Australia Record. Canberra, pp. 264.

GALLANT J. C. & DOWLING T.I. 2003. A multi-resolution index of valley bottom flatness for mapping depositional areas. Water Resources Research **39(12)**, 1347-1359.

MAGEE J. 2009. Palaeovalley Groundwater Resources in Arid and Semi-Arid Australia: A Literature Review. Geoscience Australia. Canberra. GA Record 2009/03, 224 pp.

MERNAGH T., BASTRAKOV E., CLARKE J.D.A., DE CARITAT P., ENGLISH P.M., HOWARD F.J.F., JAIRETH S., MAGEE J.W., MCPHERSON A.A., ROACH I.C., SCHRODER I.F., THOMAS M., AND WILFORD J. 2013. *A review of Australian salt lakes and assessment of their potential for strategic resources.* Record 2013/39. Geoscience Australia: Canberra. pp. 243.

Quartz-dominated Cenozoic gravels in SE Australia: Where did all the quartz come from?

Brad Pillans and Hamish Leitch

Research School of Earth Sciences, The Australian National University, Acton ACT 2601

Many Cenozoic gravel deposits in SE Australia are dominated by quartz, whereas modern stream gravels are polymict. Where did all the quartz come from?

The lithological composition of modern bedload sediments is controlled by a number of factors, including catchment geology, source rock weathering and comminution of clasts during transport. In the Canberra region, Paleozoic metasediments, acid volcanics and granitic rocks are the dominant rock types, with minor mafic intrusives and Cenozoic basalts. Quartz veins are pervasive, but are volumetrically minor (<5%).

Samples of modern bedload sediments were collected from 7 sites and Cenozoic gravel deposits were sampled at 2 additional sites. Approximately 250 gravel clasts were collected at each site, in the size range 2-5 cm (long-axis). This size range was chosen because it was ubiquitous at all sites and it was a convenient size to allow easy collection and visual inspection of a statistically significant population of clasts.

Quartz clasts comprise between 10 and 50% of modern bedload sediments, whereas they comprise >95% of clasts in the two Cenozoic deposits (Table 1). Clasts were dominantly sub-rounded, except at one site (Paddy's River) where the clasts were dominantly rounded (visual roundness classes of Powell (1953)).

Table 1. Site details of modern and Cenozoic fluvial gravels in the Canberra region

Site No.	Site	Location	Quartz clasts (%)	Age	Modal roundness
1	Fyshwick gravels	35°19.201'E; 149°10.105'E	96.1	Cenozoic	Sub-rounded
2	Geary's Gap gravels	35°06.433'S; 149°21.905'E	96.3	Cenozoic	Sub-rounded
3	Butmaroo Creek	35°12.582'S; 149°29.637'E	46.4	Modern	Sub-rounded
4	Molonglo River (Lower)	35°17.101'S; 149°02.257'E	38.5	Modern	Sub-rounded
5	Bridge Creek (tributary of Butmaroo Ck)	35°11.909'S; 149°30.218'E	25.1	Modern	Sub-rounded
6	Molonglo River (upper)	35°19.569'S; 149°14.843'E	21.4	Modern	Sub-rounded
7	Queanbeyan River (tributary of Molonglo R.)	35°21.918'S; 149°14.321'E	20.2	Modern	Sub-rounded
8	Gibraltar Creek (tributary of Paddys River)	35°21.918'S; 149°57.134'E	13.8	Modern	Sub-rounded
9	Paddys River	35°28.887'S; 148°56.402'E	12.4	Modern	Rounded

The Fyshwick Gravels were once thought to be Permian fluvioglacial deposits but are more likely to be late Cenozoic fluvial sediments deposited by the paleo-Molonglo River. They outcrop, spectacularly, in a road cutting on the Monaro Highway, near the light industrial suburb of Fyshwick, in Canberra, in the middle reaches of the Molonglo River catchment. The gravels consist almost entirely quartz clasts. Bedding is preserved and they are clast-supported. There is no evidence of *in situ* weathering and destruction of other lithologies, so post-depositional weathering of less resistant clasts cannot explain the high concentration of quartz clasts relative to modern bedload sediments.

The Molonglo River (a tributary of the Murrumbidgee River), is about 100 km long, with a catchment area of about 200,000 ha, so it's not a big river. The geology is varied, including Paleozoic granite, volcanics and metasediments, with common quartz veins, but quartz clasts make up less than 40% of the modern bedload in the lower part of the catchment (Site 4) and around 20% in the middle-upper parts of the catchment (Sites 6 and 7). For a smallish river, like the Molonglo, comminution of less resistant lithologies and concentration of quartz with increasing transport distance is probably not as significant as in a larger catchment (c.f. Adams 1979). Furthermore, the Fyshwick Gravels (Site 1) lie between sites 6 and 7 in the Molonglo catchment, so transport distance does not appear to be a significant factor in explaining the high concentration of quartz clasts in the Fyshwick gravels.

However, we know that rainfall was significantly higher in the Canberra region during the late Cenozoic, and there were rainforest elements in the vegetation. For example, Macphail *et al*. (2015) have suggested that mean annual rainfall may have been in the range 2000-3000 mm during the Pliocene. Weathering regimes may therefore have been very different from today, and perhaps deep weathering of catchment lithologies favoured the supply of quartz-rich gravelly sediment to the river systems. We plan to test this hypothesis by extending our sampling of modern bedload gravels to catchments with significantly higher rainfall.

Figure 1. Left: Quartz-dominated clasts at Site 1 (Late Cenozoic Fyshwick gravels). Right: Polymict gravels, modern Murrumbidgee River, downstream of Site 4. Largest clasts are 5 cm long.

References

ADAMS J. 1979. Wear of unsound pebbles in river headwaters. *Science* **203**, 171-172.

MACPHAIL, M., FIFIELD, L.K., PILLANS, B., DAVIES, M. AND HOPE, G., 2015. Lake George revisited: New evidence for the origin and evolution of a large closed lake, Southern Tablelands, NSW. Australia. *Australian Journal of Earth Sciences* **62**.

POWERS, M.C. 1953. A new roundness scale for sedimentary particles. *Journal of Sedimentary Petrology* **23(2)**, 117-119.

An objective and repeatable method for the construction of Hydrogeological Landscape Units

A.L. Cowood[1,2], M.J. Cracknell[3,4] and L. Moore[1]

[1] Dryland Salinity Hazard Mitigation Program, University of Canberra
[2] Institute for Applied Ecology, University of Canberra
[3]Centre of Excellence in Ore Deposits (CODES), University of Tasmania
[4]School of Physical Sciences (Earth Sciences), University of Tasmania

Introduction

The Hydrogeological Landscapes (HGL) Framework is a landscape characterisation tool. It is used to discern areas of similar physical, chemical, hydrological and biological properties, referred to as HGL Units (Muller *et al*. 2015). The HGL Framework facilitates natural resource management, where on-ground management actions are tailored to landscape facets within individual HGL Units for specific applications, such as dryland salinity, urban salinity, erosion control, wetland characterisation, climate change hazard assessment and catchment action plans (e.g., Wooldridge *et al*. 2015; Nicholson *et al*. 2014). Methodologies for constructing HGL Units typically follow the selection and manual interpretation of available spatial and field based datasets. The resulting HGL Units are then validated by an interdisciplinary expert team in conjunction with field assessments (Moore *et al*. in prep). Despite manually interpreted and validated HGL Units forming the basis for effective land management decision support systems, their subjective construction methods lack reproducibility and, as a result, their statistical validity can be difficult to quantify.

Unsupervised statistical learning algorithms, such as Self Organising Maps (SOM; Kohonen 2001), attempt to define clusters within multivariate data that represent natural groups or patterns within these data. Clusters identified by SOM are reproducible, given the same input data and operating parameters, and can be plotted on a 2D “map” representing cluster similarity in multidimensional data space. This 2D representation aids visualisation and interpretation of cluster characteristics. SOM outputs include a code-vector, summarising cluster properties. This combination of SOM code-vectors and the 2D SOM map allows one to interrogate and assess resultant clusters using qualitative and quantitative statistical methods.

This paper outlines an expansion of the HGL Framework methodology to include the automated construction and analysis of HGL Units from spatial data using SOM (SOM-HGL Units). We document a case study that compares HGL Units derived manually by domain experts and SOM-HGL Units within the South East Local Land Services region within New South Wales (Cracknell and Cowood in press).

Data and Methods

Independently, manually derived HGL Units and automatically constructed SOM-HGL Units were developed using the same spatial datasets typical of a normal HGL Framework approach (Table 1). Categorical data were combined with numeric data by the introduction of dummy variables and conversion from polygon to raster data formats where applicable. All spatial data were resampled to a coincident 500 m pixel resolution.

SOM was implemented in the R programming language (R Core Team 2015) using the *kohonen* package (Wehrens and Buydens 2007). In total, 196 SOM nodes representing initial clusters defined by a 14 x 14 2D SOM map, were generated using all available pixels (n = 234,326). A map of the spatial distribution of SOM nodes was constructed by linking SOM derived clusters to their associated pixels in a GIS. One of the fundamental challenges for unsupervised learning methods is the selection of an appropriate number of clusters. We used the Davies-Bouldin Index (DBI), a measure of cluster dispersion and similarity to objectively select an optimal number of clusters. We summarised the resulting SOM-HGL Unit polygons with attribute information indicating dominant cluster characteristics. These cluster characteristics included, for each input variable, the top and second top ranked categories based on % cover within a given SOM-HGL Unit and entropy. In this case, entropy provides a measure of the heterogeneity, or complexity, within individual SOM-HGL Units based on the proportion intersecting categories. For example, if a SOM-HGL Unit contains a single category then entropy is equal to 0, alternatively, if many categories have equivalent proportions then entropy approaches 1. For more details on SOM theory, processing methods and SOM-HGL Unit attribute definition for this study see Cracknell and Cowood (in press).

Table 1: Spatial data used to generate manually derived HGL Units and automatically constructed SOM-HGL Units.

Data (abbrev.)	Type	Scale	Comments	Sources
Surface Geology of Australia (GEO)	Polygon/ categorical	1:1,000,000	Generalised based on dominant lithological types, e.g. felsic intrusives, mafic volcanics etc. (20 classes)	Raymond and Retter (2010)
The Digital Atlas of Australian Soils (SOIL)	Polygon/ categorical	1:2,000,000	Generalised based on the level 2 soil documented by Isbell (1992), for each soil class (30 classes)	National Resource Information Centre (1991)
Vegetation Formations of NSW (VEG)	Raster/ categorical	200 m	Broad vegetation classes (13 classes)	Keith and Simpson (2010)
Australian Land Use and Management Classification (LAND)	Polygon/ categorical	1:50,000	Broad land use classes (14 classes)	ABARES (2011)
Digital Elevation Model (DEM)	Raster/ numeric	30 m		NSW OEH corporate data
Slope (SLOPE)	Raster/ numeric	30 m	Derived from DEM	NSW OEH corporate data
Topographic Wetness Index (TWI)	Raster/ numeric	90 m	Derived by combining partial contributing area and percent slope, computed from hydrologically enforced and smoothed DEMs respectively	Gallant and Austin (2012)
BIOCLIM Annual Precipitation model (RAIN)	Raster/ numeric	250 m	Based on ANUCLIM Beta climate model	Xu and Hutchinson (2011)

Results and Discussion

Initially, 65 HGL Units were manually interpreted across the study area. In comparison, the optimal number of SOM-HGL Units was defined as 76 using the DBI (Figure 1). The approximately equal number of units generated independently by the different approaches, suggest they are capturing similar landscape characteristics. A single HGL Unit was, on average, represented by full or partial cover of 20.71 SOM-HGL Units (min. = 1, max. = 42). On average, the top four SOM-HGL Units (ranked by % area) covered 78.56% of an individual HGL Unit (min. = 48.84%, max. = 100%). A single SOM-HGL Unit was, on average, present in 17.71 HGL Units (min. = 1, max. = 53), equivalent to 9.64% (min.=1.88%, max.=100%) of the total area covered by an individual HGL Unit.

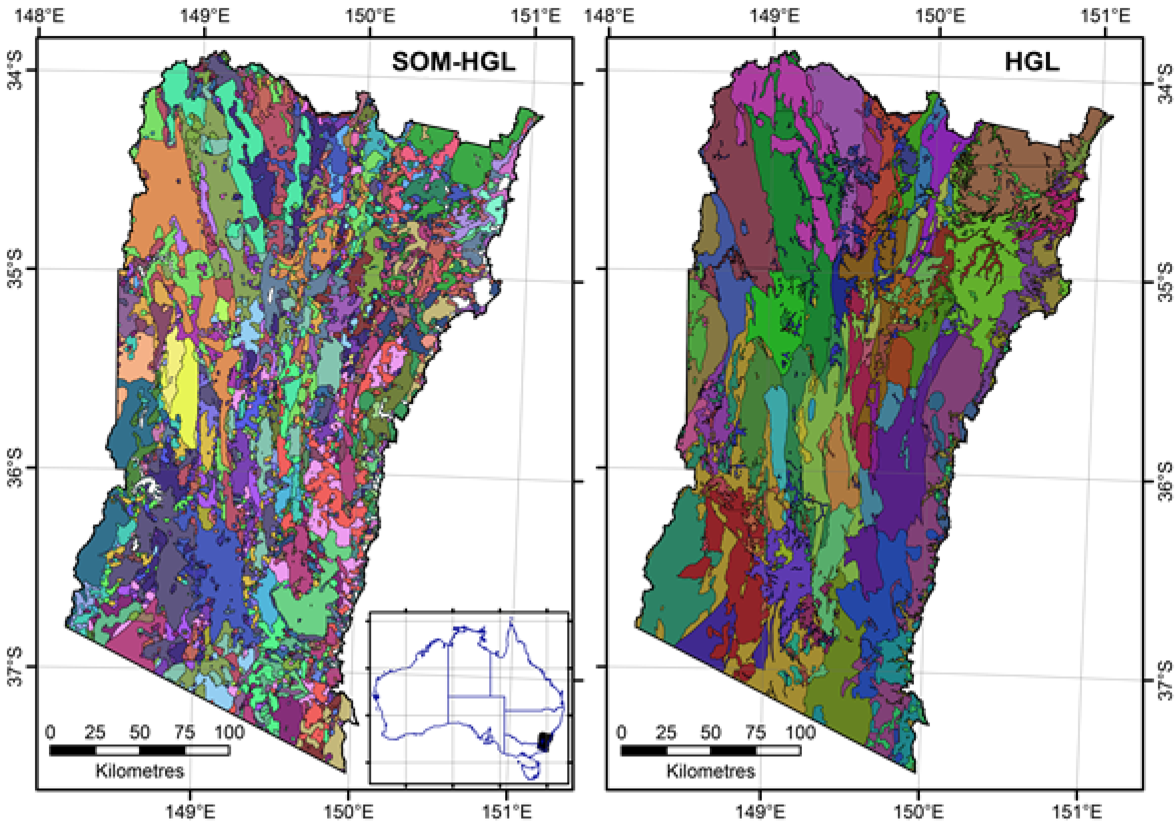

Figure 1: Comparison of 76 automatically constructed SOM-HGL Units (left) and 65 manually derived HGL Units (right). Inset shows location of the South East Local Land Services region within New South Wales.

At first glance there does not appear to be significant spatial coincidence between HGL Units and SOM-HGL Units. Closer inspection reveals HGL Units are often represented by multiple smaller SOM-HGL Units. For example, a comparison of the Windellama HGL Unit and the top four SOM-HGL Units (based on % area) covering this HGL Unit indicates close spatial relationships (Figure 2). Grouped SOM-HGL units are spatially contiguous and cover the majority of the Windellama HGL Unit (75.39%). The SOM-HGL Units can also be found grouped together as distinct regions to the northwest and southeast of Windellama. This suggests neighbouring areas share similar characteristics with the Windellama HGL. Conceptually, HGL Units account for a certain level of internal variation which is normally captured as the HGL Unit is broken down into landscape facets, referred to as Management Areas. The use of top ranked and second top ranked SOM-HGL Unit attributes are able to better capture patterns of internal HGL Unit variation. As a result of the SOM-HGL Unit comparison, the initial 65 HGL Units were expanded to a total of 74 and several HGL Unit boundaries were refined.

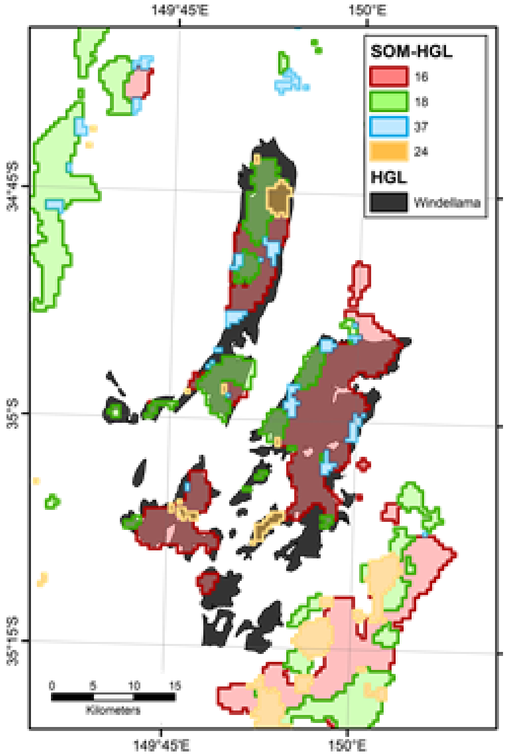

Figure 2: Comparison of top four ranked SOM-HGL Units (based on % area coverage) for the Windellama HGL.

Geological and/or soil units are typically used as a base layer for manual HGL Unit development given that these properties play a major role in the development of the physical, chemical and hydrological characteristics of the landscape. Other data, such as precipitation and vegetation, are used to distinguish areas of similarity or dissimilarity. Table 2 shows that SOM-HGL Units display a strong correlation with categorical data, particularly geological units. SOM-HGL Unit top ranked geological class proportions are the highest of all input data (mean = 0.81). Furthermore, both geological unit second ranked class proportions (mean = 0.09) and entropy (mean = 0.22) are considerably lower than any other input dataset. These findings support the use of geology as an important and fundamental base layer during HGL Unit interpretation.

Table 2: Statistical summary of SOM-HGL Unit (n = 76) top ranked (1°), second ranked (2°) class proportion and entropy.

			DEM	SLOPE	TWI	RAIN	GEO	SOIL	VEG	LAND
Class proportion	1°	Mean	0.58	0.48	0.48	0.56	0.81	0.60	0.69	0.78
		Median	0.54	0.45	0.45	0.50	0.88	0.56	0.74	0.81
		St. dev.	0.19	0.18	0.17	0.18	0.16	0.24	0.16	0.17
	2°	Mean	0.22	0.22	0.19	0.23	0.09	0.16	0.15	0.13
		Median	0.22	0.22	0.19	0.25	0.05	0.15	0.12	0.09
		St. dev.	0.10	0.06	0.06	0.09	0.09	0.10	0.09	0.10
Entropy		Mean	0.64	0.79	0.82	0.66	0.22	0.34	0.38	0.26
		Median	0.69	0.84	0.88	0.71	0.19	0.38	0.36	0.25
		St. dev.	0.24	0.20	0.18	0.22	0.14	0.19	0.13	0.14

Spatial data used to construct SOM-HGL Units in this study have been commonly used to derive landscape hydrological characteristics in other studies. For example, Coram *et al*. (2001) determined the hydrogeology of groundwater flow systems (GFS) through analysis of analogous data. The GFS has previously been used to inform salinity management in Australia (Walker *et al*. 2003). These data are also consistent with the methodology of Winter (2001) and Wolock *et al*. (2004) who employed cluster analysis to delineate hydrologic landscapes for wetland management applications using metrics of landform, geology, soil and climate. Currently, the HGL Framework methodology uses landscape characteristics present within HGL Units to infer established hydrological properties and processes identified in the literature, including those mentioned above. To increase the functionality of determining hydrological characterisation in SOM-HGL Units, future analyses using a restricted set of data representing hydrological information, such as GFS and weathering intensity index (Wilford 2012), should be undertaken.

The SOM-HGL Unit methodology is easily transferable to other regions, applicable at any scale and dependent only on the availability of spatial data across a given area. We suggest applying these techniques to the definition, or validation, of HGL Units within key agricultural regions such as the Murray-Darling Basin. The resulting statistically assessable SOM-HGL Units will provide information invaluable to land management decision support systems, such as those attempting to assess and mitigate against the significant challenges facing soil and groundwater conservation strategies in a rapidly changing climate.

Conclusions

The addition of SOM, an unsupervised statistical learning algorithm, to the HGL Framework methodology provides a statistically robust, automated technique for the objective construction of HGL Units. SOM-HGL Units are shown to closely correspond to manually derived HGL Units while also defining additional levels of landscape detail. The integration of SOM to the HGL Framework provides qualitative and quantitative statistical evidence for the definition, validation and refinement of manually derived HGL Units. This in turn increases confidence in the assessment of developed HGL Units, especially where opportunities for field-based validation are limited due to site accessibility or financial constraints. The scope of potential applications of our SOM-based methodology to the definition of HGL Units is limited only by the selection of appropriate input data. The SOM-HGL approach provides a statistically robust tool for land management decision support systems attempting to conserve soil and groundwater resources in a rapidly changing climate.

References

CORAM J.E., DYSON P.R. AND EVANS W.R. 2001. *An Evaluation Framework for Dryland Salinity, A report prepared for the National Land and Water Resources Audit Dryland Salinity Project*. Bureau of Rural Sciences, Canberra, Australia.

CRACKNELL M.J. AND COWOOD A.L. in press. Construction and analysis of Hydrogeological Landscape Units using Self-Organising Maps. Accepted for publication in *Soil Research*.

KOHONEN T. 2001 *Self-Organizing Maps*. Springer, Berlin.

MOORE C.L., JENKINS B.R., COWOOD A.L., NICHOLSON A., MULLER R., WOOLDRIDGE A., COOK W., WILFORD J.R., LITTLEBOY M., WINKLER M. AND HARVEY K. in prep. Hydrogeological Landscapes Framework, a biophysical approach to landscape characterisation and salinity hazard assessment. Submitted to *Catena*.

MULLER R., NICHOLSON A., WOOLDRIDGE A., JENKINS B., WINKLER M., COOK W., GRANT S. AND Moore C.L. 2015. *Hydrogeological Landscapes for the Eastern Murray Catchment*. Office of Environment and Heritage, Sydney, NSW.

NICHOLSON A., COWOOD A.L., MULLER R., WOOLDRIDGE A. AND COOK W. 2014. *Impact of regional corridor plantings on water quality – South East Local Land Services*. NSW Department of Primary Industries, Sydney, Australia.

R CORE TEAM. 2015. *R: A Language and Environment for Statistical Computing*. R Foundation for Statistical Computing, Vienna, Austria.

WALKER G., GILFEDDER M., EVANS R., DYSON P. AND STUAFFACHER M. 2003. *Groundwater Flow Systems Framework–Essential Tools for Planning Salinity Management*. Murray Darling Basin Commission.

WINTER T.C, 2001. The concept of hydrologic landscapes. *Journal of the American Water Resource Association*, **37**, 335-349.

WILFORD J. 2012. A weathering intensity index for the Australian continent using airborne gamma-ray spectrometry and digital terrain analysis. *Geoderma,* **183–184**, 124–142.

WEHRENS R. AND BUYDENS L.M.C. 2007. Self- and super-organising maps in R: the kohonen package. *Journal of Statistical Software*, **21**, 1–19.

WOLOCK D.M., WINTER T.C. AND MCMAHON G. 2004. Delineation and evaluation of Hydrologic-Landscape Regions in the United States using Geographic Information System tools and multivariate statistical analyses. *Environmental Management*, **34 (Supplement 1)**, S71-S88.

WOOLDRIDGE A., NICHOLSON A., MULLER R., JENKINS B.R., WILFORD J. AND WINKLER M. 2015., *Guidelines for managing salinity in rural areas*. Office of Environment and Heritage NSW, Sydney, Australia.

Cover Characterisation and Shallow Basement Mapping using Airborne Electromagnetic Data: examples from the Southern Thomson Project

I.C. Roach and A.A. McPherson

Geoscience Australia, GPO Box 378, Canberra ACT 2601

Introduction

The Southern Thomson Orogen VTEMplus® AEM Survey (Roach, 2015) was undertaken as part of Geoscience Australia's contribution to the Australian Academy of Science's UNCOVER initiative, adopted as part of the Australian Government's National Mineral Exploration Strategy. Survey planning was in conjunction with our State survey partners, the Geological Survey of New South Wales and the Geological Survey of Queensland. The aim of the survey was to demonstrate the application of the AEM technique as an under-cover mapping and exploration tool by generating new data and information regarding depth to basement (DTB) and cover character in the under-explored southern Thomson Orogen region (Figure 1). The ultimate goal of the Southern Thomson Project is to encourage industry investment in this poorly understood area to discover a new minerals province.

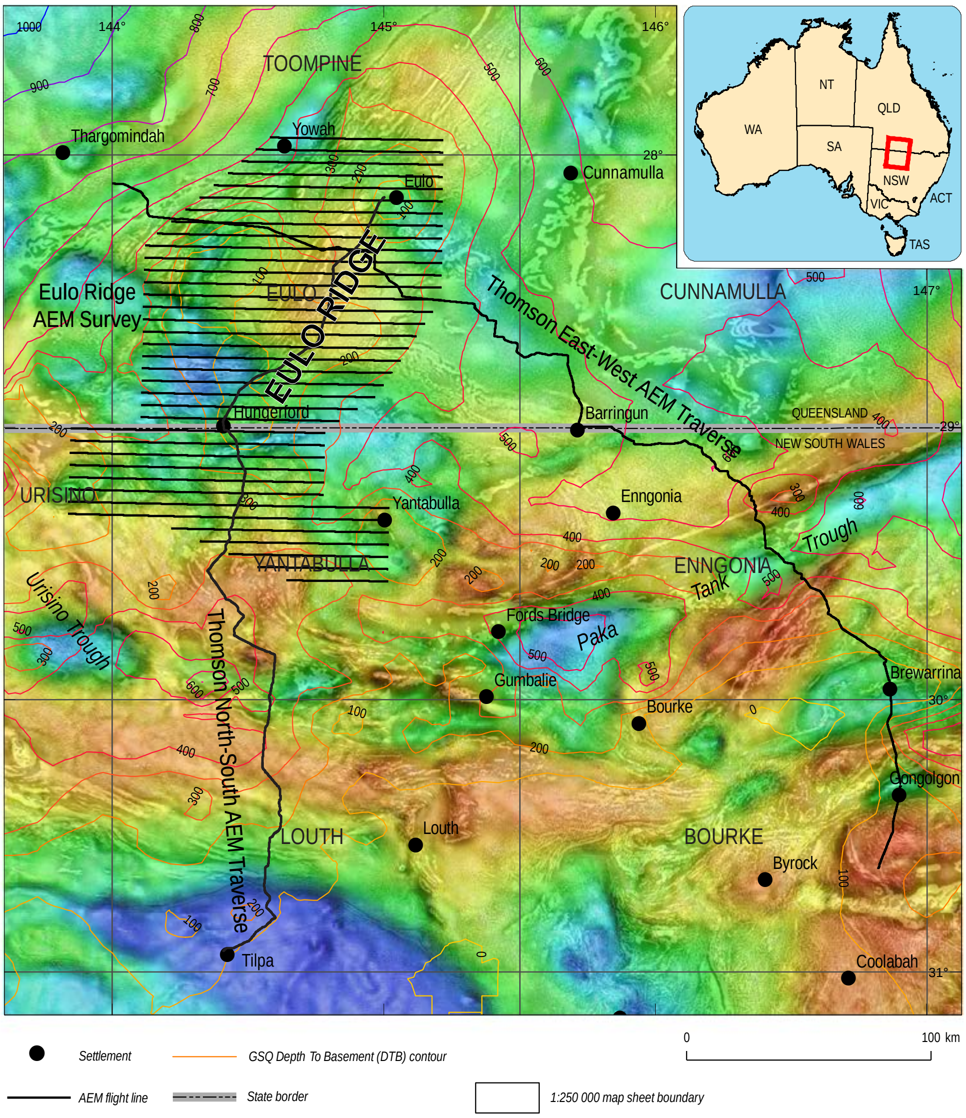

Figure 1: Location of the Southern Thomson Orogen VTEMplus® AEM Survey, showing flight lines and corresponding 1:250 000 scale map sheets. The map shows the GSQ water bore-derived depth to basement (DTB) model contour lines modelling the depth to Paleozoic basement. The image background is grey-scale reduced to pole 1st vertical derivative magnetics coloured by Bouguer gravity anomaly (red = high, blue = low). From Roach (2015).

Airborne electromagnetic (AEM) data has been used world-wide by the minerals industry to target exploration drilling for shallowly-buried basement-hosted mineral systems at depths of 150-200 m below surface, and in exploring for the distal footprints of mineral systems within the overlying basin cover sequences, summarised in Roach *et al.* (2014). Southern Thomson Orogen VTEMplus® AEM Survey focussed on the Eulo Ridge, which is an uplifted portion of Paleozoic basement that influences groundwater flow in the Great Artesian Basin (Smerdon *et al.*, 2012) (Figure 1). The Survey was flown in two parts: (1) A regular survey across the Eulo Ridge comprising east-west flight lines at a 5 km line spacing intended to maximise the potential for mapping shallow basement on and around Eulo Ridge; and (2) Two single-line traverses, one extending north from Tilpa (NSW) to Eulo (Qld) via Hungerford, and the other extending approximately north-west from Gongolgon (NSW) to south-east of Thargomindah (Qld) via Brewarrina and Barringun (Figure 1). The single-line traverses complement new gravity and magnetotelluric data acquisition to model the deeper crustal structure of the southern Thomson Orogen and the Thomson-Lachlan orogen boundary.

Regional Geology

The basement geology in the Eulo Ridge area is dominated by Paleozoic felsic intrusive, clastic sedimentary and metasedimentary rocks; other rock types such as mafic to intermediate volcanic and ultramafic rocks are interpreted to occur as minor components. Very few geochronological data are available to accurately date the basement rocks, but ages for the metasedimentary rocks are Cambro-Ordovician, similar to the Lachlan Orogen to the south; refer to Hegarty (2010), and Purdy *et al.* (2013a); Purdy *et al.* (2013b); Purdy *et al.* (2014) for further detail. In the wider study area in Figure 1, the Late Devonian basins of the Urisino Trough and Paka Tank Trough occur in the southwest and southeast, filled with Mulga Downs Group sedimentary rocks (Scheibner and Basden, 1998). The Paleozoic basement of the Eulo Ridge is covered predominantly by sediments of the Mesozoic (Jurassic to Cretaceous) Eromanga Basin. In the Eulo Ridge area the succession consists of the Hooray Sandstone (a prominent aquifer) overlain respectively by the Cadna-owie, Wallumbilla and Winton formations (Hawke and Cramsie, 1984). The Wallumbilla Formation consists of the upper Coreena Member (a moderately productive aquifer) and the lower Doncaster Member (pyritic black shale). The Wallumbilla Formation is the correlative of the Marree Subgroup in South Australia, with the Coreena Member being equivalent to the Oodnadatta Formation and the Doncaster Member being the equivalent of the Bulldog Shale (Krieg, 1995; Scheibner and Basden, 1998; Jell *et al.*, 2013). The Mesozoic sequence is overlain by the Cenozoic Glendower and Whitula formations of the Lake Eyre Basin, which are the correlatives of the Eyre and Namba formations in South Australia, respectively (Scheibner and Basden, 1998; Jell *et al.*, 2013). The Glendower Formation now exists as topographically-inverted, silica-indurated, palaeodrainage system remnants, while the Whitula Formation has been largely removed by erosion.

Data Processing and Results

The Southern Thomson Project area is a challenging environment for AEM data acquisition; high near-surface electrical conductivities due to the presence of salt lakes, saline groundwater and electrically conductive basin cover make for difficult acquisition conditions and anticipated poor AEM signal penetration. Despite these difficulties, results were generally very positive due to the selection of an appropriate AEM system for these conditions. The AEM data were inverted using the Geoscience Australia Layered Earth Inversion Sample By Sample (GALEISBS) algorithm (Brodie and Sambridge, 2009; Brodie and Sambridge, 2012) and the new Geoscience Australia Reversible Jump Markov Chain Monte Carlo (GARJMCMC) data inversion algorithm (Brodie, 2015) on the National Computational Infrastructure (NCI) supercomputer at the Australian National University. The inverted AEM data, together with a comprehensive National Groundwater Information System (NGIS) water bore (BOM, 2014) and stratigraphic drill hole database, has allowed us to make a number of high-confidence correlations between the inverted AEM data and regional geology and hydrostratigraphy.

Figures 2 and 3 are 3D block models, developed in GOCAD® software, illustrating examples of poor and good AEM signal penetration in the Eulo Ridge AEM Survey area. Average signal penetration (depth of investigation) is calculated to be 166.9 m, varying between 8.6 m in highly electrically conductive terrain to 467.5 m in highly electrically resistive terrain. The electrical responses of cover and basement units can be gauged by creating a series of these 3D block models, which are then used to develop empirical rules for interpretation along the AEM flight lines. This allowed us to map the hydrostratigraphy of the Eromanga Basin, the basement-cover interface and electrical conductivity features within Paleozoic basement with a high degree of confidence. Paleozoic basement units are overall generally electrically resistive, except the Girilambone Group of the Cobar Supergroup which is moderately conductive, allowing basement to be mapped under the moderately to highly electrically conductive Mesozoic and Cenozoic cover.

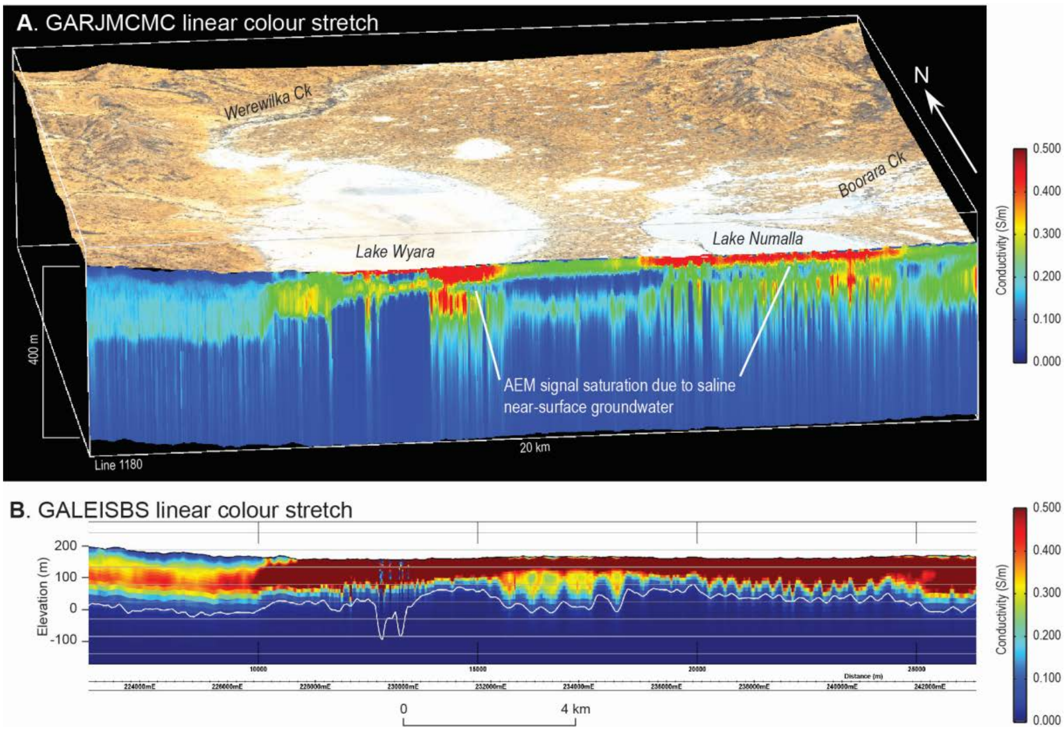

Figure 2: An example of poor AEM signal penetration in highly conductive ground over the Eulo Ridge due to high groundwater salinity. A: GOCAD block model showing a SPOT satellite image mosaic draped over topography and a portion of a GARJMCMC inversion conductivity section of line 1180. B: GALEISBS inversion conductivity section of the same portion of line 1180 showing the variation in the depth of investigation due to high near-surface groundwater salinity. From Roach (2015).

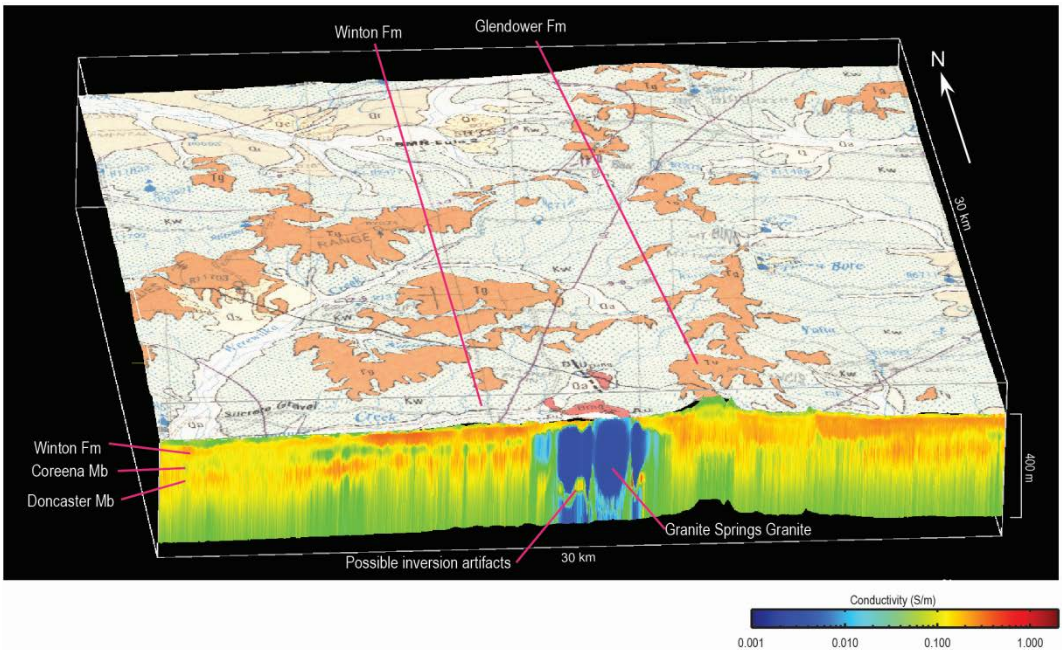

Figure 3: A GOCAD block model of the Granite Springs area on the EULO 1:250 000 geological sheet (Senior, 1971) illustrating sub-horizontal sedimentary rocks of the Eromanga Basin onlapping a poorly exposed granite pluton. This model uses a logarithmically colour stretched GARJMCMC conductivity section to highlight the difference between moderate to strong conductors in the Eromanga Basin cover sequence and the highly resistive granite bedrock. From Roach (2015).

Figure 4 illustrates AEM electrical conductivity sections and drill hole basement intersections displayed over first vertical derivative total magnetics (TMI 1VD) in ArcGIS software. The addition of off-line stratigraphic and water bore lithological data permits better cross-line extrapolations from the AEM interpretations, resulting in a more robust 3D model of the basement-cover interface and DTB in the survey area (Figure 5). During the interpretation a number of basement-intersecting drill holes and coincident electrical conductivity anomalies were also identified in the AEM dataset, defining new near-surface basement features not previously identified by 1:250 000 scale surface geological mapping.

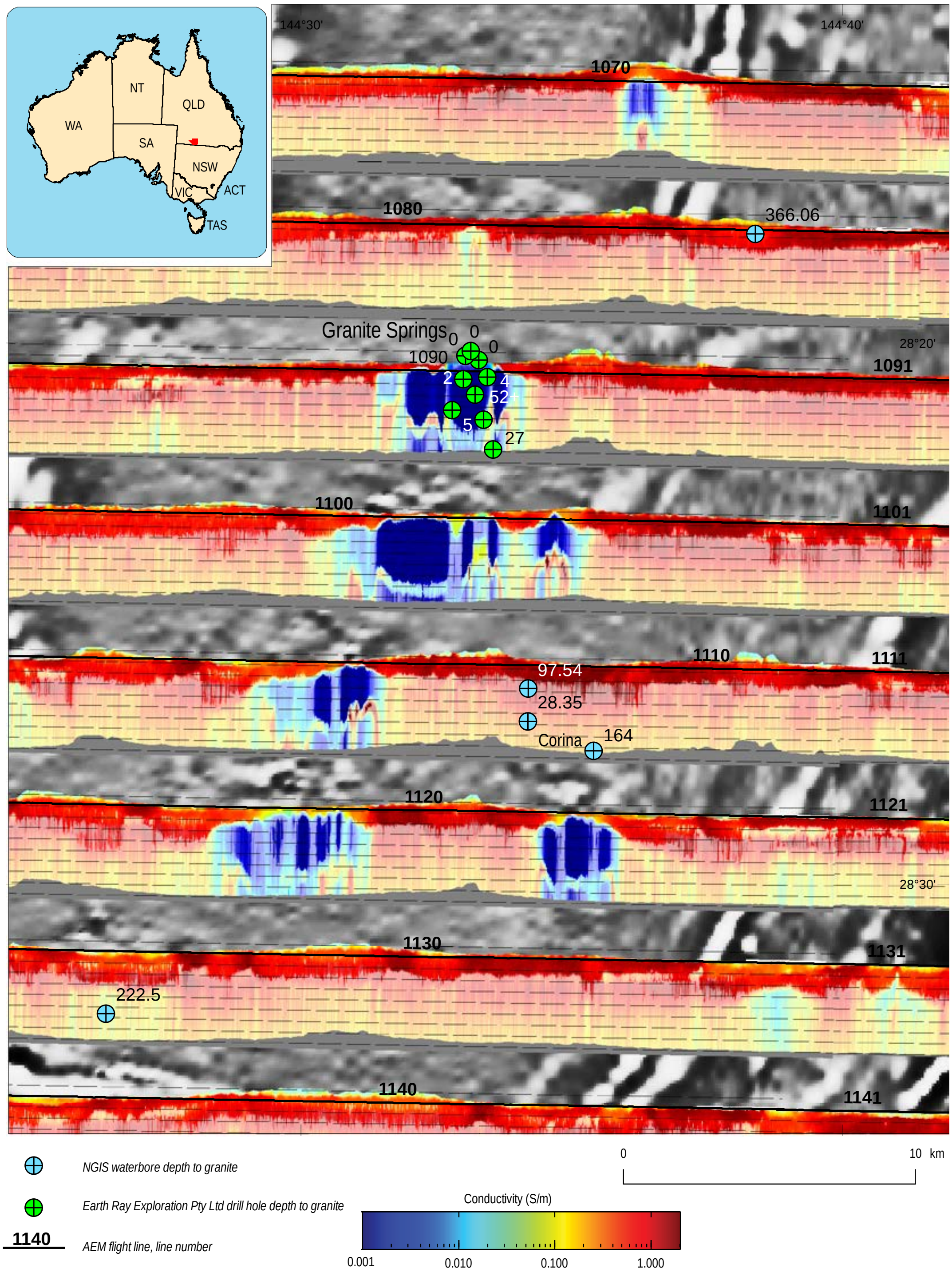

Figure 4: Plan view of logarithmic colour stretched GARJMCMC electrical conductivity sections from the Granite Springs area of the Eulo Ridge over the TMI 1VD magnetics map. Conductivity sections are rotated 90 degrees to lie in the plane of the map; flight lines (5000 m separation; flight lines numbered) and industry boreholes/NGIS water bores (annotated with depth to granite, where recorded) are also shown, indicating cover thickness. Note the shallow resistive basement extending north and (predominantly) south of Granite Springs; this has not previously been mapped. From Roach (2015).

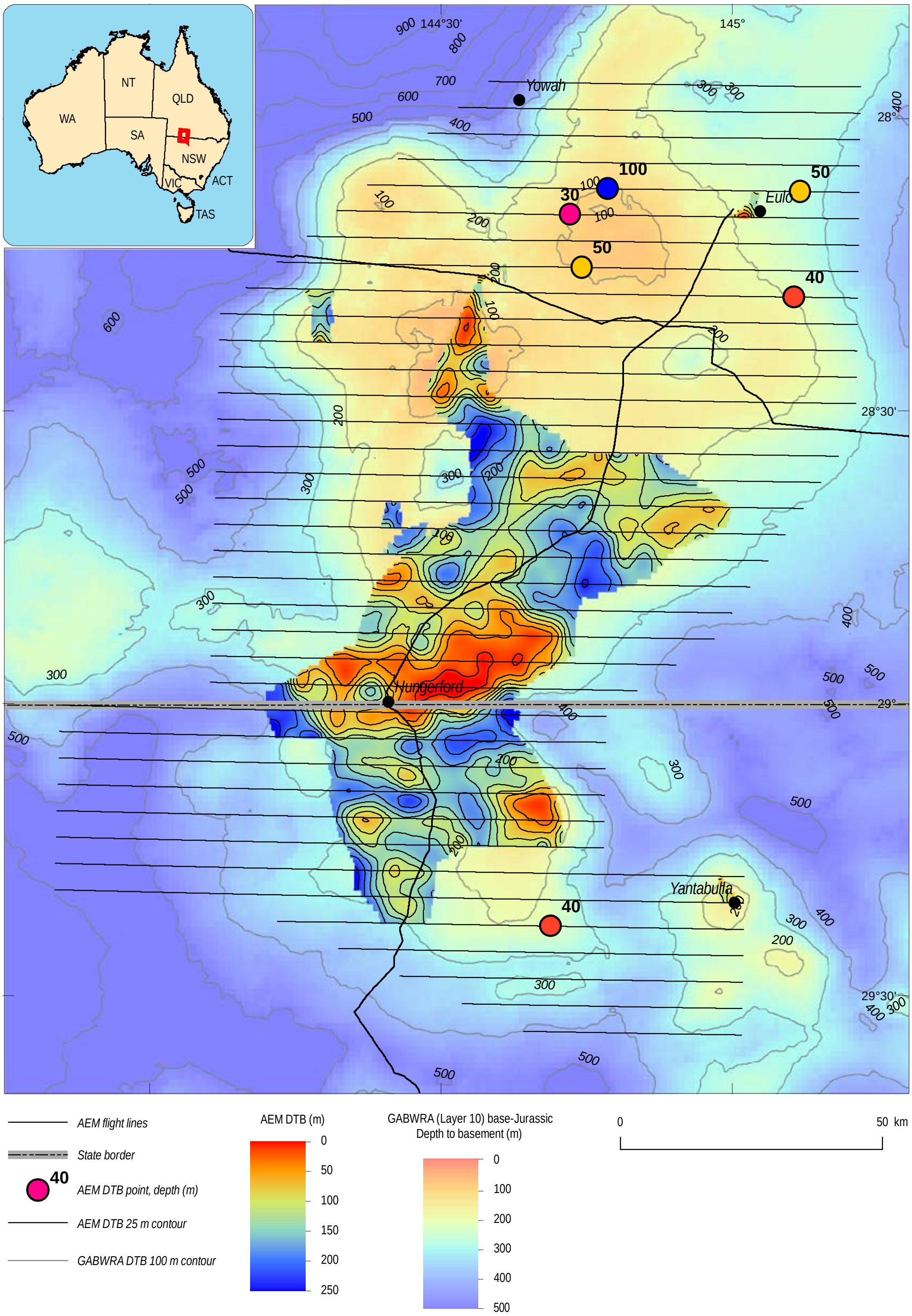

Figure 5: AEM DTB model and single basement highs observed in the AEM data. The background: DTB model is derived from the Great Artesian Basin Water Resource Assessment (GABWRA) base-Jurassic (Layer 10) surface of Ransley and Smerdon (2012). The coloured, labelled points are previously-unmapped resistive basement "islands" occurring on one flight line only, labelled with depth from surface in metres. From Roach (2015).

Conclusion

The Southern Thomson Orogen VTEMplus® AEM Survey successfully demonstrates the use of AEM as a regional geological mapping tool for characterising the basement-cover interface and under-cover geology in a region where no previous AEM data existed, and under difficult circumstances, i.e. under electrically conductive cover. Survey highlights include:

- Successful interpretation and mapping of the basement-cover interface over 3446 km^2 of the Eulo Ridge. This is despite the impediments of varying thicknesses of conductive cover, and saline ephemeral drainage systems over the survey area.
- Mapping of extensive resistive basement terrains, and previously-unrecognised basement 'islands', under shallow cover.
- Identification of highly complex basement palaeotopography.
- Higher-resolution hydrostratigraphic mapping of the Eromanga and Lake Eyre basins.
- 3D mapping of post-depositional fault systems that modify the landscape.
- High resolution mapping of weathering profiles in the Cobar Basin.

The recognition and mapping of new near-surface Paleozoic basement terrain dramatically increases the amount of ground potentially available for exploration drilling in the region by providing explorers more surety of reaching basement targets, and informing mineral systems models, thus reducing exploration risk. The next step of the Southern Thomson Project is to take the DTB interpretation developed in this study and drill near-surface Paleozoic basement features to learn more about the composition and age of the basement. This will inform mineral systems models and increase our knowledge of the mineral prospectivity of this greenfields region.

Acknowledgements
This paper is published with the permission of the CEO, Geoscience Australia. The authors thank Martin Smith and Murray Richardson for their thoughtful reviews.

References

BOM, 2014. National Groundwater Information System. Online: http://www.bom.gov.au/water/groundwater/ngis/.

BRODIE, R. AND SAMBRIDGE, M., 2009. Holistic inversion of frequency-domain airborne electromagnetic data with minimal prior information. Exploration Geophysics 40, 765-778.

BRODIE, R. C., 2015. AEM data acquisition and processing. In: Roach, I. C. (editor) The Southern Thomson Orogen VTEMplus® AEM survey. Geoscience Australia, Canberra. Record 2015/29.

BRODIE, R. C. AND SAMBRIDGE, M., 2012. Transdimensional Monte Carlo Inversion of AEM data. In: 22nd International Geophysical Conference and Exhibition, Brisbane. Australian Society of Exploration Geophysicists. Online: http://www.publish.csiro.au/?act=view_file&file_id=ASEG2012ab095.pdf.

HAWKE, J. M. AND CRAMSIE, J. N., 1984. Contributions to the geology of the Great Australian Basin in New South Wales. Geological Survey of New South Wales Bulletin 31, NSW Department of Mineral Resources, Sydney, 295 pp.

HEGARTY, R., 2010. Preliminary geophysical–geological interpretation map of the Thomson Orogen. Thomson Orogen - Release of Provisional and Preliminary Information [DVD], Geological Survey of New South Wales, Department of Industry & Investment, Maitland, NSW.

JELL, P. A., DRAPER, J. J. AND MCKELLAR, J., 2013. 7.1 Great Australian Superbasin. In: Jell, P. A. (editor) Geology of Queensland. Geological Survey of Queensland, Brisbane. 517 p.

KRIEG, G. W., 1995. Chapter 9: Mesozoic. In: Drexel, J. F. and Preiss, W. V. (editors) The Geology of South Australia Volume 2: The Phanerozoic. Geological Survey of South Australia, Adelaide. Bulletin 54, 93 p.

PURDY, D., HEGARTY, R., DOUBLIER, M. AND SIMPSON, J., 2014. Interpreting basement geology in the southern Thomson Orogen. In: Proceedings of the Australian Earth Sciences Convention 2014, Newcastle, Australia. Geological Society of Australia.

PURDY, D., CARR, P. A., BROWN, D. D., SIMPSON, J., HEGARTY, R. AND DOUBLIER, M. P., 2013a. Basement geology of the Southern Thomson Orogen. In: Digging Deeper 2013 Conference Proceedings, Brisbane. Geological Survey of Queensland, 39-52 pp.

PURDY, D. J., CARR, P. A. AND BROWN, D. D., 2013b. A review of the geology, mineralisation and geothermal energy potential of the Thomson Orogen in Queensland. Geological Survey of Queensland Record 2013/01, Geological Survey of Queensland, Brisbane. Record 2013/01, 206 pp.

RANSLEY, T. R. AND SMERDON, B. D. (editors), 2012. Hydrostratigraphy, hydrogeology and system conceptualisation of the Great Artesian Basin. A technical report to the Australian Government from the CSIRO Great Artesian Basin Water Resource Assessment. CSIRO Water for a Healthy Country Flagship, Australia. 285 pp.

ROACH, I. C. (editor) 2015. The Southern Thomson Orogen VTEMplus® AEM survey: Using airborne electromagnetics as an UNCOVER application. Geoscience Australia, Canberra. Geoscience Australia Record 2015/29. Available at http://www.ga.gov.au/metadata-gateway/metadata/record/83844.

ROACH, I. C., JAIRETH, S. AND COSTELLOE, M. T., 2014. Applying regional airborne electromagnetic (AEM) surveying to understand the architecture of sandstone-hosted uranium mineral systems in the Callabonna Sub-basin, Lake Frome region, South Australia. Australian Journal of Earth Sciences 61(5), 659-688. Available at: http://www.tandfonline.com/doi/full/10.1080/08120099.2014.908951.

SCHEIBNER, E. AND BASDEN, H., 1998. Geology of New South Wales - Synthesis. Geological Survey of New South Wales, Sydney. 2, 666 pp.

SENIOR, B. R., 1971. EULO 1:250 000 Geological Series - Explanatory Notes. Bureau of Mineral Resources, Geology and Geophysics, Canberra.

SMERDON, B. D., RANSLEY, T. R., RADKE, B. M. AND KELLETT, J. R., 2012. Water resource assessment for the Great Artesian Basin. A report to the Australian Government from the CSIRO Great Artesian Basin Water Resource Assessment. CSIRO Water for a Healthy Country Flagship, Australia.

Comprehensive new public datasets helping to understand cover and mineral potential in the Stavely Region, western Victoria.

Matilda Thomas[1], Anthony Schofield[1], Pauline English[1], Tony Meixner[1] and Georgina Gordon[2]

[1]Geoscience Australia, GPO Box 378, Canberra ACT 2601
[2] Geological Survey of South Australia, DSD, Australia, GPO Box 320, Adelaide SA 5001

Introduction

The Stavely Project is a collaborative venture between Geoscience Australia (GA) and the Geological Survey of Victoria (GSV) and additional government, industry and academic partners around Australia. The project aims to provide a framework for discovery of new mineral resources in the Stavely region, via the acquisition and delivery of pre-competitive geoscientific data (see Roach *et al*., this volume*)*. The Stavely Project area is located from 230 km to 300 km west and northwest of Melbourne, in western Victoria, south-eastern Australia (Figure 1). 14 pre-competitive stratigraphic drill holes were drilled in 2014 (Figure 2). Drilling was undertaken to test regional geological interpretations and recover material for detailed lithological, petrophysical, geochemical and geochronological analysis. Site-specific geophysical data was acquired to test the cover thickness and geophysical properties at selected drill sites for cover mapping and characterisation.

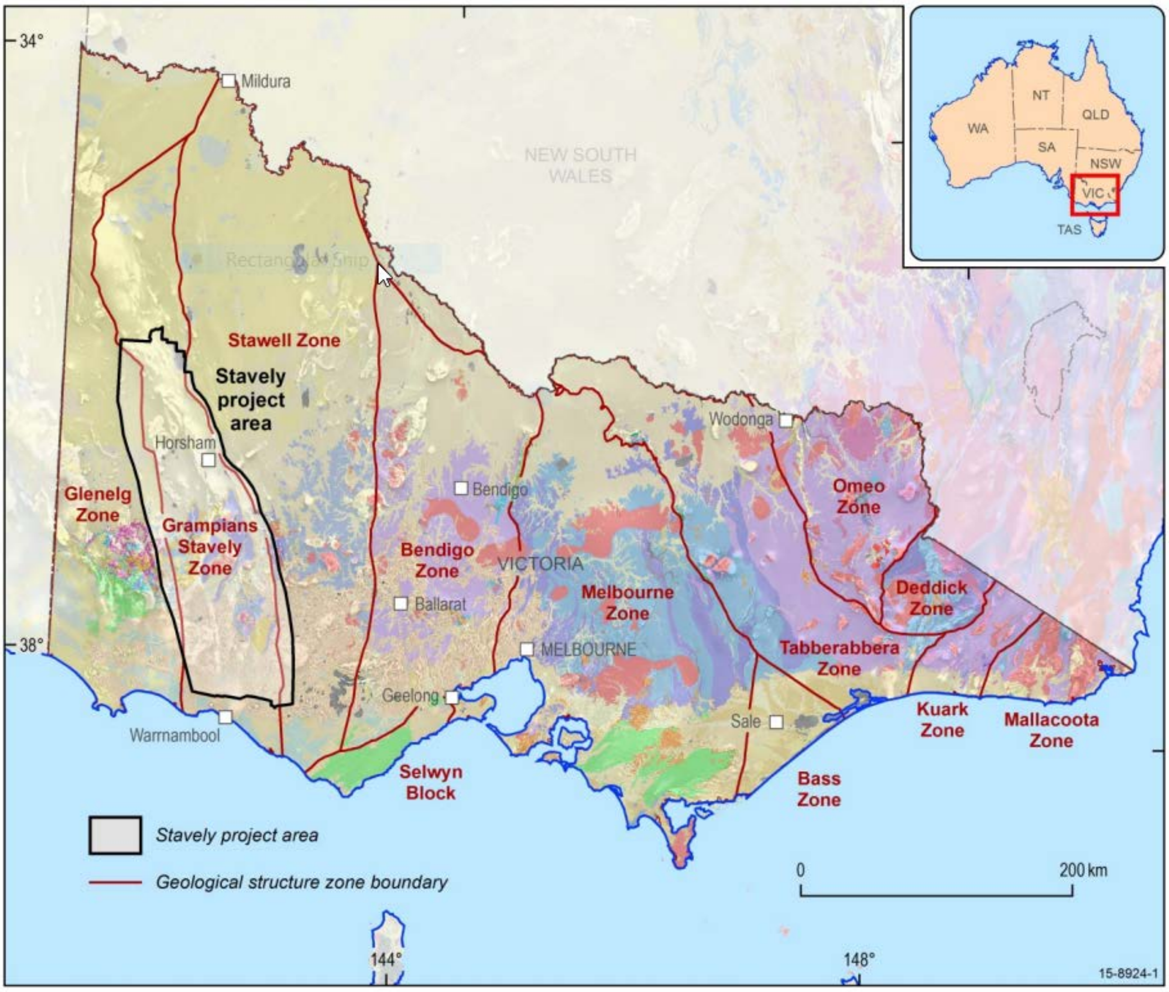

Figure 1: Location of the Stavely region and structural zones of Victoria. Figure adapted from VandenBerg *et al*. (2000).

Local basement comprises poorly explored Cambrian mafic-felsic igneous rocks. These are considered to form part of a volcanic arc system (the Stavely Arc), developed on the eastern Gondwana margin during the Early to Middle Cambrian. This basement is buried by variable thicknesses of non-mineralised cover rocks, including Mesozoic-Cenozoic fill in the Murray and

Otway basins and Cenozoic lavas of the Newer Volcanic Group. While a combination of existing exposure, regional airborne geophysics and historical open-file drilling reports has allowed the delineation of the volcanic belts under younger cover, the buried parts of the Stavely Arc remain largely untested for their mineral systems potential.

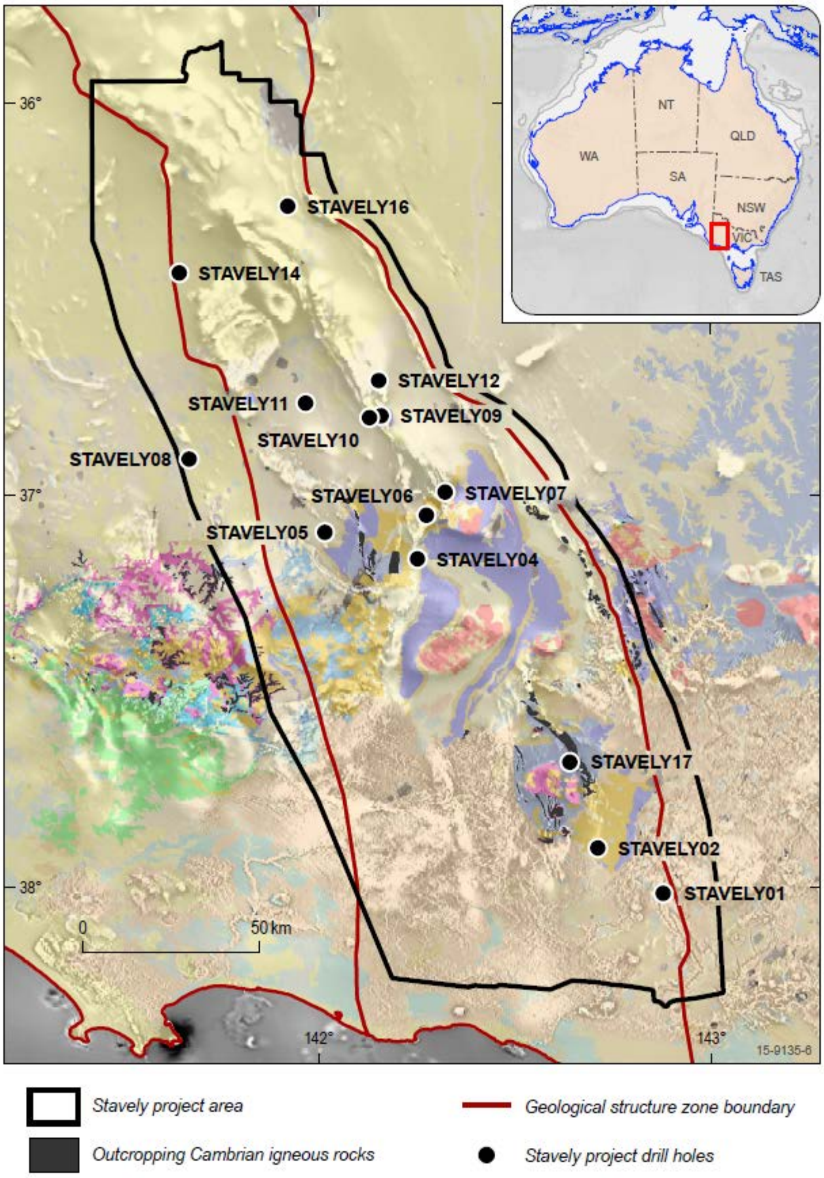

Figure 2. Location of the Stavely Project area showing the locations of new holes drilled for the project. Background: semi-transparent 1:1 million scale Geological Map of Australia (Raymond, 2010) overlain on a first vertical derivative total magnetic intensity greyscale image.

Stavely sonic drilling and cover materials sampling program

Where unconsolidated Murray Basin sediments overlie basement rocks, around 1100 m of sonic pre-collars were drilled on 11 of the 17 holes followed by approximately 1600 m of diamond drilling to complete basement core tails (STAVELY14 and 16 were sonic-only holes into deep sediments). The sonic drilling technique uses audible frequency vibration, rather than fast rotation, to advance a coring drill bit and steel casing. The sonic drilling technique has significant advantages over traditional rotary coring techniques including: almost 100% core recovery in unconsolidated materials, particularly sands and gravels; preservation of changes in facies; and the avoidance of contamination by drilling fluid, allowing for pore fluid samples to be collected and analysed.

Sonic pre-collars were completed for 11 of the 14 drill holes, providing a full stratigraphic sequence from surface to basement; these are a valuable resource and reference, now archived at the GSV core library. Sonic drilling generally employed a six inch sonic coring system over-ridden with eight inch outer casing. Sonic drill core logs were completed by a cover specialist with extensive experience of Murray Basin stratigraphy (J. Clarke).

Sonic and diamond logs were produced by comparing field geological logs with core photographs and checking against sample material taken at intervals of approximately 0.5-1.0 m. Lithological and stratigraphic contacts were then further refined using down-hole geophysical data and HyLogger™ hyperspectral data, which was used to detect variations in mineralogy. Stratigraphic unit attribution was made using lithological correlations with known Murray Basin stratigraphy. In order to refine and check stratigraphic picks, 12 samples were sent for foraminiferal biostratigraphy analysis, and an additional 11 samples were sent for palynostratigraphic age determinations. The sonic cores were sub-sampled, including an extensive pore-fluid sample collection (yet to be analysed), halved and placed in custom six-inch core trays after the completion of the drilling. After air drying, the cores were shipped for spectral scanning at the Geological Survey of South Australia's HyLogger™ facility in Adelaide.

Spectral scanning program

HyLogger™ spectral data were collected on all project cores, as described in Thomas *et al*. (2015), which includes detailed methods and procedures. Infrared reflectance spectroscopy was collected using a HyLogger™ 3-3 instrument with a spectral ranges of 380–2500 nm (visible and short wave infrared, VSWIR), and 6000–14,500 nm (thermal infrared, TIR). Reflectance spectroscopy can identify a range of different minerals, from iron oxides in the visible wavelengths, through to clay minerals and carbonate species in the SWIR and tecto-silicates in the TIR. Spectral data such as HyLogger™ can help increase value for money in drilling programs (especially if used early) by assisting the geologists with detailed mineralogical information, and by identifying mineral chemistry variations that may be indicators or markers for depth of weathering, bedrock/cover boundaries and favourable alteration and/or mineralisation.

In addition to collecting spectral information, the HyLogger™ produces high resolution digital imagery to allow geologists to visually characterise the colour and texture of the materials being logged. Macro images of core sections and drill hole mosaics (composite images of core trays arranged in order of depth) are produced to allow geologists to identify changes in colour and structure over the full depth of the drill hole (Figure 3).

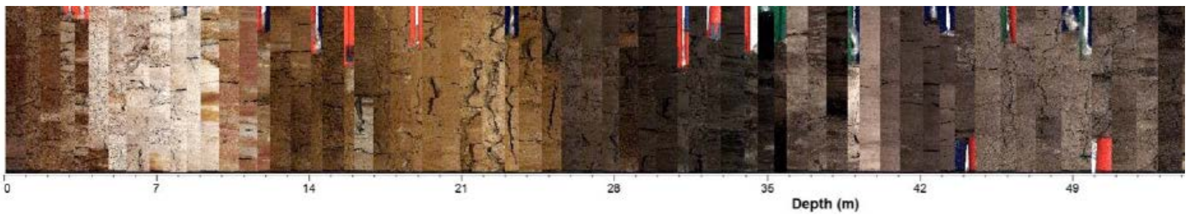

Figure 3: Core tray layout: mosaiced high resolution core scan images of STAVELY10. Note: brightly coloured sections are packing "noodles" to keep soft core sections intact.

The HyLogger™ data and specialist spectral interpretation and processing software (The Spectral Geologist – Hot Core, version 7.1.0) were used to aid in the identification and classification of weathering and alteration zones. The data also allow identification of surface weathering penetration (e.g. using kaolin and iron oxide mineral content), and any persistent mineral assemblages which might be important to mineral systems development. The specialist software allows for export in other data formats for combination with other data (e.g. Figure 4), as well as identification of minerals present in the SWIR and TIR wavelengths, and provides several viewing options to help study and interpret/present the data (see Figures 5 and 6.).

In the sonic core, kaolinite occurrence delineated depth of surface weathering, and oxidation zones associated with groundwater aquifers could be identified using iron oxide and clay mineralogy as mineralogical indicators (e.g. Lawrie *et al. 2012*).

Diamond core spectra identified a regionally extensive epidote-chlorite-carbonate-sericite assemblage in most drill holes, which could be interpreted as a regional metamorphic product and/or possible large scale hydrothermal alteration, with more definitive hydrothermal alteration mineralogy found in some drill holes, such as STAVELY17 (Schofield *et al.,* in prep).

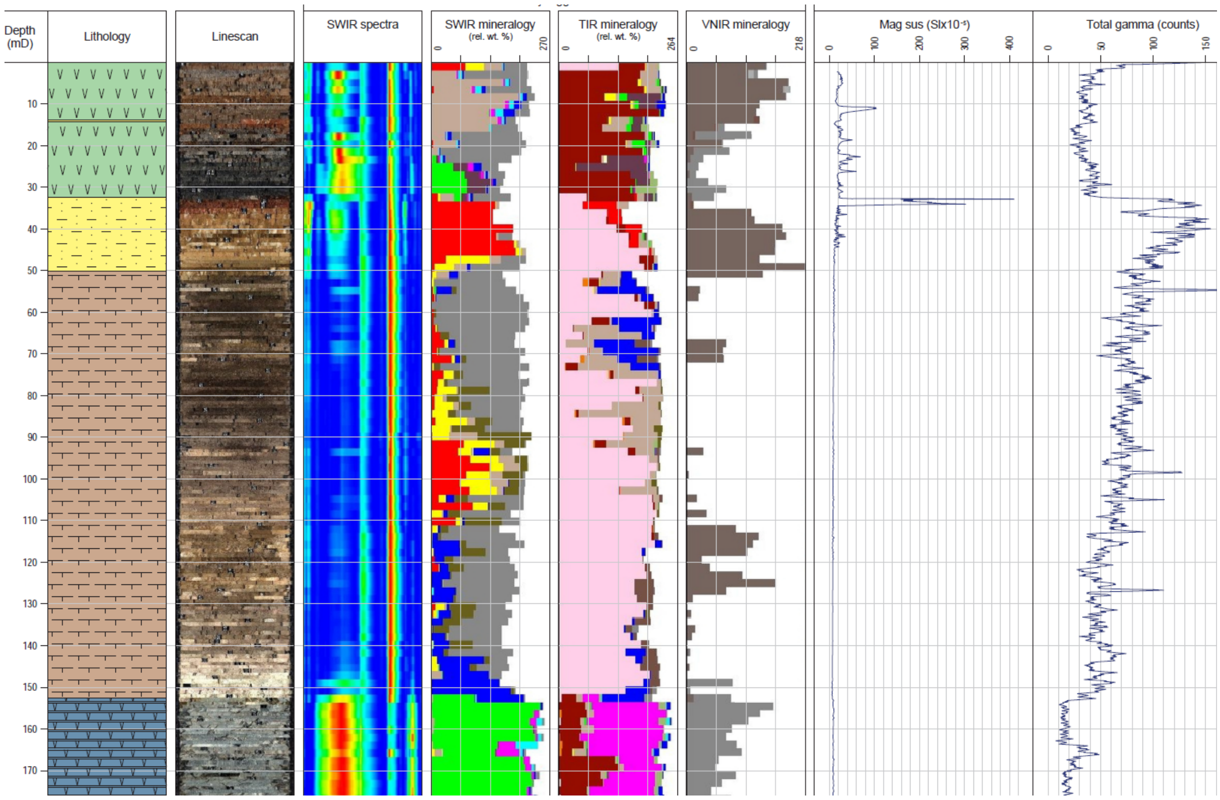

Figure 4. Example of HyLogger™ plots integrated with other data: from left to right, are: Depth (m), lithology, linescan image, SWIR spectra, SWIR mineralogy, TIR mineralogy, VNIR mineralogy, magnetic susceptibility and total gamma.

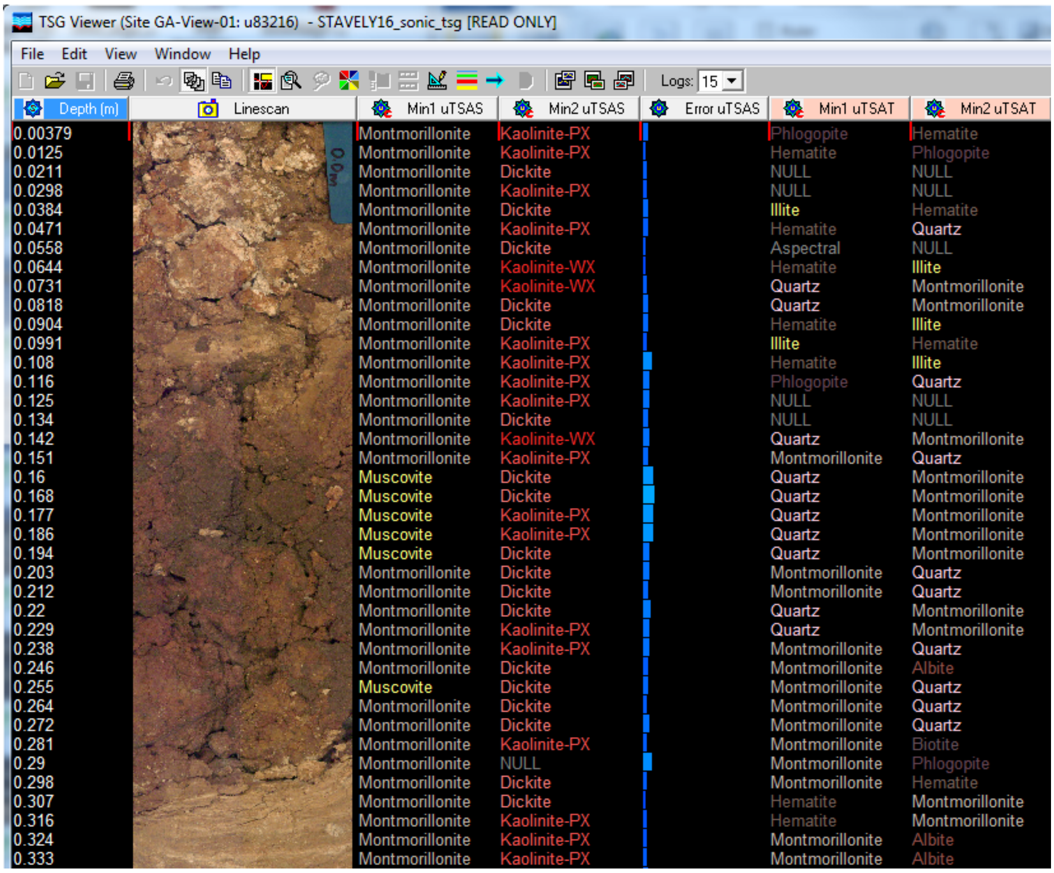

Depth (m)	Linescan	Min1 uTSAS	Min2 uTSAS	Error uTSAS	Min1 uTSAT	Min2 uTSAT
0.00379		Montmorillonite	Kaolinite-PX		Phlogopite	Hematite
0.0125		Montmorillonite	Kaolinite-PX		Hematite	Phlogopite
0.0211		Montmorillonite	Dickite		NULL	NULL
0.0298		Montmorillonite	Kaolinite-PX		NULL	NULL
0.0384		Montmorillonite	Dickite		Illite	Hematite
0.0471		Montmorillonite	Kaolinite-PX		Hematite	Quartz
0.0558		Montmorillonite	Dickite		Aspectral	NULL
0.0644		Montmorillonite	Kaolinite-WX		Hematite	Illite
0.0731		Montmorillonite	Kaolinite-WX		Quartz	Montmorillonite
0.0818		Montmorillonite	Dickite		Quartz	Montmorillonite
0.0904		Montmorillonite	Dickite		Hematite	Illite
0.0991		Montmorillonite	Kaolinite-PX		Illite	Hematite
0.108		Montmorillonite	Kaolinite-PX		Hematite	Illite
0.116		Montmorillonite	Kaolinite-PX		Phlogopite	Quartz
0.125		Montmorillonite	Kaolinite-PX		NULL	NULL
0.134		Montmorillonite	Dickite		NULL	NULL
0.142		Montmorillonite	Kaolinite-WX		Quartz	Montmorillonite
0.151		Montmorillonite	Kaolinite-PX		Montmorillonite	Quartz
0.16		Muscovite	Dickite		Quartz	Montmorillonite
0.168		Muscovite	Dickite		Quartz	Montmorillonite
0.177		Muscovite	Kaolinite-PX		Quartz	Montmorillonite
0.186		Muscovite	Kaolinite-PX		Quartz	Montmorillonite
0.194		Muscovite	Dickite		Quartz	Montmorillonite
0.203		Montmorillonite	Dickite		Montmorillonite	Quartz
0.212		Montmorillonite	Dickite		Montmorillonite	Quartz
0.22		Montmorillonite	Dickite		Quartz	Montmorillonite
0.229		Montmorillonite	Kaolinite-PX		Quartz	Montmorillonite
0.238		Montmorillonite	Kaolinite-PX		Montmorillonite	Quartz
0.246		Montmorillonite	Dickite		Montmorillonite	Albite
0.255		Muscovite	Dickite		Montmorillonite	Quartz
0.264		Montmorillonite	Dickite		Montmorillonite	Quartz
0.272		Montmorillonite	Dickite		Montmorillonite	Quartz
0.281		Montmorillonite	Kaolinite-PX		Montmorillonite	Biotite
0.29		Montmorillonite	NULL		Montmorillonite	Phlogopite
0.298		Montmorillonite	Dickite		Montmorillonite	Hematite
0.307		Montmorillonite	Dickite		Hematite	Montmorillonite
0.316		Montmorillonite	Kaolinite-PX		Hematite	Montmorillonite
0.324		Montmorillonite	Kaolinite-PX		Montmorillonite	Albite
0.333		Montmorillonite	Kaolinite-PX		Montmorillonite	Albite

Figure 5. Extract from The Spectral Geologist software: "Log screen" - from left to right, are: Depth (m), Continuous colour linescan image, the first mineral identified: Min1 TSAS (SWIR), the second mineral identified: Min2 TSAS (SWIR), TSAS Error rating, the first thermal mineral identified: Min1 TSAT (TIR), and the second thermal mineral: Min2 TSAT (TIR).

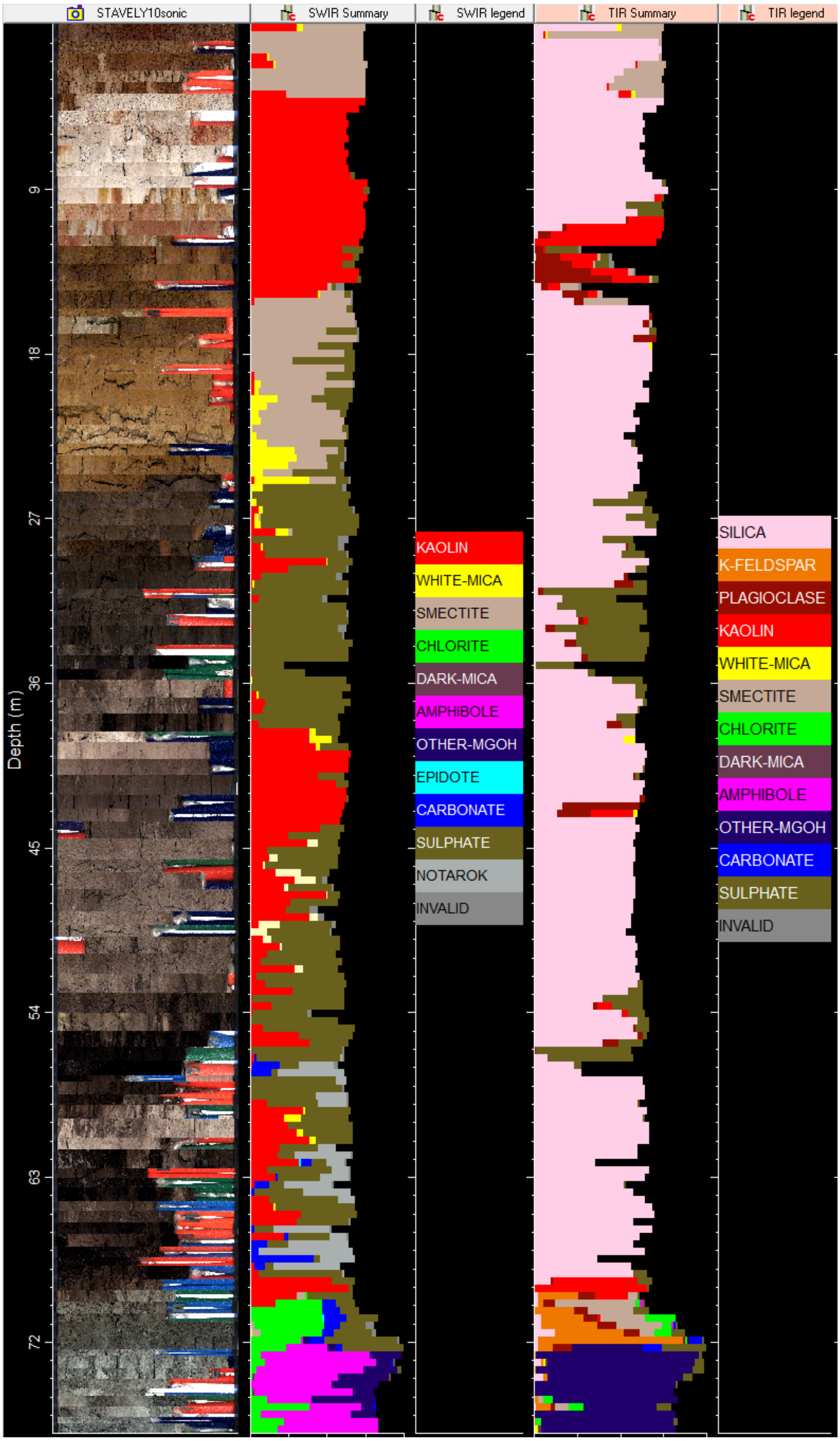

Figure 6. Extract from The Spectral Geologist software: "Hole" screen - from left to right, are: Depth (m), colour tray images (coloured sections are core packing noodles), main SWIR mineral group identified (SWIR Summary) the SWIR mineral group legend, main TIR mineral group identified (TIR summary), the TIR mineral group legend.

Comparison to geophysics

Preliminary comparison and analysis of the HyLogger™ results with the pre-drilling and down-hole geophysics show promising correlations, suggesting that methods using very different physical properties on different material (i.e. down-hole onsite geophysics versus spectral absorption of core in trays) provide consistent information about depth to basement. The HyLogger's™ SWIR mineralogy from the sonic and diamond core indicates elevated kaolinite sample counts (~70%) at the top of basement that gradually decrease with depth. This is correlated with interpretation of a weathered layer in the refraction seismic survey from the Stavely drill site locations (Meixner *et al.,* 2016). Kaolinite, as an indicator of weathering depth, indicates that the refraction data has successfully predicted a weathered layer at the top of basement, and that the HyLogger™ spectral results can be validated using a separate physical property measurement.

In addition, the geophysical cover thickness prediction at STAVELY09 overestimated the cover thickness by 42 m, or 32 m when considering the uncertainty range of the cover thickness estimate at this site (Meixner *et al.,*2016). Downhole density logs, however, show no jump in the density value at the cover/basement interface. Therefore the top 30 m of the intersected volcanic basement rocks appear to have the same density as the overlying sediments before density gradually increases, indicating that the top interval of the basement is highly weathered. This interpretation is supported by the hyperspectral data from the sonic and diamond core for STAVELY09 that show elevated SWIR sample counts (~70%) for kaolinite at 99.5 m - the top of the volcanic basement rocks - before decreasing to 0% at 128 m. This cross-correlation with the HyLogger™ data indicates that the refraction method at STAVELY09 has successfully predicted the depth of the transition to higher density and, therefore, a higher velocity unweathered basement.

Conclusions

The Stavely Project cover sampling program has amassed over 1000 ~350 g samples collected from the sonic cores, available from GA for further research. The cores themselves present a stratigraphically continuous and detailed archive of Murray Basin sands and many other materials, and are stored at the GSV core library in Werribee, Victoria. The HyLogger data is a versatile, data-rich and accessible digital record, which along with the project reports, palynological data, pore-fluid samples, geophysical data and additional upcoming data releases, comprises a comprehensive public resource which it is hoped will be used in future research by students and others interested in developing cover and mineral systems studies in the region.

Acknowledgements

GSV, GSSA (Steve Hill, Alan Mauger and Sam Williams), Carsten Laukamp (CSIRO) and Jon Clarke are gratefully acknowledged for their support and contributions to this project. Thanks to Patrice de Caritat and Ian Roach for helpful reviews of this document. This paper is published with the permission of the CEO, Geoscience Australia.

References

LAWRIE, K.C., BRODIE R.S., TAN, K.P., GIBSON, D., MAGEE, J., CLARKE, J.D.A., HALAS, L., GOW, L., SOMERVILLE, P., APPS, H.E., CHRISTENSEN, N.B., BRODIE, R.C., ABRAHAM, J., SMITH, M., PAGE, D., DILLON, P., VANDERZALM, J., MIOTLINSKI, K., HOSTETLER, S., DAVIS, A., LEY-COOPER, A.Y., SCHONING, G., BARRY, K. AND LEVETT, K. 2012. BHMAR Project: Data Acquisition, processing, analysis and interpretation methods. Geoscience Australia Record 2012/11. 804p.

MEIXNER, A.J., NAKAMURA, A., CZARNOTA, K., GORBATOV, A., MCALPINE, S.R.B., NICOLL, M.G., GOODWIN, J.A., AND SIMPSON, R. in prep. Regional geology and mineral systems of the Stavely region, western Victoria. Data release 4 – Pre-drilling geophysics. Record 2016/xx. Geoscience Australia, Canberra.

ROACH I.C., BLEWETT R.S., CZARNOTA K., CARITAT P. DE, MCPHERSON A.A., MEIXNER A.J., NEUMANN N., SCHOFIELD A., THOMAS M. AND WILFORD J. 2016. Regolith studies and the UNCOVER Initiative at Geoscience Australia. *This volume*.

SCHOFIELD, A., CAYLEY, R.A., BARTON, T., TAYLOR, D., NICOLL, M. & CAIRNS, C., 2015. Regional geology and mineral systems of the Stavely region, western Victoria: Data release 1 - Stratigraphic drilling field data. Record 2015/013. Geoscience Australia, Canberra. http://dx.doi.org/10.11636/Record.2015.013

SCHOFIELD, A*., et al*. in prep. Mineral systems of the Stavely region, western Victoria. Geoscience Australia, Canberra.

THOMAS, M., SCHOFIELD, A., GORDON, G., DUNCAN, R. AND HAYDON, S., 2015. Regional geology and mineral systems of the Stavely region, western Victoria: Data release 2 – HyLogger data and catalogue. Geoscience Australia, Canberra. Record 2015/27. Online: http://www.ga.gov.au/metadata-gateway/metadata/record/gcat_84572.

VANDENBERG, A.H.M., WILLMAN, C.E., MAHER, S., SIMONS, B.A., CAYLEY, R.A., TAYLOR, D.H., MORAND, V.J., MOORE, D.H. AND RADOJKOVIC, A. 2000. The Tasman Fold Belt system in Victoria: geology and mineralisation of Proterozoic to Carboniferous rocks. Geological Survey of Victoria Special Publication. Department of Natural Resources and Environment, Melbourne.

Recognition of geochemical footprints of mineral systems at the regional to continental scales

Patrice de Caritat[1], Phil Main[1], Eric Grunsky[2] and Alan Mann[3]

[1]Geoscience Australia, GPO Box 378, Canberra, ACT 2601, Australia
[2]Department of Earth and Environmental Sciences, University of Waterloo, Waterloo, Canada N2L 3G1
[3]Geochemical Consultant, PO Box 778, South Fremantle, WA 6162, Australia

Multivariate statistical analysis was applied to surface regolith geochemical data obtained by the same chemical digestion method in (1) the southern Thomson region of northern New South Wales/southern Queensland, and (2) across the continent (National Geochemical Survey of Australia). Despite contrasting scales and sample densities, interesting parallels between the two study areas were observed. (1) The composition of Principal Component 1 (PC1), which explains the most variation in each dataset, is almost identical at the regional and continental scales (Ca-Sr-Cu-Au association as one end-member; REEs-Th as the other). (2) The spatial patterns of PC1 in both studies are surprisingly compatible, given the considerable differences in scales and data densities. (3) A geochemical vector developed by a local explorer and our statistical analysis have independently yielded a similar geochemical indicator (PC1 above), one that is a proven empirical vector to mineralisation on the ground and, additionally, that statistically accounts for the most variability in the data. (4) If the Ca-Sr-Cu-Au association is indicative of Cu-Au mineralisation in the southern Thomson region, as suggested by local exploration results, then a number of areas with this same characteristic geochemical fingerprint are highlighted and are potentially worthy of further investigations, both at the regional scale and at the national scale. We conclude that in terms of the UNCOVER initiative, this study shows that potentially valuable information is held within the geochemical composition of surface transported regolith, allowing discrimination between more and less prospective regions and districts.

A preliminary investigation in to pedogenic effects on rare earth element concentrations in Victorian soils

Oliver Gore, Vanessa Wong, Sasha Wilson, Simon Jowitt[1]

[1]School of Earth, Atmosphere and Environment, Monash University; Wellington Rd Clayton, VIC 3800

Introduction

Rare earth elements (REE) are a group of 17 metals that include the lanthanides, Sc and Y (IUPAC, 2005). These are often grouped into the light rare earth elements (LREE: La-Eu), heavy rare earth elements (HREE: Gd-Lu) and occasionally the medium rare earth elements (MREE: often Sm-Dy). The REE are critical for many modern technologies including consumer electronics, medicine and communication. However, a combination of increasing global demand for REE and concerns on their security of supply means that alternative sources of these critical metals may need to be found.

Several soil- and regolith-hosted REE resources have already been identified, including heavy mineral sand deposits in the Wimmera region of western Victoria (Weng *et al*., 2015), alluvial or placer deposits in the Northern Territory (Crossland, 2013), ionic adsorption clay deposits in southern China (Weng *et al*., 2015), development of REE-enriched regolith over highly enriched lithologies (Jaireth *et al*., 2014), and anthropogenic REE enrichment such as in mine tailings (Weng *et al*., 2015).

One of the major controls on the concentrations of the REE in soils is the abundance of these elements in the parent material, as the majority of REE concentrations are largely inherited rather than acquired. Enrichment of REE in overlying soils and regolith compared to common protolith has been identified in several studies. For example, Mongelli *et al.,* (2013) found that LREE elements were enriched in subsoils developed over volcanic rocks. REE were also enriched by 2-3 times in subsoil above a Granodiorite (Nesbitt and Markovics, 1997). Furthermore Ce has been found to be enriched up to 12 times above protolith in a granite weathering profile (Taunton *et al*., 2000).

The mobilisation of REE in regolith results in the distribution patterns that are identified. Factors that control mobilisation during weathering include distribution of REE in protolith minerals and their resistivity to weathering. Dissolution of easily weathered accessory minerals like apatite and allanite can deplete upper horizons of REE (Braun *et al*., 1993) whilst weathering of resistant minerals can result in HREE enriched horizons. The pH of the soils can also effect mobility, whereby acidic conditions in soils tend to increase REE dissolution whereas alkaline conditions favour REE fixation (Laveuf and Cornu, 2009).

Weathering of granitic parent material can also lead to relative enrichment of the MREE, with the REE largely adsorbed to clay minerals. These clay minerals can include kaolinite and amorphous Fe oxides (Compton *et al*., 2003). Therefore, as most soil profiles increase in clay content with depth, REE can be leached from upper soil horizons, resulting in enrichment in lower soil horizons due to adsorption at depth to clay minerals (Compton *et al*., 2003).

Accessory minerals in the solum or parent material, such as P-bearing minerals, can influence the processes of enrichment and depletion. REE concentrations are frequently positively correlated to phosphates and P-bearing minerals (e.g., Peng *et al*., 2014). Weathering or dissolution of these less resistant phosphate-minerals such as apatite is likely to release the LREE, whereas the HREE are likely to reside in more resistant minerals such as anatase, monazite, sphene, ilmenite, rutile and zircon (Aide and Smith-Aide, 2003).

Although proximal carbonatite-related regolith material is already a key REE resource, it is likely that soils and regolith material developed from other REE-enriched material may have the potential to host economic concentrations of the REE. REE-enriched lithologies such as the alkaline potassic-to-ultrapotassic volcanics and intrusives of the Newer Volcanics in Victoria has the potential as parental materials for REE-enriched regolith and soil material.

Fe and Mn oxides can scavenge REE via sorption processes, resulting in REE enrichment with the formation of Fe/Mn oxides in the regolith profile (Laveuf and Cornu, 2009). Amorphous Fe oxides can provide a number of sites for adsorption, which preferentially sorb LREE compared to HREE, resulting in enrichment in LREE (Compton *et al*., 2003). However, the REE economic enrichment potential of soils other than laterites and of soils formed above, more common, low to moderately REE-enriched protoliths remains largely unexplored.

This study aims to identify the relationships between the regolith and protolith in terms of REE concentrations in Victoria. Specifically, the study will determine i) the REE concentrations of the regolith relative to the protolith, and therefore, if enrichment occurs, ii) where enrichment occurs in the regolith profile, and iii) determining the effects of pedogensis on REE enrichment

Materials and Methods

Site Description

Four sites were sampled in Victoria, southern Australia; Lysterfield Granodiorite (LG), Lake Purrumbete Maar (PB), and the Victoria Valley Granite (VVG) and the Western Aegerine Granite (WAG) units of the Victoria Valley Batholith (Fig. 1).

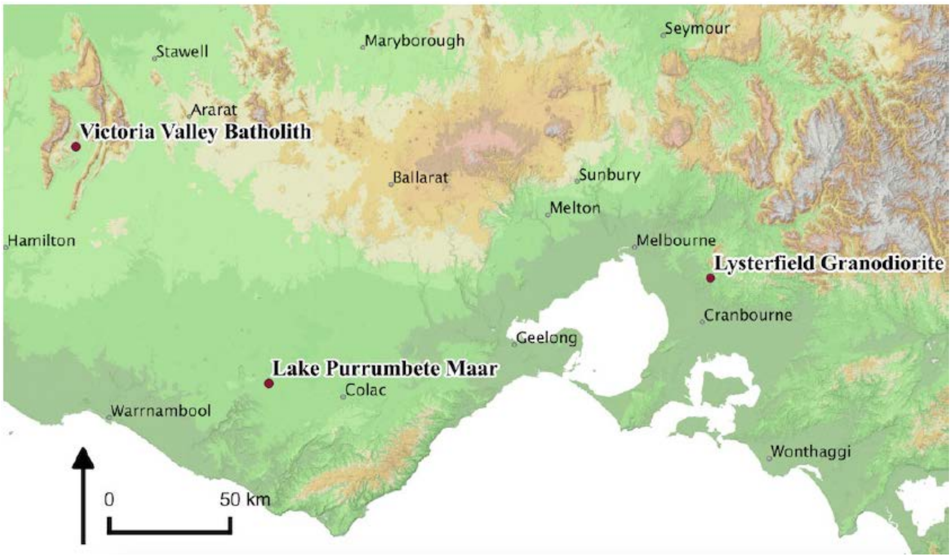

Figure 1. Location of the field sites

The LG site was located near the crest of a hill with a moderate slope and was mostly cleared of native vegetation. The major soil unit reported over the LG are Brown Chromosols (Macmillan *et al*., 1997; Isbell, 2002), which contain loam topsoils over sandy to medium clay subsoils that diffusely transition to weathered granodiorite (Macmillan *et al*., 1997). The LG soils are slightly acidic with low water holding capacity with low nutrient concentrations (Van de Graaff and Wootton 1996; Macmillan *et al*., 1997).

Lake Purrumbete Maar (PB) is a Pleistocene eruption sequence within the Newer Volcanics Province (NVP) of South East Australia. The maar is mostly alkaline, nepheline-normative and basanitic with some randomly distributed nepheline-normative trachybasalts (Jordan *et al*., 2015). All of the PB volcanics are LREE-enriched and are free of Eu anomalies with La concentrations between 73.2-103.1 mg/kg (Jordan *et al.,* 2015). Slight Ce anomalies at the base of the deposit suggest slight alteration or assimilation of altered material in these samples prior to soil formation (Jordan *et al*., 2015). The Purrumbete Maar lake is surrounded by undulating rises. The soils are developed on scoria and ash ejected from the maar and are shallow to moderately deep, friable gradational soils that are often stony. The LG field site was situated on small stony hills with sparse vegetation.

The Victoria Valley Batholith is an A type granitic batholith emplaced in the Grampians-Stavely Zone during the early Devonian (~396 Ma) (Hergt *et al.* 2007). Both VVG and WAG have large negative Eu anomalies. VVG contains between 37.0-44.7 mg/kg La, and WAG containing much higher REE enrichment of 80-300 mg/kg La (Hergt *et al.*, 2007). The soils developed over the Victoria Valley Granite are predominately Tenosols, which are characterised by weak textural separation in the profile (Baxter and Robinson, 2012; Isbell, 2002). VVG and WAG field sites were situated in native woodland. The VVG site was located on a shallow slope and the WAG on a moderately inclined hillside.

Field sampling and analysis

Soil and rock samples were collected from each site described above. Soil was sampled using a hand auger until bedrock was reached. Rock samples were collected from nearby outcrop where possible for geochemical analysis.

Soil samples were crushed and sieved through a 2 mm sieve and pH was determined on 1:5 soil:water extracts. Soil and rock samples were milled to a fine powder in a tungsten carbide mill prior to X-Ray Diffraction (XRD) analysis. Major and trace elements were determined following digestion by aqua regia. Major elements were determined by inductively coupled plasma-atomic emission spectroscopy (ICP-AES) and trace elements, including REE, were determined by inductively coupled plasma-mass spectroscopy (ICP-MS).

Results and Discussion

Total REE content decreased relative to the protolith during the formation of all soil profiles suggesting that enrichment does not necessarily occur during pedogenesis. The surface was the most depleted of all profiles, though there were sections with less depletion (Fig 2), indicating greater controlling pressures occurring on the surface. Surface soils of other studies show high levels of depletion, which is likely to be the result of rainfall, which is slightly acidic, infiltrating in to the profiles. Similarly, all of the profiles analysed were weakly acidic, which increases the mobilisation potential of REEs, resulting in leaching and loss of dissolved REE.

In the LG and PB soils, Al_2O_3 and total REE concentrations were positively correlated, suggesting that REE are associated with clay minerals, with the relationship stronger in LREE and MREE compared to HREE. Similarly, REE concentrations also showed the same correlations with Fe_2O_3 as Al_2O_3. However, the absence of Fe-oxides in XRD suggest they are present at low concentration and that clay, not Fe-oxides, are responsible for this pattern. Furthermore, Ce/Ce* and Fe_2O_3 were negatively correlated, contrary to positive associations found in other studies (Laveuf and Cornu, 2009). However, further research is required to elucidate the relationship between REE concentrations and particle size in conjunction with quantitative XRD.

Summary

REE concentrations in LG, WAG and VVG soils were most depleted in the surface soils and showed less depletion lower in the profile while HREE fractionation increased towards the surface. Conversely, REE concentrations in the PB soils showed depletion which minimal variation with depth. Areas of high REE content were associated with high Al concentration which was most likely related to clay content. HREE fractionation is most likely driven by retention of zircon, and therefore, further research is required on the retention of zircon as a potential exploration target for HREE in weathered soils

References

AIDE, M., SMITH-AIDE, C., 2003. Assessing Soil Genesis by Rare-Earth Elemental Analysis. *Soil Science Society of America Journal*, **67**. 1470-1476.

BAXTER, N. AND ROBINSON, N. 2012 A Land Resource Assessment of the Glenelg-Hopkins region. *Agriculture Victoria*

BRAUN, J.-J., PAGEL, M., HERBILLN, A., ROSIN, C., 1993. Mobilization and redistribution of REEs and thorium in a syenitic lateritic profile: A mass balance study. *Geochimica et Cosmochimica Acta* **57**, 4419-4434.

COMPTON, J.S., WHITE, R.A., SMITH, M., 2003. Rare earth element behavior in soils and salt pan sediments of a semi-arid granitic terrain in the Western Cape, South Africa. *Chemical Geology*, **201**. 239-255.

CROSSLAND, 2013. Charley Creek Rare Earths Scoping Study Results, Crossland Strategic Metals Ltd. (Crossland), Sydney, Australia. Available from http://www.crosslanduranium.com.au/uploads/resources/ASX_Release_Charley_Ck_scoping_Study_15_Apr_13_Final.pdf, accessed 07/01/16

HERGT, J., WOODHEAD, J., AND SCHOFIELD, A. 2007. A type magmatism in the Western Lachlan Fold Belt? A study of granites and rhyolites from the Grampians region, Western Victoria. *Lithos*

ISBELL R. 2002 The Australian Soil Classification. CSIRO Publishing, Melbourne.

JAIRETH, S., HOATSON, D.M., MIEZITIS, Y. 2014. Geological setting and resources of the major rare-earth element deposits in Australia Ore Geology Reviews. **62**, 72–128.

JORDAN, S.C., JOWITT, S.M., AND CAS, R.A.F. 2015. Origin of temporal - compositional variations during the eruption of Lake Purrumbete Maar, Newer Volcanics Province, southeastern Australia. *Bulletin of Volcanology* **77**, 1–15.

LAVEUF C. & CORNU S. 2009 A review on the potentiality of Rare Earth Elements to trace pedogenetic processes, *Geoderma,* vol. 154, no. 1–2, pp. 1-12.

NESBITT, H.W., AND MARKOVICS, G. 1997. Weathering of granodioritic crust, long-term storage of elements in weathering profiles, and petrogenesis of siliciclastic sediments. *Geochimica Et Cosmochimica Acta* **61**,1653–1670
MACMILLAN, M.J., SMITH A.L. AND BAXTER, N.M. 1997 *A land capability study of the Cardinia Shire.*Centre for Land Protection Research, Department of Natural Resources and Environment, Victoria
MONGELLI, G., PATERNOSTER, M., RIZZO, G., AND SINISI, R. 2014. Trace elements and REE fractionation in subsoils developed on sedimentary and volcanic rocks: case study of the Mt. Vulture area, southern Italy. *International Journal of Earth Sciences* **103**, 1125–1140.
PENG B., RATE A., SONG Z., YU C., TANG X., XIE S., TU X. & TAN C. 2014 Geochemistry of major and trace elements and Pb–Sr isotopes of a weathering profile developed on the Lower Cambrian black shales in central Hunan, China, *Applied Geochemistry,* vol. 51, pp. 191-203.
TAUNTON A. E., WELCH S. A. AND BANFIELD J. F. 2000.Geomicrobiological controls on light rare earth element, Y and Ba distributions during granite weathering and soil formation*. Journal of Alloys Compounds* **303–304**, 30–36
VAN DE GRAAFF, R., AND WOOTTON, C. 1996. *Melbourne Soils.* Landcare Notes.
WENG Z.*,* JOWITT S.M., MUDD G.M.*.* 2015 A Detailed Assessment of Global Rare Earth Element Resources: Opportunities and Challenges, *Economic Geology,* vol. 110, no. 8, pp. 1925-1952.

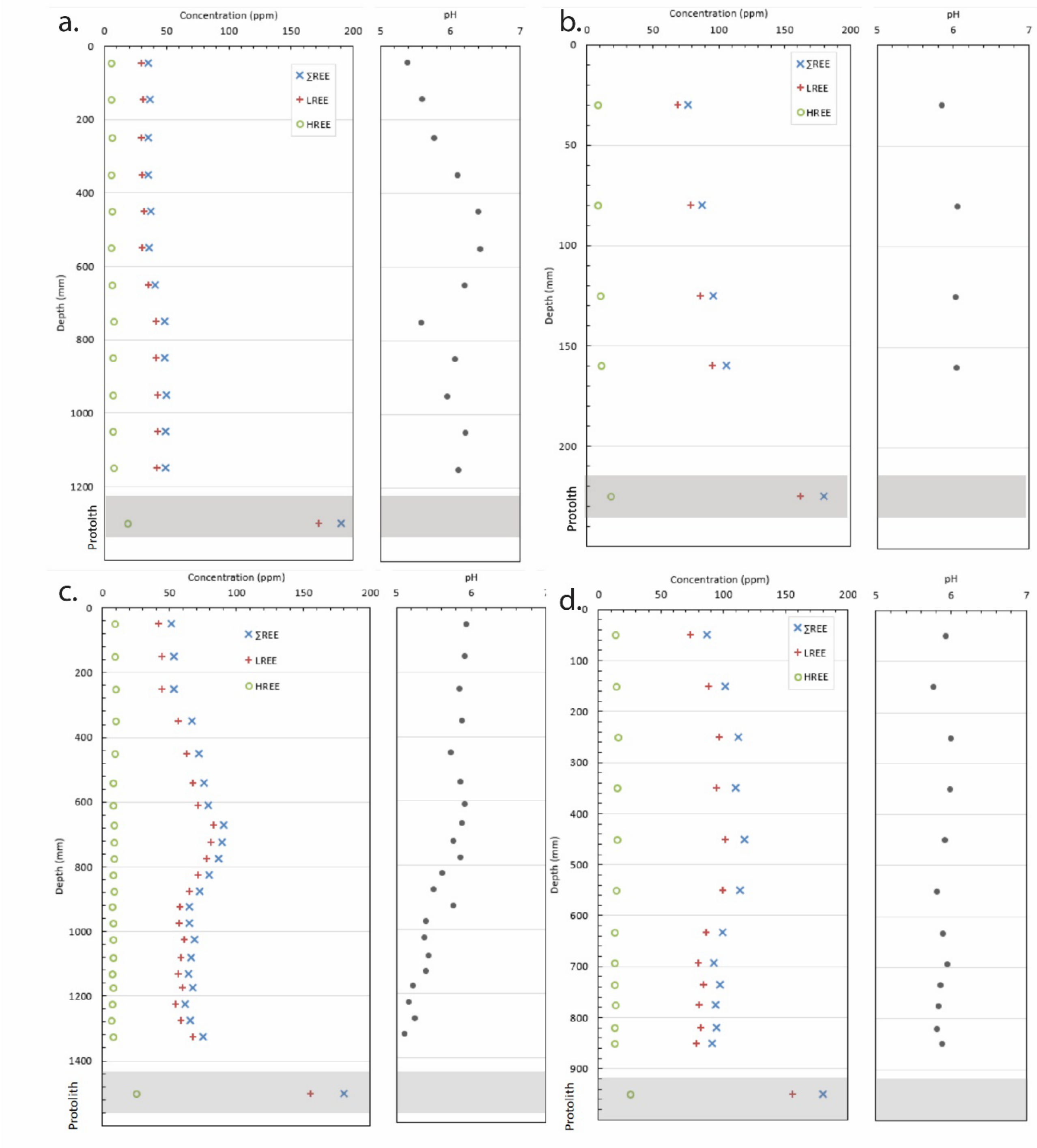

Figure 2. REE concentrations and pH of samples from a) Lysterfield Granodiorite (LG), b) Lake Purrumbete (PB), c) Victoria Valley Granite (VVG), and d) Western Aegerine Granite (WAG)

Regolith-landforms of the Balanggarra area, north Kimberley

N. de Souza Kovacs

Geological Survey of Western Australia, 100 Plain St, East Perth WA 6004

The Balanggarra 1:250 000 regolith-landform map was produced to complement a regolith geochemistry program carried out in 2013. The map covers 10 500 km^2 in the north Kimberley (Fig 1), and shows the distribution of different regolith types in a landform context, and their relationship to bedrock (de Souza Kovacs, 2015).

Identification of different regolith-landform units was carried out using remotely-sensed data and existing geological information. Published geological maps were used in conjunction with geophysical (radiometrics, magnetics) and satellite (Landsat™, ASTER) imagery to identify bedrock and regolith composition, whereas digital elevation models, orthophotos, and Google Earth® imagery were used to delineate landform types. Ground observations from the Geological Survey of Western Australia (GSWA) database and observations made during the regolith sampling program were used to refine interpretations.

Regolith-landforms distribution and composition

The bedrock geology comprises Paleoproterozoic and Mesoproterozoic mafic igneous and siliciclastic sedimentary rocks (Tyler *et al.*, 2012), with lithologies dominated by quartz-rich sandstones, siltstone and basalt. The Balanggarra landscape is predominantly erosional, dominated by 60% exposed bedrock, with 40% regolith cover. The regolith cover is approximately 10% residual/relict, and 30% depositional regolith. The distribution of different regolith-landform units in the area reflects the combination of bedrock composition and structure, physiography, and chemical and physical weathering processes. The regolith is compositionally similar to the bedrock, largely developed in situ, and shows little evidence of transport. Siliciclastic sedimentary rocks are the least weathered rocks, forming weakly dissected high plateaus. Although the regolith derived from siliciclastics sedimentary rocks is the most abundant type by area (about 27%), regolith profiles are quartz-rich, homogeneous and thin compared to the thicker and more compositionally diverse profiles developed on basalt. Regolith derived from basalt of the Carson Volcanics occupies 7% of the area, with ferruginous and aluminous duricrust developed on mesas and hilltops. Downslope from the mesas, the regolith consists of pisolite-rich colluvium occupying very low angle slopes and pediplains, and black soils on alluvial plains.

Alluvial and coastal regolith makes up 9 % of regolith and cannot be tied to any specific rock type.

Residual and relict regolith

Residual-relict regolith has been divided into four residual (i.e., in situ) units and one transported (i.e., relict) unit. Two of the residual units, a ferruginous duricrust and an aluminous duricrust, are found on the Carson Volcanics. These regolith profiles have an upper part composed of pisolitic ferruginous and/or aluminous duricrust up to 3 metres thick (Morris *et al*., 2015). Two other residual units are developed on quartz-rich sandstones, as an in situ ferruginous duricrust and a residual sand. The ferruginous duricrust is composed of ferruginised sandstone in a Fe-rich matrix, occupying the top of round sandstone hills; whereas the in situ residual sand is characterised by shallow profiles, made up of unconsolidated quartz-rich sand, ferruginised granules and sandstone clasts, occupying the highest parts of the sandstone plateau.

Transported relict regolith (ferricrete) is widespread in the project area, but occurrences are often too small to be shown at 1:250 000 map scale. This relict regolith is characterised by ferruginous indurated gravels often along drainage depressions. A more extensive relict unit is found adjacent to the Carson Volcanics over the King Leopold Sandstone, in the northwest of the mapped area. It may represent weathered Carson Volcanics which was subsequently transported and deposited on the sandstone.

Conclusion

Regolith accounts for approximately 40% of the Balanggarra area. Most of the regolith is compositionally similar to the underlying bedrock, indicating either in situ development of regolith or only short transportation. Scattered mesas of in situ aluminous and ferruginous duricrust probably represent remnants of a previously more extensive land surface. Regolith profiles are notably more extensive and well developed on basaltic rocks of the Carson Volcanics. The susceptibility of mafic volcanic rocks to chemical weathering has resulted in a broader and more subdued landscape compared to the relatively rugged plateaus, cliffs and gorges characteristic of areas of quartz-rich siliciclastic rocks. Quartz-rich siliciclastic rocks are less susceptible to chemical weathering resulting in thinner and compositionally less diverse regolith.

The Balanggarra regolith-landform map shows the distribution of different regolith types, and forms the basis for interpreting regolith geochemical data as well as providing a better understanding of the evolution of the Kimberley landscape.

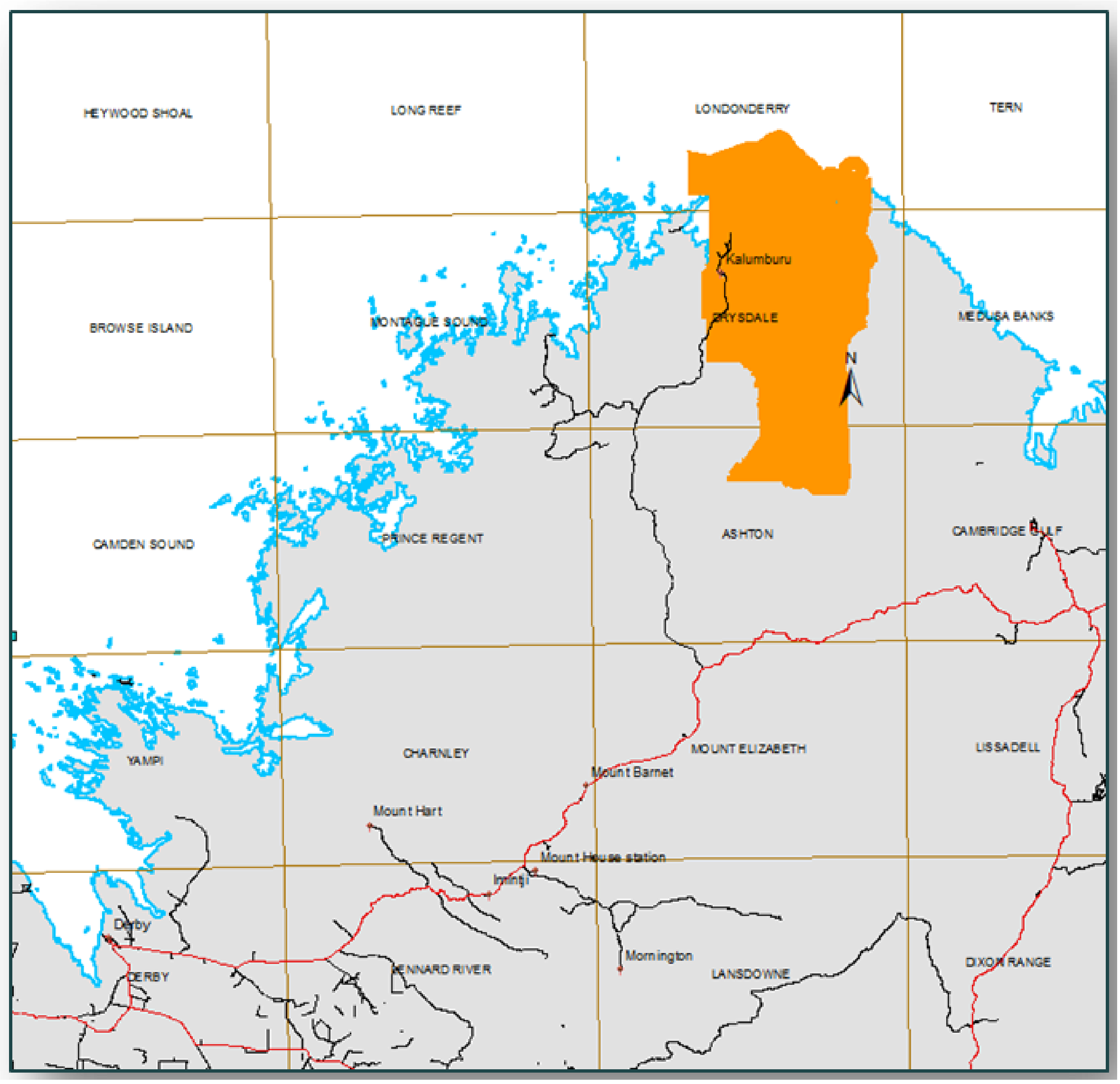

Figure 1: Location map of the Balanggarra area within the north Kimberley region.

References

DE SOUZA KOVACS, N 2015. Interpreted regolith–landform geology of the Balanggarra area, north Kimberley, in Regolith chemistry of the Balanggarra area, north Kimberley by PA Morris, AJ Scheib and N de Souza Kovacs: Geological Survey of Western Australia, Record 2015/9, Plate 1.

MORRIS, PA, SCHEIB, AJ AND DE SOUZA KOVACS, N 2015. Regolith chemistry of the Balanggarra area, north Kimberley: Geological Survey of Western Australia, Record 2015/9, 142p.

TYLER I. M., HOCKING R. M. & HAINES P. W. 2012. Geological evolution of the Kimberley region of Western Australia. *Episodes: Geological newsletter: International Union of Geological Sciences*, 35, issue 1 March 2012 Geology in the Oceania Region – Special Issue for the 34 IGC, Brisbane, August 2012, 298 – 306p

Tectonic Geomorphology in Australia: Earthquakes and more…

A. A. McPherson and D. J. Clark

Geoscience Australia, GPO Box 378, Canberra ACT 2601

Introduction

Tectono-geomorphic landscape features in Australia, many of which are neotectonic, can be interpreted in the context of long-term patterns of large earthquake occurrence, and used to inform contemporary earthquake hazard science. Such features often represent our only means of defining seismic source parameters such as fault slip-rate, large earthquake recurrence and magnitude. They therefore provide an avenue for extending the short historic catalogue of seismicity to timeframes commensurate with the slow strain accumulation rates characteristic of intraplate environments (Clark *et al*., 2012). In addition to supporting seismic hazard assessment, an analysis of tectono-geomorphic landscape evolution might also be used to inform studies in a range of other disciplines. Here we present the example of the Avonmore Scarp in the Campaspe River valley of north-central Victoria, a tectono-geomorphic (and neotectonic) feature which has implications not only for seismic hazard in central Victoria, but also for mineral and groundwater resources.

Geological and Geomorphic Setting

The northerly-draining Campaspe River valley is located to the east of Bendigo in central Victoria (Figure 1). Forming part of the Lachlan Fold Belt, the Paleozoic basement rocks of the area are generally highly deformed, steeply-dipping and are dominated locally by Ordovician turbidites of the Castlemaine Supergroup (Edwards *et al*., 1998; Wohlt & Edwards, 1999). The west-side up north-south trending Avonmore Scarp (Neivandt, 1990; Cherry & Neivandt, 1995) coincides, at least in part, with the Meadow Valley Fault (Figure 1) (Edwards *et al*., 1998; Wohlt & Edwards, 1999). Cayley *et al*. (2011) interpret this as one of several moderately west-dipping listric faults that link into a master thrust at depth. Gold-bearing structures at the Fosterville Mine (Figure 1) are recognised as a series of west-dipping faults breaching a parasitic fold on the western limb of an east-verging fold system. Related mineralised faults extend over a strike length of 14 km within the mining lease (Boucher *et al*., 2008). The Lockington deposits, buried under shallow basin cover to the north (Figure 1), exhibit a similar structural style but are additionally characterised by the presence of younger, shallowly west-dipping thrust faults which cross-cut both limbs of the fold system and which host Fosterville-style gold mineralisation (Boucher, 2008).

Consistent with others areas of the eastern Riverine Plain, the Paleozoic basement within the Campaspe River valley is covered by a Cenozoic Murray Basin sequence comprising carbonaceous sediments of the mid-Eocene to mid-Miocene Olney Formation (the upper member of the Renmark Group). The Renmark Group is overlain by alluvial deposits of the Mio-Pliocene Calivil Formation, which are in turn conformably overlain by aggraded floodplain deposits of the Plio-Pleistocene Shepparton Formation (Tickell & Humphrys, 1987; Brown & Stephenson, 1991). Arad & Evans (1987) suggest that the Renmark Group and Calivil Formation may be relatively indistinguishable in the area, and that the boundary between the Shepparton and Calivil formations may be ambiguous where coarse materials from the respective units interface. They estimate the total thicknesses for the Murray Basin sequences within the valley at 70-100 m in the south and 120-150 m in the north.

The geomorphic history of the Campaspe River valley is similar to other north-flowing (paleo-) drainage systems emanating from the Eastern Highlands, many of which were established by the early Cenozoic (Macumber, 1983; 1991). A paleo-valley 'deep lead' system similar to those identified locally and elsewhere in the Victorian central highlands (e.g. Canavan, 1988; Holdgate *et al*., 2006; Raiber & Webb, 2008) is recognised in the central part of the valley (Figure 1). The paleo-channel is filled with Renmark Group and Calivil Formation sediments, over which the Mio-Pliocene Coliban Basalt (Edwards *et al*., 1998) has flowed, and is in places interbedded with Shepparton Formation (Tickell, 1978; Tickell & Humphrys, 1987). The basalt, which on the basis of borehole driller's logs is in the order of 5-6 m thick, sits at a depth of around 25 m below ground surface near Goornong, and is imaged in magnetic data extending almost as far north as Elmore (Figure 1). The Huntly deep lead, a tributary of the Campaspe paleo-drainage system, sits within the Bendigo Creek valley to the west (Figure 1). The Huntly deep lead has historically been worked for alluvial gold (Canavan, 1988).

In a hydrogeological context, two dominant aquifers are recognised in the valley: (1) the Calivil/Renmark 'deep lead', and (2) shallower aquifers of the Shepparton Formation (Arad & Evans, 1987). They consider these as being hydraulically connected, with lateral [down-valley] flow in the 'deep lead' system dominating. Owing to extremely low hydraulic gradients, Arad & Evans (1987) support the assertion of Macumber (1983; 1991) that the Victorian part of the Murray Basin, including the Campaspe River valley, is hydrologically highly sensitive to perturbation.

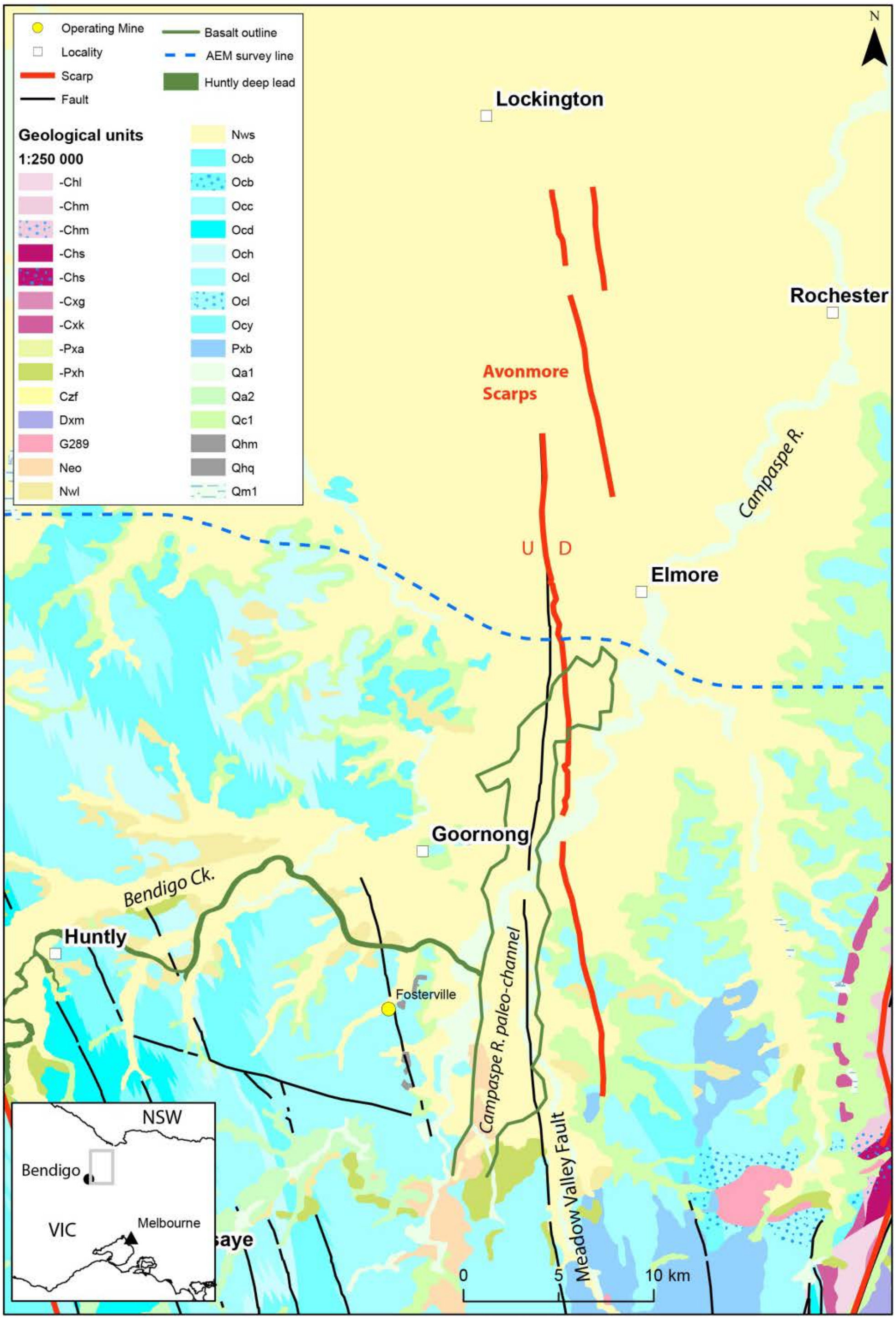

Figure 1: Location of the Avonmore Scarp within the Campaspe River valley in central Victoria. Mapped 1:250 000 geology shows the dominance of Cambro-Ordovician basement rocks which are covered in the central and northern parts of the study area by Cenozoic Murray Basin sediments (VandenBerg, 2009). The outline of the basalt-filled section of the Campaspe River paleo-channel is seen to coincide with the Meadow Valley Fault in this part of the valley, with the Huntly deep lead paleo-drainage entering from the west. The operating Fosterville Gold Mine and the locality of Lockington, near which another gold prospect has been identified, are indicated.

Investigations

Field reconnaissance in 2012 was followed by the acquisition of LiDaR digital elevation model (DEM) data in order to help characterise the generally low relief landscape. The DEM data reveal the extent and surface displacement of the Avonmore Scarp, which was revealed to be distinct from the mapped position of the Meadow Valley Fault. In addition, the data show a series of previously unrecognised *en echelon* 'scarplets' to the north-east of the main scarp (Figures 1 and 2), which approach the southern extension of the Cadell Scarp (South Echuca Scarp segment) approximately 10 km north-east of Rochester. The DEM also suggests the possibility that a footwall depression exists on the eastern side of the scarp (Figure 2) where the modern Campaspe River crosses the scarp. Lastly, the elevation data define a series of complex drainages associated with both the paleo-Campaspe River and paleo-Bendigo Creek systems (Figures 2 and 3). While further work is required, the apparent evolution of these systems is suggestive of a progressive re-direction to the north-west across the back of a tilt block associated with the Avonmore Scarp. This east to west diversion of streams has been documented elsewhere in the valley, with the Campaspe River prior streams known to have shifted from a north-east to a north-west course in association with the Echuca South scarp north-east of Rochester (Bowler & Harford, 1966).

Implications

The clear delineation of the scarp itself, and the newly identified *en echelon* steps to the north-east, has implications for strain sharing and the partitioning of slip from the controlling fault structures beneath. Follow-up investigations involving trenching of the scarp and dating of the faulting events are planned. This will allow for comparisons with the Cadell Fault, which is located only about 40 km to the north-east and has a multiple large earthquake event history (Clark *et al*., 2015). This proximity raises the question of whether all of these structures might share strain during a period of active faulting (Clark *et al*., 2012). In such a scenario the regional seismic hazard may be significantly increased.

From a mineral resources perspective, the shallowly west-dipping thrust faults identified at Lockington, which were considered to be the most recently active, are also the structures hosting mineralisation (Boucher, 2008), as seen by the anomalous bedrock Au values in Figure 4 (Arne *et al*., 2009). As such, identifying more recently mobile structures may provide further guidance in mineral exploration for Fosterville-type mineralisation.

While the fault structures themselves may have mineral resource implications, the associated landscape elements are also potentially important. The presence of a footwall depression to the east of the scarp would provide accommodation with the potential to have accumulated Au-bearing sediments (placer Au) from both the Campaspe River and Bendigo Creek systems. This is true not only for any footwall depression, but for the many paleo-drainages that criss-cross the plain, particularly those which have had any linkage to the historically prospective Bendigo Creek catchment (Figure 3).

Irrespective of any footwall depression, the presence of the scarp and underlying fault has additional connotations. With the 'deep lead' system being the dominant conduit within the valley, increases in hydraulic gradient across a bedrock faulting displacement has the potential to enhance recharge into the deep lead system. As a result the shallower Shepparton Formation aquifers may be less reliable, lower yielding and potentially with poorer water quality.

Conclusion

The tectono-geomorphic (and neotectonic) Avonmore Scarp has the potential to provide important insights into the seismic history of the underlying (and potentially linked) fault structures. Information on the structures within the basement underlying the Campaspe River valley also have the potential to inform mineral prospectivity under shallow cover and improve understanding of groundwater resource location and connectivity. Insight into the tectono-geomorphic evolution of the Campaspe River valley may shed light on distal footprints of known mineralisation in the nearby uplands developed via physical redistribution of alluvial gold-bearing materials. Such knowledge would further support informed groundwater management by elucidating potential preferred flow paths for both the 'deep lead' and Shepparton aquifer systems.

Knowledge about tectono-geomorphic landscape features has implications beyond those discussed here for the Campaspe River valley. The assessment and management of wetlanddependant ecosystems, groundwater and surface water management (including managed aquifer recharge), irrigated agriculture and CCS/CSG/tight gas exploration/extraction all stand to benefit from an improved understanding of the tectono-geomorphic evolution of the landscape. Geoscience Australia's Neotectonics Database holds information on more than such 300 features (http://www.ga.gov.au/earthquakes/staticPageController.do?page=neotectonics), many of which have very little known about them. By way of example, Figure 5 shows the Walgett Scarp, an apparent west-side up displacement which has disrupted and diverted drainage on the lower Namoi River in New South Wales. This feature may be akin to the uplifted terraces in Green Gully on the western side of the Cadell Fault in Victoria (Bowler & Harford, 1966; Clark *et al*., 2015).

Acknowledgements
This paper is published with the permission of the CEO, Geoscience Australia.

References

ARAD, A. & EVANS, R. 1987. The hydrogeology, hydrochemistry and environmental isotopes of the Campaspe River Aquifer System, north-central Victoria, Australia. Journal of Hydrology 95, 63-86.

ARNE, D.C., HOUSE, E., TURNER, G., SCOTT, K.M. & DRONSEIKA, E. 2009. Exploration for deeply buried gold deposits in northern Victoria: soil, regolith and groundwater geochemistry of the Lockington and Lockington East gold deposits. Gold Undercover Report 10: Victoria Department of Primary Industries.

BOUCHER, R.K. 2008. Stratigraphic controls on structures and mineralisation in central Victoria 4: Lockington. AIG News 94, 1-5.

BOUCHER, R.K., HITCHMAN, S.P. & ALLWOOD, K.J. 2008. Stratigraphic controls on structures and mineralisation in central Victoria 3: Fosterville. AIG News 93, 6-9.

BOWLER, J.M. & HARFORD, L.B. 1966. Quaternary tectonics and the evolution of the Riverine Plain near Echuca, Victoria. Journal of the Geological Society of Australia 13(2), 339-354.

BROWN, C.M. & STEPHENSON, A.E. 1991. Geology of the Murray Basin, southeastern Australia. Bureau of Mineral Resources, Geology & Geophysics Australia Bulletin 235, 430 p.

CANAVAN, F. 1988. Deep lead gold deposits of Victoria. Geological Society of Victoria Bulletin 62, 101 p.

CAYLEY, R.A., KORSCH, R.J., MOORE, D.H., COSTELLOE, R.D., NAKAMURA, A., WILLMAN, C.E., RAWLING, T.J., MORAND, V.J., SKLADZIEN, P.B. & O'SHEA, P.J. 2011. Crustal architecture of central Victoria: results from the 2006 deep crustal reflection seismic survey. Australian Journal of Earth Sciences 58(2), 113-156.

CHERRY, D.P. & NEIVANDT, R.W. 1995. A late Quaternary fault scarp on the Riverine Plain near Bendigo, Victoria: Geological Survey of Victoria Unpublished Report.

CLARK, D., MCPHERSON, A. & VAN DISSEN, R. 2012. Long-term behaviour of Australian Stable Continental Region (SCR) faults. Tectonophysics 566-567, 1-30. doi: http://dx.doi.org/10.1016/j.tecto.2012.07.004

CLARK, D., MCPHERSON, A., CUPPER, M., COLLINS, C. D. N., & NELSON, G. 2015. The Cadell Fault, southeastern Australia: a record of temporally clustered morphogenic seismicity in a low-strain intraplate region. In: A. Landgraf, S. Kuebler, E. Hintersburger & S. Stein (Eds.), Geological Society, London, Special Publication 432 'Seismicity, Fault Rupture and Earthquake Hazards in Slowly Deforming Regions'.

EDWARDS, J., WOHLT, K.E., SLATER, K.R., OLSHINA, A. & HUTCHINSON, D.F. 1998. Heathcote and parts of Woodend and Echuca 1:100 000 map area geological report. Geological Survey of Victoria Report 108, 212 p.

HOLDGATE, G.R., WALLACE, M.W., GALLAGHER, S.J., WITTEN, R.B., STAS, B. & WAGSTAFF, B.E. 2006. Cenozoic fault control on 'deep lead' palaeoriver systems, Central Highlands, Victoria. Australian Journal of Earth Sciences 53(3), 445-468.

MACUMBER, P.G. 1983. Interactions between groundwater and surface systems in northern Victoria. Ph.D., University of Melbourne, Melbourne.

MACUMBER, P.G. 1991. Interaction between groundwater and surface systems in northern Victoria. East Melbourne Department of Conservation and Environment Report, 345 p.

NEIVANDT, R. 1990. The geomorphology, sediments and soils of the mid Campaspe Valley, Victoria and relationships to groundwater recharge. B.Sc. (Honours), University of Melbourne, Melbourne.

RAIBER, M. & WEBB, J.A. 2008. Tectonic control of Tertiary deposition in the Streatham Deep-Lead System in western Victoria. Australian Journal of Earth Sciences 55, 493-508.

TICKELL, S.J. 1978. Geology and hydrogeology of the eastern part of the Riverine Plain in Victoria. Geological Survey of Victoria Report 1977/8, 73 p.

TICKELL, S.J. & HUMPHRYS, W.G. 1987. Groundwater resources and associated salinity problems of the Victorian part of the riverine plain. Geological Survey of Victoria Report 84.

VANDENBERG, A.H.M. 2009. Rock unit names in the Bendigo Zone portion of central Victoria, Seamless Geology Project. Geological Survey of Victoria Report 129.

WOHLT, K.E. & EDWARDS, J. 1999. Avonmore 1:50 000 geological sheet [map]. 1st Edition. Geological Survey of Victoria, Melbourne.

WOHLT, K.E. & EDWARDS, J. 1999. Avonmore 1:50 000 geological sheet [map]. 1st Edition. Geological Survey of Victoria, Melbourne.

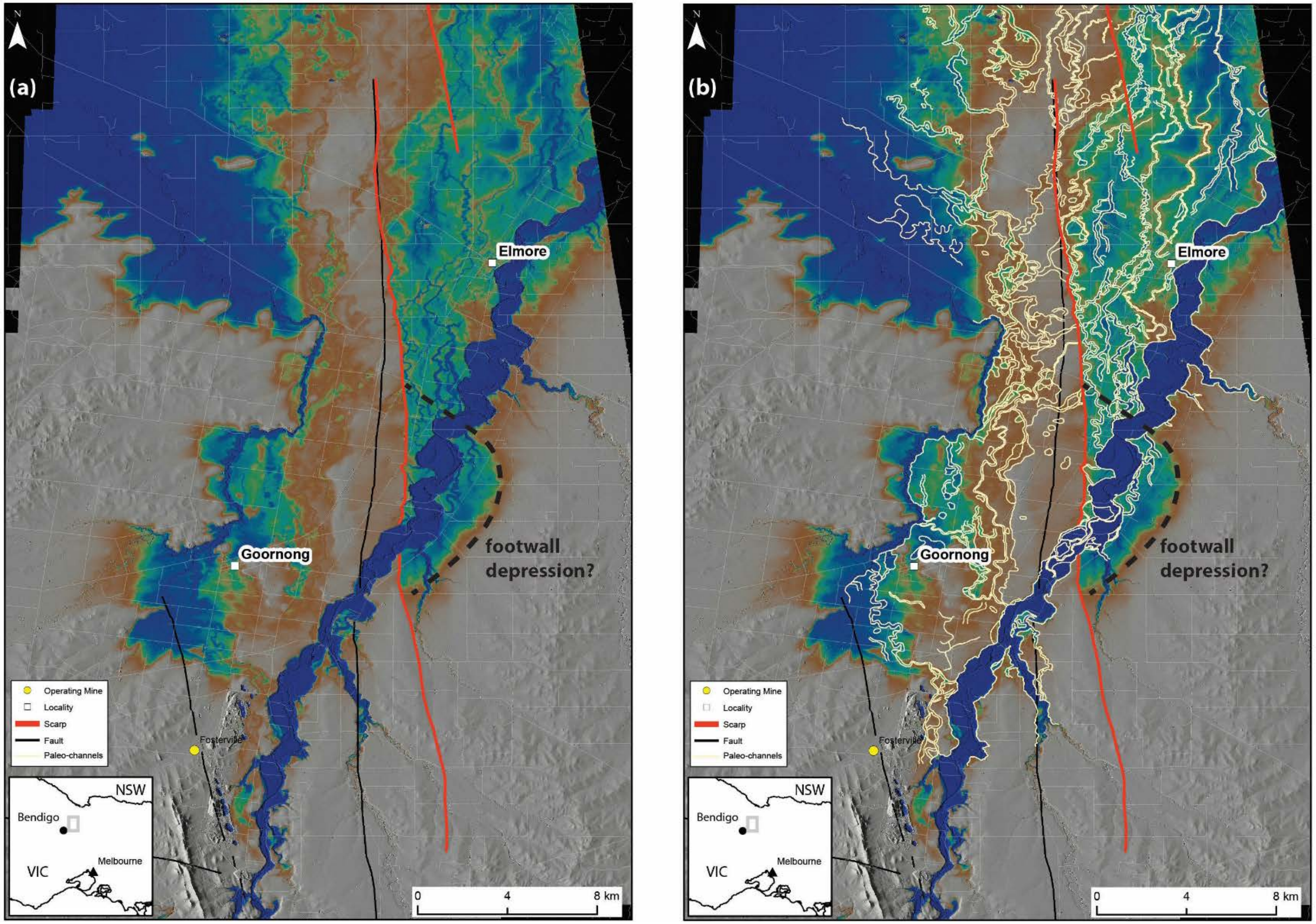

Figure 2: LiDaR 1 m digital elevation model (DEM) of the Campaspe River valley which has been tilted south to remove the gradient associated with the Campaspe River valley. **(a)** DEM showing surface expression of the Avonmore Scarp(s) and possible footwall depression east of the scarp; **(b)** as per (a) but with mapped paleo-drainage showing the multiple generations of westward drainage re-direction potentially related to episodes of movement on the fault.

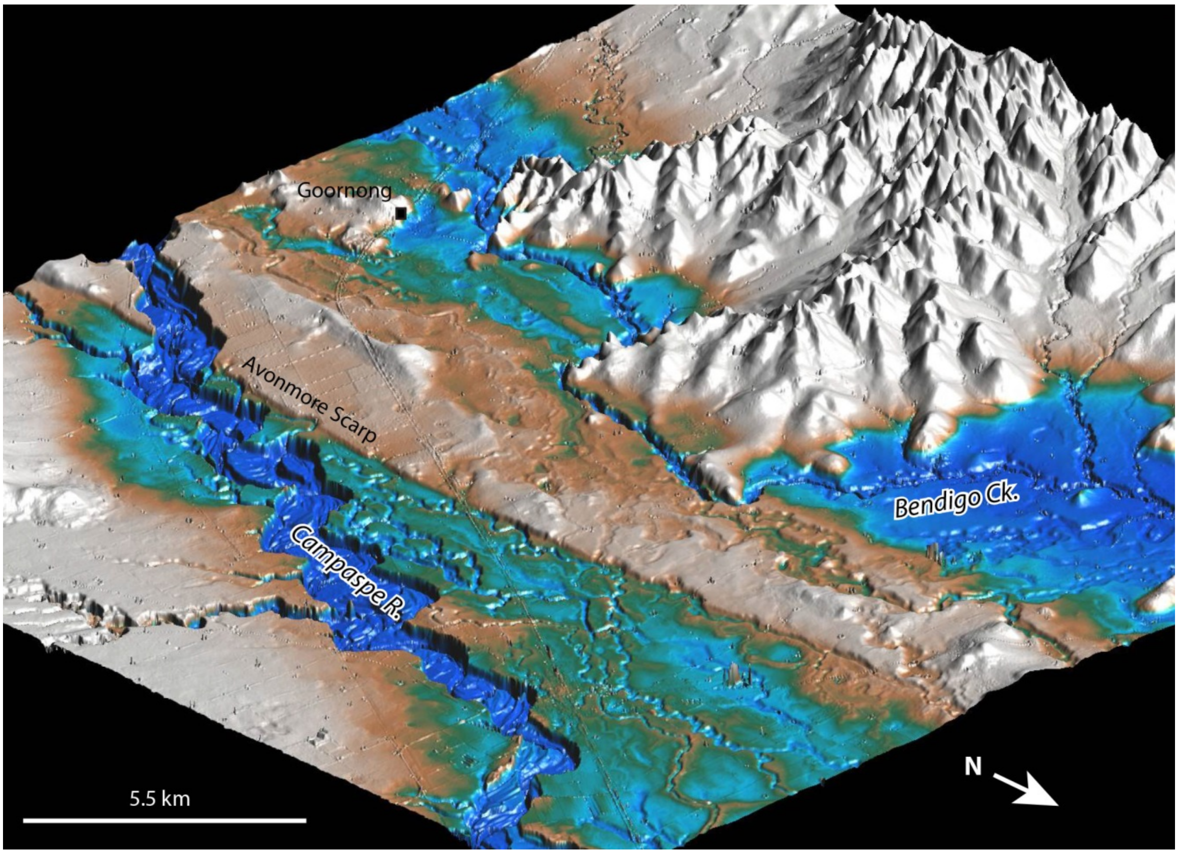

Figure 3: Vertically-exaggerated rendition (view looking south-west) of LiDaR data for the middle section of the Campaspe River valley showing part of the main Avonmore Scarp (running NW-SE) and the complex nature of both the Campaspe River and Bendigo Creek drainage (and paleo-drainage) systems.

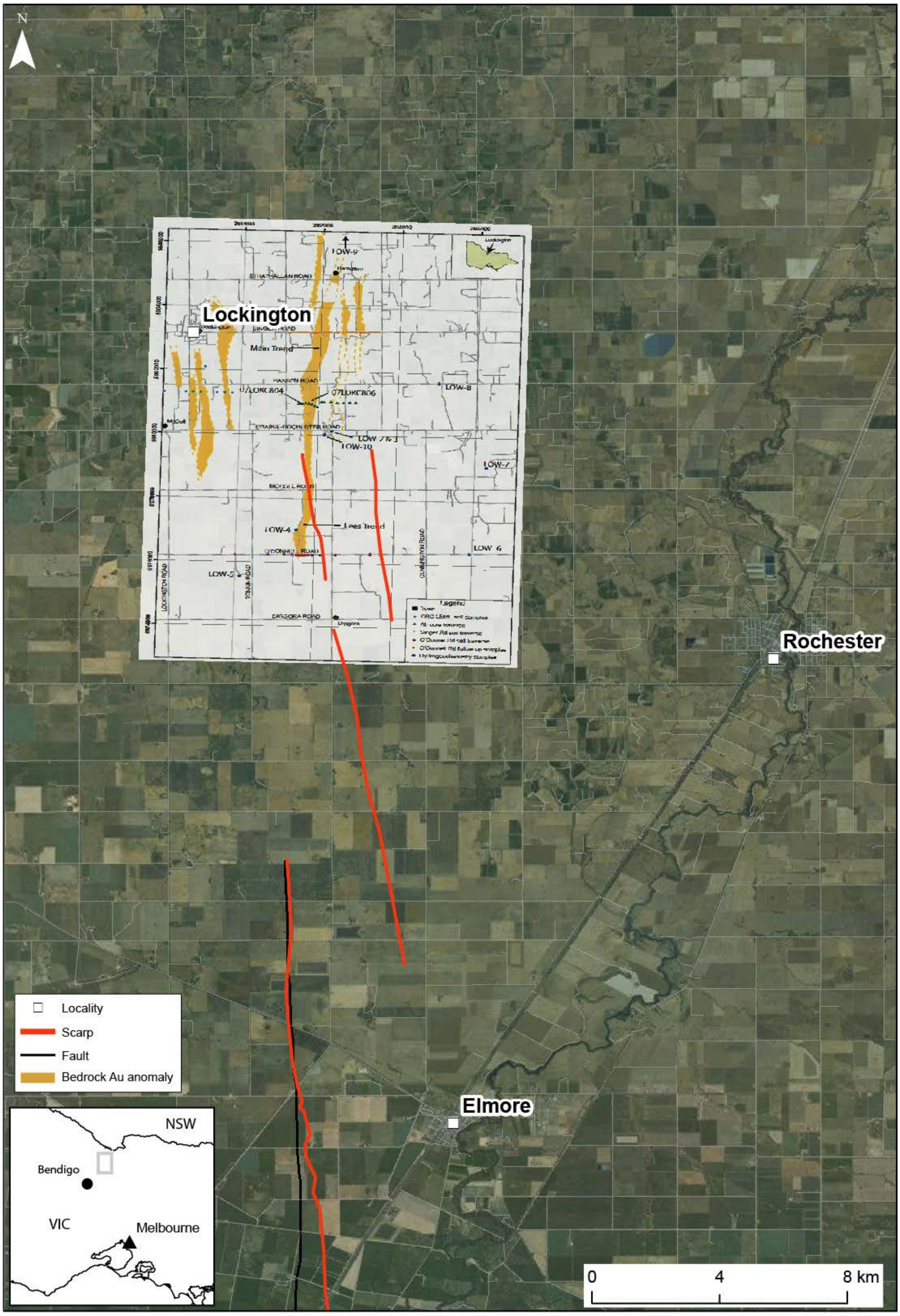

Figure 4: Location of anomalous bedrock Au values at prospects near Lockington (Arne *et al*., 2009) where shallowly west-dipping reverse faults are known to be the dominant hosts of mineralisation (Boucher, 2008).

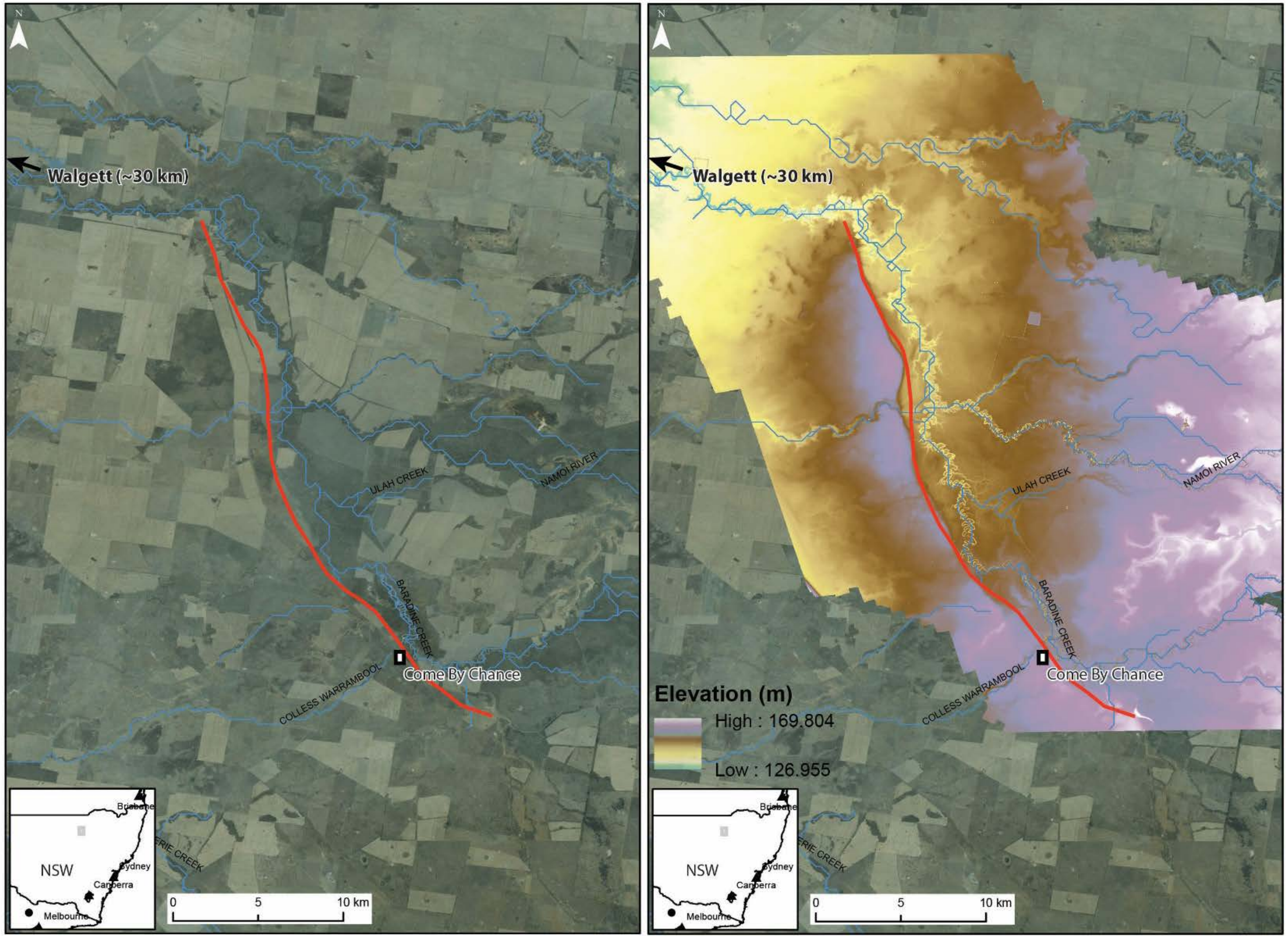

Figure 5: **LEFT**: Visible imagery of the lower Namoi River region east of Walgett (NSW) showing drainage diversion and capture of Baradine Creek and the Namoi River by a probable neotectonic fault scarp (red line). **RIGHT**: LiDaR 1 m DEM showing the west-side up displacement responsible for the drainage capture. Note the prominent westerly-draining channel in the middle of the scarp which has been abandoned by the uplift

Regional to district scale mineral footprints in the Capricorn Orogen interpreted from ASTER, soil geochemical and radiometric data

Carsten Laukamp[1]

[1] CSIRO Mineral Resources, Australian Resources Research Centre, 26 Dick Perry Avenue, Kensington, WA 6151, Australia.

Abstract

The combination of multiple surface geoscience data sets provides an opportunity for advanced characterisation of cover rocks, but also for identifying bedrock signatures and potentially mineral footprints of concealed mineral systems. Surface mineralogical and geochemical data, including ASTER imagery, GSWA's regolith geochemistry (Morris, 2005) and radiometric data, were collated to evaluate their potential for advanced regolith characterisation, mapping of bedrock lithologies and identification of mineral footprints potentially related to hydrothermal alteration. As suggested by complementary studies in the Capricorn Orogen (e.g. Lampinen et al., 2014; Wells et al., 2015), CSIRO's continental scale ASTER geoscience products are applicable for regional to district scale mapping of surface mineralogy and distinct lithologies. For example, the MgOH/Carbonate ASTER geoscience products help to trace Mesoproterozic tholeiitic dolerites that may have a genetic relationship to polymetallic deposits in the Capricorn Orogen and to discover previously unmapped occurrences of dolerites. The MgOH/Carbonate ASTER geoscience products are also sensitive to the occurrence of calcretes and limestones, which can be distinguished from the dolerites by a comparison with other ASTER geoscience products. To enhance the ability for spatially continuous mapping of dolerites, the green vegetation mask, normally applied to the publically available MgOH/Carbonate Group Content image (Cudahy et al., 2012), was relaxed. This resulted in improved mapping in areas where the previously applied masking removed most of the pixels (e.g. west of Abra). However, in other areas such as north of Abra, where dolerites were already identified by the continental scale ASTER geoscience products, the relaxation of the green vegetation masks led to dolerites being confused with vegetation. This can be partly overcome by using the MgOH/Carbonate composition map, which helps to distinguish vegetation from dolerites (and carbonate successions).

A comparison of the AlOH Group Composition maps with K radiometrics (Figure 1.) suggests the potential exists for identifying bedrock signatures in the Edmund Basin by tracing lithologies that

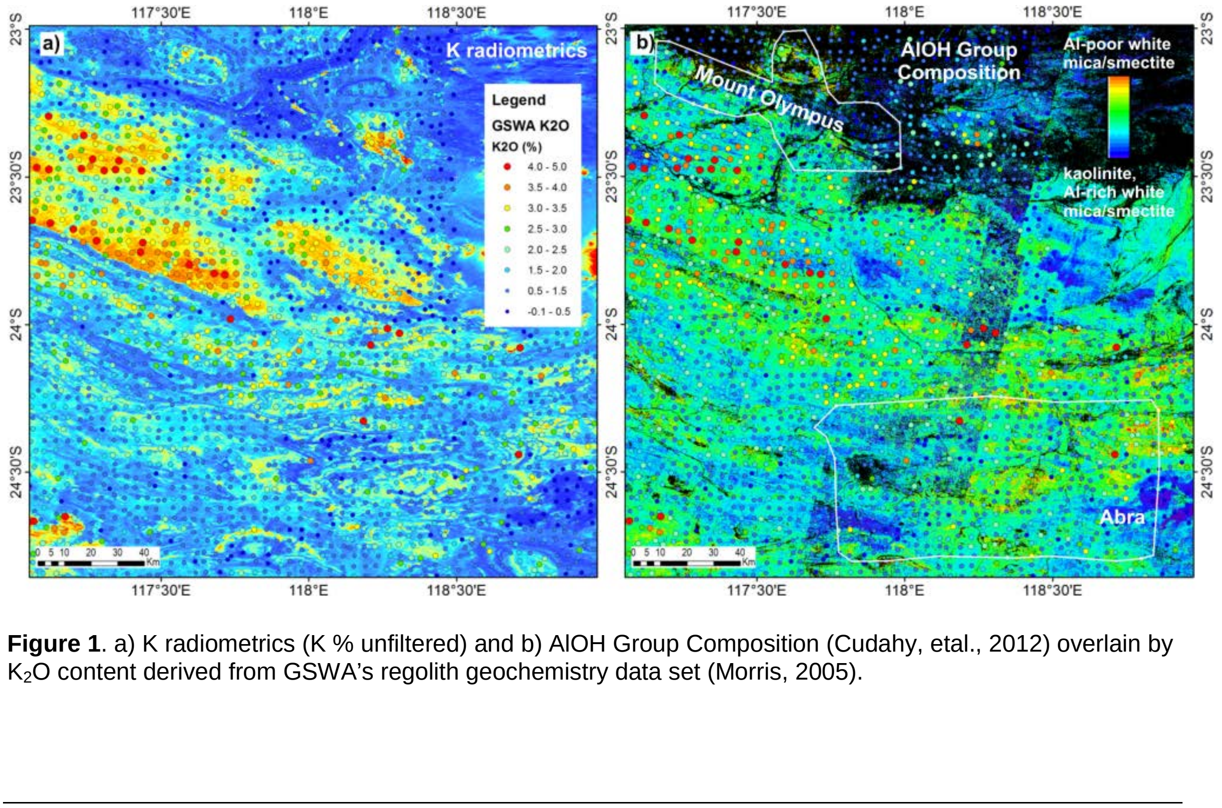

Figure 1. a) K radiometrics (K % unfiltered) and b) AlOH Group Composition (Cudahy, etal., 2012) overlain by K_2O content derived from GSWA's regolith geochemistry data set (Morris, 2005).

contain white micas. Both types of remote sensing data show good correlations from the regional to district scale. A preliminary comparison of the remote sensing data with K contents derived from GSWA's regolith geochemistry data set, supports the regional patterns of elevated K (K radiometrics) in areas with increased relative abundance of white mica and decreased kaolin abundance (AlOH Group Composition). However, on the local scale, the broad sampling pattern of the regolith geochemistry data set complicates any comparison with remote sensing data.

In summary, publically available surface geoscience data can greatly assist exploration in the Capricorn Orogen, by 1) advanced regolith characterisation, 2) identifying previously unmapped occurrences of lithologies that may be genetically linked to economic deposits, and 3) to trace bedrock signatures for improved geological mapping. Recent work on comparing the spatially comprehensive surface with subsurface geoscience data (e.g. HyLogging, AEM) in Western Australia (Laukamp *et al*., 2015; Wells *et al*., 2015) has demonstrated the potential for uncovering concealed stratigraphy and mineral footprints potentially related to hydrothermal alteration.

References

CUDAHY, T, CACCETTA, M, LAU, I, RODGER, A, LAUKAMP, C, ONG, C, CHIA, J, COLLINGS, S, RANKINE, T, FRASER, R, WOODCOCK, R, VOTE, J, WARREN, P, THOMAS, M, TYLER, I, MAUGER, A, CLOSE, D, JONES, M, ABRAMS, M 2012, Satellite ASTER geoscience map of Australia. Version 1. CSIRO Australia, Data Access Portal, https://data.csiro.au/dap. DOI: 10.4225/08/51400D6F7B335

MORRIS P.A. (2005). GSWA's Regional Regolith Geochemistry. http://www.dmp.wa.gov.au/6564.aspx

LAMPINEN, H., LAUKAMP, C., OCCHIPINTI, S., FIORENTINI, M., MCCUAIG, C., MILLER, J. (2014): Comparison of hyperspectral signatures and geochemistry in regolith samples to ASTER data. Edmund Basin, Capricorn Orogen, Western Australia.- CET Corporate Members' Day 2014. 4pp.

LAUKAMP, C., SALAMA, W., GONZÁLEZ-ÁLVAREZ, I. (2015): Proximal and remote spectroscopic characterisation of regolith in the Albany-Fraser Orogen (Western Australia).- Ore Geology Reviews, 73 (3), 540-554.

WELLS, M., LAUKAMP, C., HANCOCK, L. (2015): Integrated Spectral Mapping of Precious and Base Metal Related Mineral Footprints, Nanjilgardy Fault, WA.- CSIRO report EP155294, 88p.

About anatase

Tony Eggleton[1] & Graham Taylor[2]

[1]Research School of Earth Sciences, ANU, Canberra (tony.eggleton@anu.edu.au)

[2] University of Canberra (graham.taylor@canberra.edu.au)

Excluding detrital rutile and ilmenite, titanium in regolith is largely present as anatase. The solubility of titanium in regolith water is low, though not at all well constrained. Broadly it is thought to be least at mid-pH and rise towards the acid and alkaline ends (Knauss *et al*. 2001), much like aluminium but not like silicon which does not become more soluble at low pH.

Silcrete is a regolith formation characterized by a very high silica content, commonly >90% SiO_2 as quartz, and almost ubiquitously a few percent TiO_2 as anatase. An average of 170 silcrete analysis from the literature, confined to those having ≥ 90% SiO_2, shows these silcretes average 1% TiO_2. The question of the origin of this anatase has vexed geologists for years: is it detrital/eluviated anatase or was it precipitated from a solution? The distribution of anatase within silcrete admits in most instances of either interpretation; the anatase typically forms caps or coatings on the upper side of quartz grains suggesting gravity as a contributing agent. It is generally thought that titanium does not move far during mineral alteration.

Part of the answer may lie in assessing the source of the titania, and many studies have addressed this. (see e.g. Hutton *et al.* 1972, Milnes *et al.* 1992). The issue is clouded by the difficulty of distinguishing titania concentrated by subtraction of other components from titania introduced from elsewhere. In an attempt to contribute to this particular aspect, we compared the titania and zirconium content of typical silcretes of silica cemented stream sediments with that of Australian stream sediments from the de Caritat & Cooper (2011) collation of 1,320 samples. We find that the concentration factor from average sediment to silcrete is the same for Zr and TiO_2. Assuming that Zr in silcrete is all detrital we suggest that perhaps titania in such silcretes was, like the Zr, in the original sediment, not introduced from outside, as Hutton *et al*. (1972) concluded. Calculating the composition of the average stream sediment after subtraction of all soluble elements leaves 95.7% SiO_2, much as is in silcrete, with a silica concentration factor of 1.8, similar to that found for Ti and Zr. Does this tell us that the silica in silcrete is also derived from within the silcreted sediment?

As a second line of attack we have looked at the character of anatase in silcrete, its morphology and mode of aggregation. Images of anatase in silcrete show a morphology not unlike those seen as *de novo* crystals in weathered minerals and comparable to those formed in synthetic studies.

Taken together, our results suggest that anatase precipitates as a pure mass in some silcretes, but it co-precipitates with quartz in others. Either way, we feel confident to conclude that the anatase is precipitated between the quartz framework grains of silcrete, and is not washed in as particles.

References

DE CARITAT P. & COOPER M. 2011. *National Geochemical Survey of Australia: The Geochemical Atlas of Australia: Dataset*. Geoscience Australia, Canberra. http://dx.doi.org/10.4225/25/54CAB00B4C9AB

HUTTON J.T., TWIDALE C.R., MILNES A.R AND ROSSER, H. 1972. Composition and genesis of silcretes and silcrete skins from the Arcoona Plateau, South Australia. *Journal of the Geological Society of Australia* 19, 31-39.

KNAUSS K.G., DIBLEY M.J. AND SHAW, H.F. 2001. *Applied Geochemistry* 16, 1115-1128.Ti(IV) hydrolysis constants derived from rutile solubility measurements made from 100 to 300°C.

MILNES, A. R. AND THIRY, M. 1992. Silcretes. In: Martini I.P & Chesworth W. (eds) *Weathering, soils & paleosols.*, 349-377. Elsevier.

Landscape evolution of the Clarence River catchment:

Weird rivers and wild ideas

K.G. McQueen

Institute for Applied Ecology, University of Canberra, ACT 2601

The Clarence River catchment in northern New South Wales is the largest river system on the southeast coast of Australia. It has a total area of 22,400 km^2 with large gorges and deep valley systems on its western and southwestern margins. In the east the catchment is defined by a lowland fluvio-lacustrine, flood plain developed in two basins separated by a northerly trending ridge and marked by various anabranches and connected lagoons. Even a cursory examination of the catchment features suggests a remarkable complexity in its landscape evolution.

Features of the catchment

A key feature of the Clarence River catchment is a large, elongate erosional 'bowl' to the west and southwest of the main river, separating a coastal terrain and present coastline from the Great Divide (Figure 1). Within this area there is a northeast trending drainage network in the west and a northerly trending drainage in the south. Where this drainage intersects the Clarence River it is redirected to the southeast and then to the northeast before entering the Pacific Ocean. The eastern tributaries of the river are relatively short with west and southwest trends.

For most of its southerly direction the Clarence River (indigenous *Breimba*) closely follows the eroded western edge of the Mesozoic Clarence-Moreton Basin (Figure 2). Small, perched outliers of Triassic sediments indicate that this basin extended a short distance to the west before development of the present river channel. The river overlies Mesozoic sediments and Palaeozoic bedrock suggesting that its course has been superimposed from a Mesozoic cover. Typically there are large Quaternary sediment deposits flanking the river where it transects the Mesozoic sediments, but these are absent or minor where it cuts the Palaeozoic bedrock. Significant areas of Quaternary sediments are preserved around Tabulam, upstream from Grafton and in areas downstream from Grafton within the fault-bounded Grafton Trough.

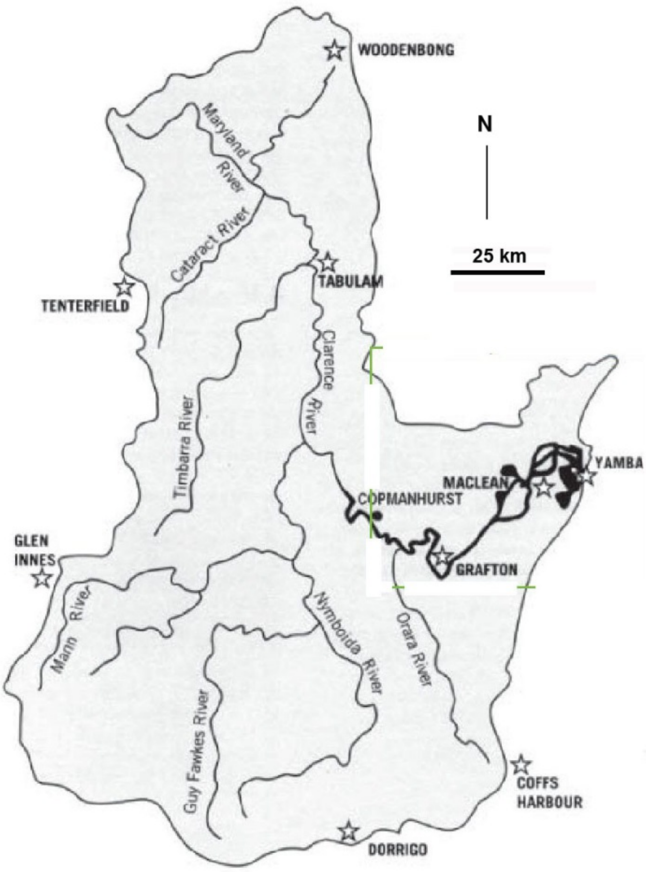

Figure 1: Area of the Clarence River catchment in north-eastern New South Wales showing the major rivers. The western boundary of the catchment marks the Great Divide in this region. Also shown are some of the towns within and around the catchment (modified from Independent inquiry into the Clarence River System: Final report. Healthy Rivers Commission of New South Wales. 1999).

The north-eastern boundary of the catchment is defined by the Richmond Range, probably developed by post-Cetaceous tectonism along reactivated basin structures and later Tertiary volcanism (O'Brien *et al.* 1994). Partly capping and to the east of this range are large areas of Miocene volcanic rocks, mainly basaltic lavas, of the eroded Tweed Volcano. This area contains the Richmond and Tweed River catchments developed during erosion of the shield volcano. North of the Clarence River catchment there are small scattered remnants of older Tertiary volcanic rocks representing the Focal Peak Volcano and west of these a larger area of basalts forming part of the Main Range Volcano (Figure 2; Ollier & Haworth 1994). The southern boundary of the catchment is defined by the Ebor Volcano, also of Miocene age (Figure 2, Ollier 1982; Ashley *et al*. 1995).

To the east, the catchment is bounded by the Coast Range, defined by Palaeozoic basement and up-faulted Mesozoic rocks (Figure 2). The lower Clarence River breaches a low range at Grafton and then flows northeast across the underlying Grafton Trough. After branching, the river passes through two narrow gaps in a ridge of resistant Kangaroo Creek Sandstone, the Maclean-Tyndale Ridge, and enters the ocean at Illuka-Yamba through a gap in the Coast Range. The lower floodplain is divided into two Quaternary depositional basins by the Maclean-Tyndale Ridge and these basins feature a number anabranches and lagoons including two large lakes, The Broadwater and Lake Wooloweyah.

Locally, drainage in the catchment is partly controlled by the underlying rock types and structures. For example, within the Clarence-Moreton Basin many drainage lines follow the contacts of more resistant rock units, particularly the Kangaroo Creek Sandstone (Wells & O'Brien 1994a). Elements of radial and annular drainage are present on the Tertiary volcanic rocks, including in the adjacent Richmond River catchment and north of Ebor, reflecting the original volcano morphologies. The northerly trend of several rivers in the Palaeozoic basement of the south-western part of the catchment is strongly influenced by the major Demon Fault structure (Figure 2).

Age data and events

A framework of age data can be used to constrain key events in the landscape history of the Clarence River catchment (Table 1). Major events influencing the long term catchment evolution include:

- Initiation of the Clarence-Moreton Basin in the Late Triassic;
- Progressive infilling of the basin from erosion of the surrounding Palaeozoic basement through the Jurassic and possibly into the early Early Cretaceous, largely in a terrestrial fluviatile environment;
- Deformation of the basin and ongoing erosion;
- Eruption of a series of large central-style volcanoes in the Miocene with accompanying thermal doming and subsequent faulting to form topographic irregularities in the Clarence-Morton Basin.

Table 1: Compilation of age data relevant to the landscape evolution of the Clarence River catchment. K/Ar ages are corrected to current IUGS standard.

Feature	**Geological Age**	**Numerical Age Range Ma**	**Reference**
Present drainage	Miocene-Quaternary		Pickett & McKenzie 1984
Ebor Volcano	Miocene	20-19	Wellman & McDougal 1974 Ashely *et al*. 1995
Tweed Volcano	Miocene	23-21	Wellman & McDougal 1974 Jones 1987
Focal Peak Volcano	Late Oligocene	ca. 24	McDougall & Wilkinson 1967 Jones 1987
Main Range Volcano	Late Oligocene-Miocene	25-18	Ewart & Grenfell 1985 Lafferty & Golding 1985
Continental margin rift	Cretaceous	73-52	Gaina *et al*. 1998
Clarence-Moreton Basin	Late Triassic-Late Jurassic		Wells & O'Brien 1994b
Basin basement	Silurian-Triassic		Wells & O'Brien 1994a

The Clarence-Moreton Basin is a framed basin representing a narrow southern extension of the contemporaneous Eromanga-Surat basin system. It developed prior to major continental rifting that formed the Tasman Sea. Deformation of the basin fill may have accompanied this rifting and was followed in the Cenozoic by further faulting, doming and uplift, probably accompanying and following the major volcanism in the Late Oligocene to Early Miocene (e.g. O'Brien *et al*., 1994).

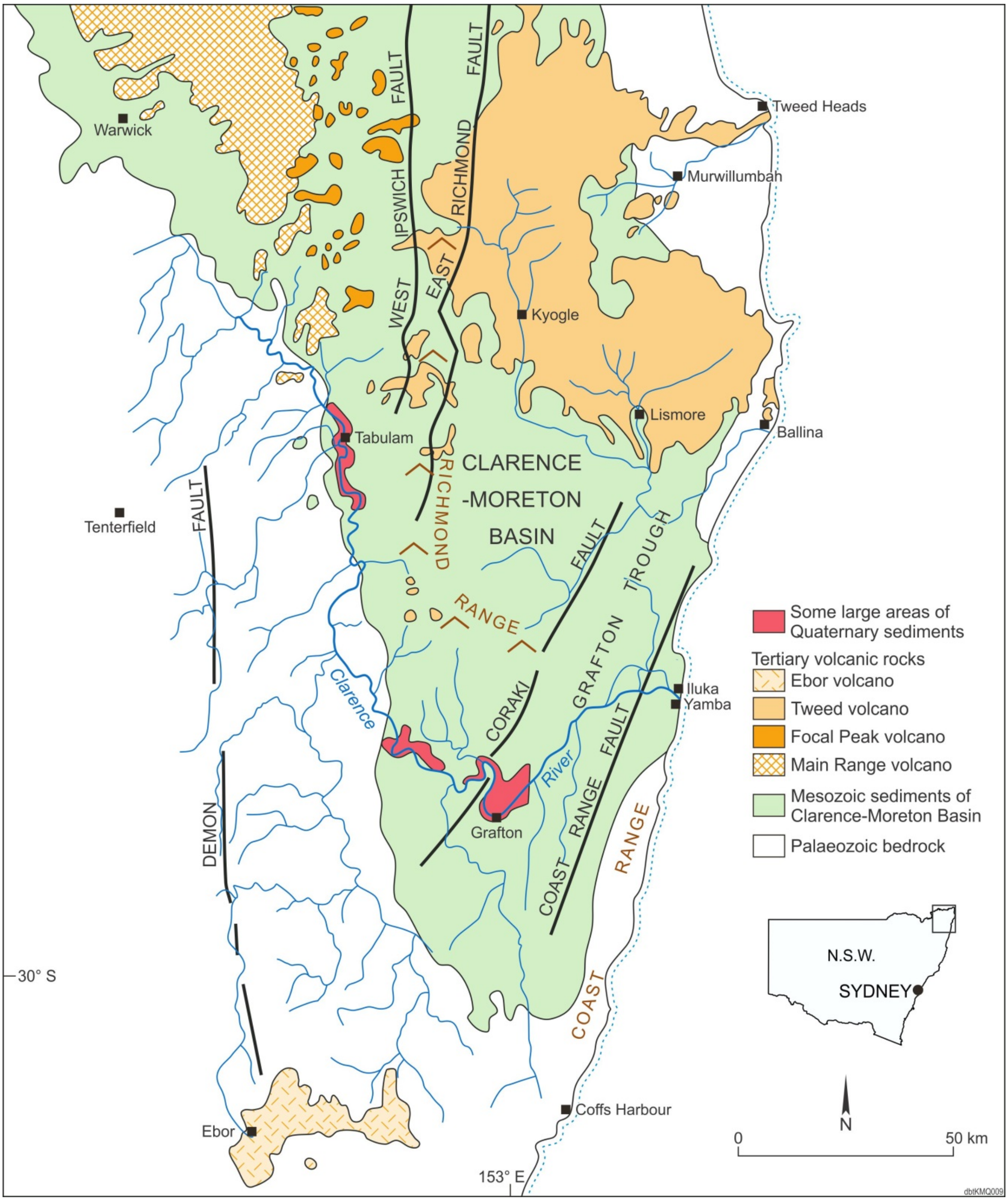

Figure 2: Map of the Clarence River catchment area showing the main drainage lines and key geological features (from Wells & O'Brien 1994a). Inset shows area location in northern New South Wales.

Discussion

The most striking and intriguing feature of the Clarence River catchment is the dramatic change in drainage direction along its north-western margin. Ollier and Haworth (1994) refer to the 'barbed' tributaries in this area and propose a model of river reversal to explain the pattern. This model includes a north-flowing proto Clarence River with a simple 'normal' dendritic drainage pattern located roughly in the present position and developed in the Palaeozoic bedrock. They suggest that this ancient river connected with a proto Condamine River to the north, noting that the head of the present Clarence River appears aligned with the head of the Condamine River on the other side of the Great Divide, a feature first pointed out by Griffith Taylor (1911). They further suggest that most of the river valley was filled with Mesozoic sediments during deposition in the Clarence-Moreton

Basin. Following basin infill and relative uplift to form a divide in the border region, drainage was reversed in the northern Clarence valley and separated from the Condamine River (Figure 3-2a).

While plausible from a broad view of the drainage pattern, a number of aspects are hard to explain by this simple reversal model and the story is likely to be more complicated in detail. The model needs to explain why the main north-south valley was developed along the western margin of the Clarnece-Moreton Basin, particularly during the Mesozoic. It is more likely that drainage was into the basin from the west, east and south, with river systems developed across the basin surface. If the proto Clarence valley predated initiation of the basin, the model needs to explain how this valley was re-exhumed by a superimposed post-Mesozoic drainage in the same position.

An alternate model is that a drainage network developed following initiation and subsidence of the Clarence-Moreton Basin with rivers feeding sediment into the basin from its margins. The resulting drainage pattern developed and persisted through the Mesozoic, but was disrupted by tectonic movements accompanying deformation, probably beginning with Late Cretaceous continental rifting to form the Tasman Sea. Doming and major volcanic eruption in the Miocene, followed by further faulting, progressively disrupted and diverted the drainage across the basin. This resulted in a new Clarence River valley west of the Richmond Range with south-flowing drainage. Where this valley intersected the older drainage network in the west it caused redirection of flow and the distinctive 'barbed' tributary pattern. In the south, the river course was controlled by other topographic features related to structures and rock types in the underlying Mesozoic basin. It was able to flow around the southern end of the Richmond Range and after breaching a low ridge continue northeast across more easily eroded sediments west of the Coast Range (Figure 3-2b).

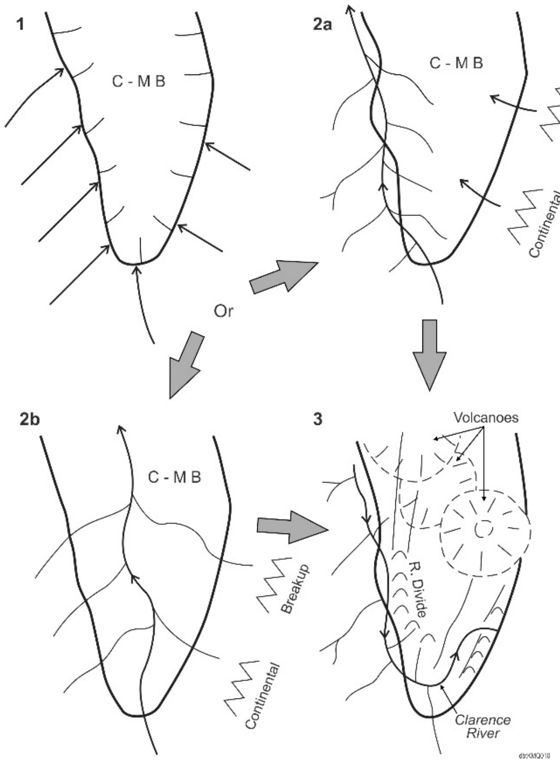

Figure 3: Summary of two possible landscape evolution models for the Clarence River catchment.

Stage 1 shows initiation of the Clarence-Moreton Basin in the Late Triassic.
Stage 2 shows infilling of the basin during the Jurassic, rifting to the east during continental breakup to form the Tasman Sea after major deposition ended in the Cretaceous. **2a** shows model 1 with development of a north-flowing proto Clarence River along the western edge of the Clarence-Moreton Basin. **2b** shows model 2 with development of a north-flowing river system into and within the Clarence-Moreton Basin.
Stage 3 shows disruption of the drainage within the Clarence-Moreton Basin by Cenozoic volcanism and tectonism with development of the present south and northeast directed flow of the Clarence River.
C-MB = Clarence-Moreton Basin; R. Divide = Richmond Range and divide.

The detailed mechanisms of drainage reversal or diversion warrant further research and field evidence. Reversal of drainage or blockage in a valley can be accompanied by damming and formation of lakes. Interestingly, there are large areas of sediments along key sections of the Clarence River, which have been mapped as Quaternary alluvium (e.g. near Tabulam and upstream from Grafton). It would be worth investigating these, particularly the higher terraces, to see if they contain lake sediments.

Conclusions and suggestions for further research
Two possible models for the development of the present Clarence River catchment include:
1. Drainage Reversal (e.g. Taylor 1911; Haworth & Ollier 1992; Ollier & Haworth 1994);

The drainage network developed around a major north-flowing river, bordering the western edge of the Clarence-Moreton Base, with later reversal in flow to the south as a result of uplift and blockage near the current headwaters.

2. Drainage Diversion (here proposed).

The drainage to the west of Clarence-Moreton Basin is inherited from an earlier network which fed north and northeast into the basin during the Mesozoic. Volcanism and uplift within the basin during the Cenozoic blocked and diverted the drainage to form a new south draining river west of the Richmond Range and along the western margin of the Clarence-Moreton Basin.

Both models imply that the present western and southern drainage network of the Clarence River catchment is inherited from an old Mesozoic drainage initiated in the Triassic with ongoing incision and lowering.

Further research is needed to conclusively establish the landscape evolution of the Clarence River catchment and region. Field observations should focus on checking the possibility of lake deposits and high-level gravels related to drainage disruption, as well as locating Mesozoic sedimentary outliers that could help define the former extent and elevation of the Clarence Moreton Basin surface. More detailed investigation of both pre- and post-volcanic, Cenozoic sedimentary deposits could shed new light on the landscape history. Landscape features preserved beneath the volcanic deposits would provide useful information on the early Cenozoic drainage pattern, prior to disruption.

To date, there has been limited work on the nature of weathering profiles in the Clarence River region. Such research could provide useful information about paleo--climatic conditions and erosion rates.

References

ANON. 1999. *Independent inquiry into the Clarence River System: Final report*. Healthy Rivers Commission of New South Wales, Sydney, 281 pp.

ASHLEY P.M., DUNCAN R.A. & FEEBREY C.A. 1995. Ebor Volcano and Crescent Complex New South Wales: age and geological development. *Australian Journal of Earth Sciences* **42,** 471-480.

EWART A. & GRENFELL A. 1985. *Cainozoic volcanic centres in southeastern Queensland, with special reference to the Main Range, Bunya Mountains, and the volcanic centres of the northern Brisbane coastal region*. Papers of the Department of Geology, University of Queensland **11(3),** 1-57.

GAINA C., ROEST W.R., MULLER R.D. & SYMONDS P. 1998. The opening of the Tasman Sea: A gravity anomaly animation. *Earth Interactions* **2(4)** pp, 1-23.

HAWORTH R.J. & OLLIER C.D. 1992. Continental rifting and drainage reversal: the Clarence Valley, New South Wales. *Earth Surface Processes and Landforms* **17**, 387-397.

JONES D.G. 1987. *K-Ar isotopic dates, New South Wales*. Geological Survey of NSW Report **1986/237**.

LAFFERTY S. & GOLDING S.D. 1985. *Isotope Geology Laboratory Report No.3 1975-1984*. Department of Geology and Mineralogy, University of Queensland, Brisbane, Queensland, Australia, 147 pp.

O'BRIEN P.E., KORSCH R.J., WELLS A.T., SEXTON M.J. & WAKE-DYSTER K. 1994. Structure and tectonics of the Clarence-Moreton Basin. *In* Wells A.T. & O'Brien P.E. eds *Geology and Petroleum Potential of the Clarence-Moreton Basin*. Australian Geological Survey Organisation, **Bulletin 241**, pp. 195-216.

OLLIER C. D. 1882. Geomorphology and tectonics of the Dorrigo Plateau. *Journal of the Geological Society of Australia* **29,** 431-435.

OLLIER C.D. AND HAWORTH R.J. 1994. Geomorphology of the Clarence-Moreton Basin. *In* Wells A.T. & O'Brien P.E. eds *Geology and Petroleum Potential of the Clarence-Moreton Basin*. Australian Geological Survey Organisation, **Bulletin 241**, pp. 291-302.

PICKETT J.W. & MCKENZIE K.G. 1984. Environmental interpretations of Late Pleistocene ostracoda assemblages from the Richmond River Valley, New South Wales. *Royal Society of Victoria Proceedings* **96(4)** 227-242.

TAYLOR G. 1911. *Physiography of Eastern Australia*. Commonwealth Bureau of Meteorology, Melbourne, **Bulletin 8,** 18 pp.

WELLS A.T. & O'BRIEN P.E. 1994a. *Geology of the Clarence Moreton Basin (1:500 000 scale map),* Australian Geological Survey Organisation, Canberra.

WELLS A.T. & O'BRIEN P.E. 1994b. Lithostratigraphic framework of the Clarence-Moreton Basin. *In* Wells A.T. & O'Brien P.E. eds *Geology and Petroleum Potential of the Clarence-Moreton Basin*. Australian Geological Survey Organisation, **Bulletin 241**, pp. 4-47.

Regolith Modelling – The Bulldog Shale

G.A.Gordon[1,] B.J.Morris[1] and J.Talbot[1]

[1]Department of State Development, Geological Survey of South Australia, GPO Box 320, Adelaide SA 5001

The opal fields in South Australia, particularly the Coober Pedy Precious Opal Field, are world renowned for the production of precious opal. Precious and potch opal are found in deeply weathered, Early Cretaceous, white to mauve, marine Bulldog Shale, which underlies the red-brown silty and bouldery, Tertiary to Quaternary Russo Beds.

Weathering during the Tertiary Period, with a periodic lowering of the water table, produced kaolin rich weathered, bleached and porous silty or sandy claystone down to a depth of about 20m, followed by 20m of partly weathered mauve, gray brown or yellow-brown claystone. Below this the fresh shale is a dark grey, silty or sandy smectite-rich claystone, commonly pyritic and carbonaceous. Precious and potch opal, often with associated alunite, gypsum and iron oxides, are generally found near the base of the upper weathered zone infilling cracks, joints and occasionally replacing fossils.

A series of over 700 shallow auger drill holes were taken at two metre intervals from Coober Pedy, Lambina and Andamooka opal fields as part of the South Australian Governments' Plan for Accelerating Exploration Initiative. The aim of the program was to explore for new opal fields, away from established workings. The 714 drill holes were collected into chip trays and scanned using the HyLogger™ spectral scanning technology at the Glenside Core Storage Facility in Adelaide. The aim of scanning the samples was to rapidly log the very large number of samples produced during the exploration program; and to learn more about the weathering profile of the precious opal field, and the relationship of mineralogy to opal formation at these fields.

The HyLogger™ instrumentation rapidly measures drill core using infrared reflectance spectroscopy, and high-resolution linescan digital imagery. The spectral range includes 380 nm-2500 nm (visible and short wave infrared, VisSWIR), and also 6000 nm-14,500 nm (thermal infrared, TIR). Reflectance spectroscopy can identify a range of different minerals, from iron oxides in the visible wavelengths, through to clay minerals (including kaolinite and alunite), and carbonate species in the SWIR; and tectosilicates (opal, garnet, feldspar) in the TIR. These minerals are important for identifying the weathering profile and the relationship to opal formation. The spectral characteristics at were then extracted from TSG™, and plotted across each region, using GOCAD modelling software, producing a regional regolith profile for opal field area.

At Andamooka the weathered profile of the Bulldog Shale is similar to Coober Pedy, and consists of three main zones. An upper highly weathered kaolinized and bleached zone (known locally as '*kopi*'). A middle light brown, grey and yellowish impermeable claystone (known locally as '*mud*'), dominated by smectite – montmorillonite. A lower zone of pale yellow to red and brown bouldery silt (known locally as '*bulldust*').

The spectrally modelled profile reflects montmorillonite dominates the upper intervals of many drill samples, and grades down into a zone rich in gypsum. Underlying the gypsum is a zone dominated by well crystalline kaolinite zone, and finally at the base lies the alunite. The alunite zone is dominated by sodium rich alunite species although the potassic species is also present in places and this may reflect a change in host rock chemistry or salinity of the water-table.

Silcretes of the NE Eyre Peninsula and their association with the underlying bedrock

Carmen B.E. Krapf and Mario X. Werner

Geological Survey of South Australia, DSD, Australia, GPO Box 320, Adelaide SA 5001

The NE Eyre Peninsula is situated at the south-eastern margin of the Gawler Craton which consists of variably deformed and metamorphosed Mesoarchean to Palaeoproterozoic basement rocks. In this region the basement rocks of the Gawler Craton are successively overlain by flat-lying and unmetamorphosed rocks of the early Mesoproterozoic Gawler Range Volcanics, fluvial redbed sediments of the middle Mesoproterozoic Pandurra Formation deposited in the intracratonic Carriewerloo Basin, and continental to marine Neoproterozoic rocks of the Stuart Shelf forming part of the Adelaide Rift Complex. Cenozoic sedimentary deposits are found as thin relicts throughout the area.

Despite extensive bedrock outcrops large areas of the NE Eyre Peninsula are covered by a wide variety of in-situ and transported regolith with silcretes forming the most common induration type. Weathering and erosion of these silcretes has resulted in the widespread formation of silcrete lags throughout the area.

Recent geological mapping in the Roopena and Augusta 1:100.000 mapsheet areas revealed a close relationship between silcrete morphology and the underlying bedrock lithology.

Silcrete skins associated with quartzite blocks

Silcrete skins are frequently found on joint blocks of the Neoproterozoic Simmons Quartzite (Fig. 1a). These silcrete rinds consist of variably sized angular residual quartz grains and clasts of granular silcrete irregularly distributed within a pale purple-grey microcrystalline silica matrix. The boundary between the quartzite and the skin silcrete is usually very sharp but can also be transitional over a few millimetres. The thickness of the skins ranges from 2 mm up to <5 cm.

Silcretes associated with conglomerates

Columnar to cone-shaped silcretes with an attached rock clast (Fig. 1b) occur within pebbly to cobbly lags of weathered conglomerates and conglomeratic sandstones. These silcrete columns have formed in-situ within the conglomerates and have a convex lamellar internal structure formed by alternating silica- and titania-rich cutans of variable thickness ranging from microscopic up to several millimetres.

In other cases conglomerates have been eroded, reworked and silicified after deposition resulting in the formation of a silicified conglomerate. These silcrete conglomerates are characterised by a polymict, often well-rounded gravel clast assemblage, including quartzite, rhyolite, jasper, chert clasts.

Silcretes associated with sandstones

Silcretes have formed in sandstones of various stratigraghic units and hence a clear association between silcretes and individual sandstone units is problematic. Generally, silcretes formed in sandstones show a wide variety of morphologies including fragmental, laminar, pisolitic, massive, nodular and columnar. The silcrete matrix is mainly very fine-grained and locally contains well-rounded quartz grains. Underlying sandstones are often variably weathered and hence the sandstone-silcrete contact is transitional.

During mapping a previously undescribed, extensive and up to 10 m thick Tertiary sandstone unit has been found. In this yellowish to cream-coloured, moderately to well-sorted, medium-grained sandstone a variety of silcrete morphologies have formed. The most impressive silcrete morphology associated with this unit is the formation of two in-situ columnar silcrete horizons, each up to 70 cm thick and exposed over nearly 50 m along the cutbank of a creek (Fig. 1c). The two horizons are 50 cm apart separated by only slightly silicified, plane bedded sandstone. Individual silcrete columns are 10 to 20 cm wide. These two pedogenic columnar silcrete horizons may have formed as a response to changes in the water table during their formation. Exclusively found within this Tertiary sandstone are silicified plant casts and rhizomorphs. As all other sedimentary units are Neoproterozoic or older in age these silcretes can be assigned to this new recognised Tertiary sandstone unit. Also exclusively found with this sandstone unit are pisolite-like silcretes characterised by quartz grains or clasts coated concentrically with laminae of micro-quartz and quartzose detritus. Individual pisolites are 0.5 to 2cm in diameter.

Silcretes associated with shales and siltstones

Shales and siltstones of the Stuart Shelf's Tent Hill Formation are cropping out extensively in the eastern part of the mapping area. However, in many places these shales and siltstones are completely weathered to white, massive kaolinitc saprolite. These kaolinitic weathered sediments often grade upwards into yellowish to cream-coloured, massive, very fine-grained porcellanites and in some places are topped by columnar silcretes. Locally, a breccia-like porcellanitic silcrete developed from silicification of kaolinitic shale clasts embedded in a powdery weathering material (Fig. 1d).

Silcretes associated with quartz veins

Silicified colluvium entirely composed of angular vein quartz clasts occurs in the direct vicinity of quartz vein ridges in the western part of the mapping area.

Groundwater Silcretes

All previously described silcretes are of pedogenic origin and are the dominant silcrete form in the mapping area. However, a few isolated outcrops of groundwater silcretes have been found. These are overall grey massive silcretes some of which have flutey surfaces.

Relating silcrete morphologies to bedrock lithologies can provide a useful mapping tool in interpreting covered and underlying stratigraphic units but care has to be taken as not all silcrete morphologies are exclusively associated with a specific bedrock lithology.

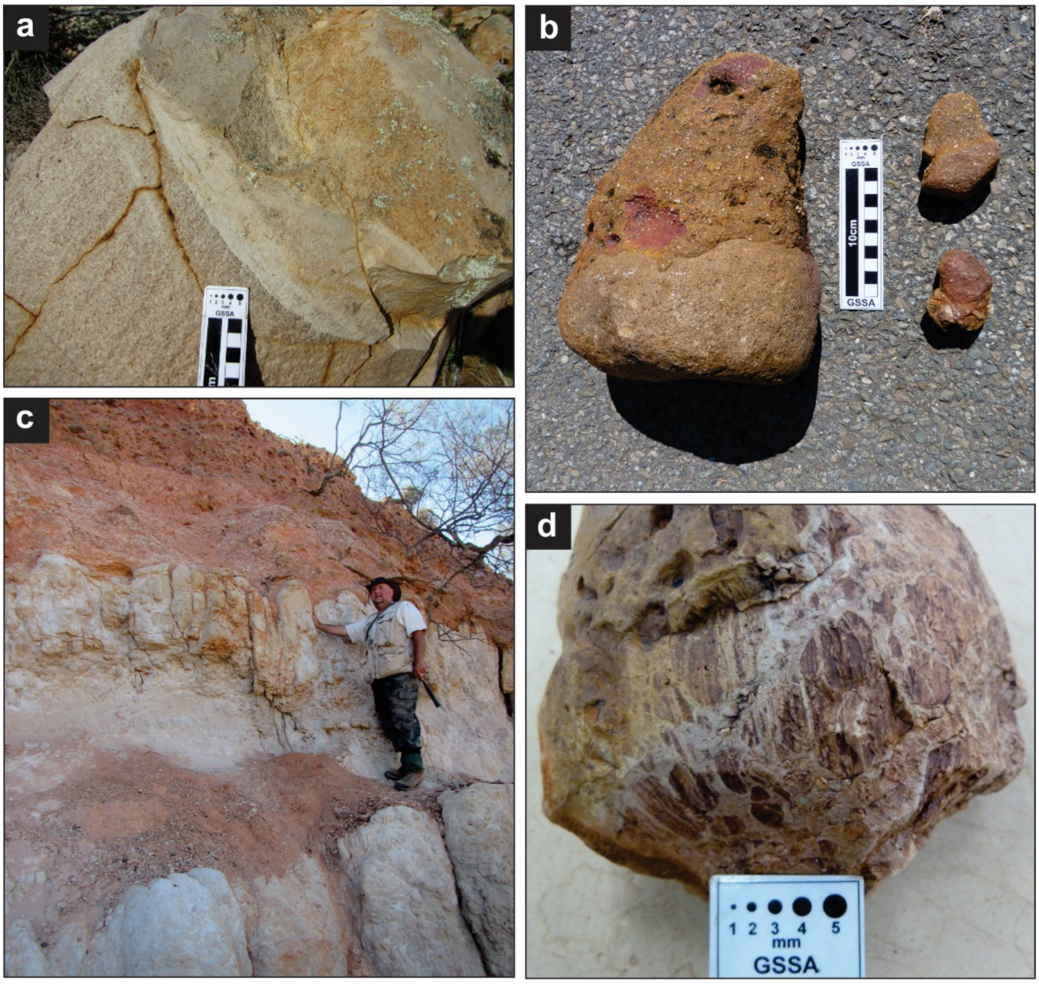

Figure 1: a) Silcrete skin on Simmons Quartzite block; b) columnar to cone-shaped silcretes with an attached rock clast; c) two in-situ columnar silcrete horizons formed in Tertiary sandstone; d) silicified shale clasts in porcellanitic silcrete.

Regolith and the Selection of Landing Sites for Crewed Missions to Mars

Jonathan Clarke[1], David Willson[1, 2], and Heather Smith[2]

[1]Mars Society Australia, c/o 43 Michell St, Monash, ACT 2904, Australia, jon.clarke@bigpond.com
[2]NASA Ames Research Center, Moffett Field CA 94035, USA

Introduction

Regolith geology has been, and continues to be essential to understanding surfaces of other solar system bodies, such as on Mars. Large volumes of high quality imagery of the surface of Mars, and continuing exploration programs by NASA and other space agencies around the world have benefited from Australian regolith understanding and insight through analogue research (West *et al.* 2010, Hobbs *et al.* 2016). This paper outlines the role that regolith sciences, especially Australian regolith science, can play in understanding and exploring extra-terrestrial regolith, with particular application preparation and selection of sites for potential crewed missions to Mars.

Martian Regolith – what we know now, and where to from here

Almost everything known about the martian regolith has been obtained by robotic spacecraft. While much is possible using the extensive data available from these missions (e.g. Gendrin *et al.* 2005, Squyres *et al.* 2012), effective Mars exploration will require astronauts on the surface (Crawford 2012). Hence the commencement of the selection processes for potential exploration zones for such missions (LPI 2015), even though such landings are at least several decades in the future. Selection of such sites will require detailed understanding of regolith characteristics, building on experience with site selection for robotic missions (e.g. Golembek *et al.* 2003, Grant *et al.* 2010).

Geoscience goals for regolith research on Mars by crewed missions include characterising the composition of surface units and evaluating the diverse geologic processes and palaeoenvironments that have affected the martian crust; geochronology, stratigraphy and exposure age determination; constraining the geophysics of the martian interior; and determining crustal evolutionary trends (Beaty and Niles 2015, LPI 2015). Dating of planetary surfaces, palaeonvironmental reconstruction, cycling of dust and gases through the atmosphere and surface, characterisation of the surface - requires an understanding of regolith processes for their interpretation - the preservation of biosignatures and the search for evidence of past or even present signs of life, each require an understanding of regolith processes for their interpretation.

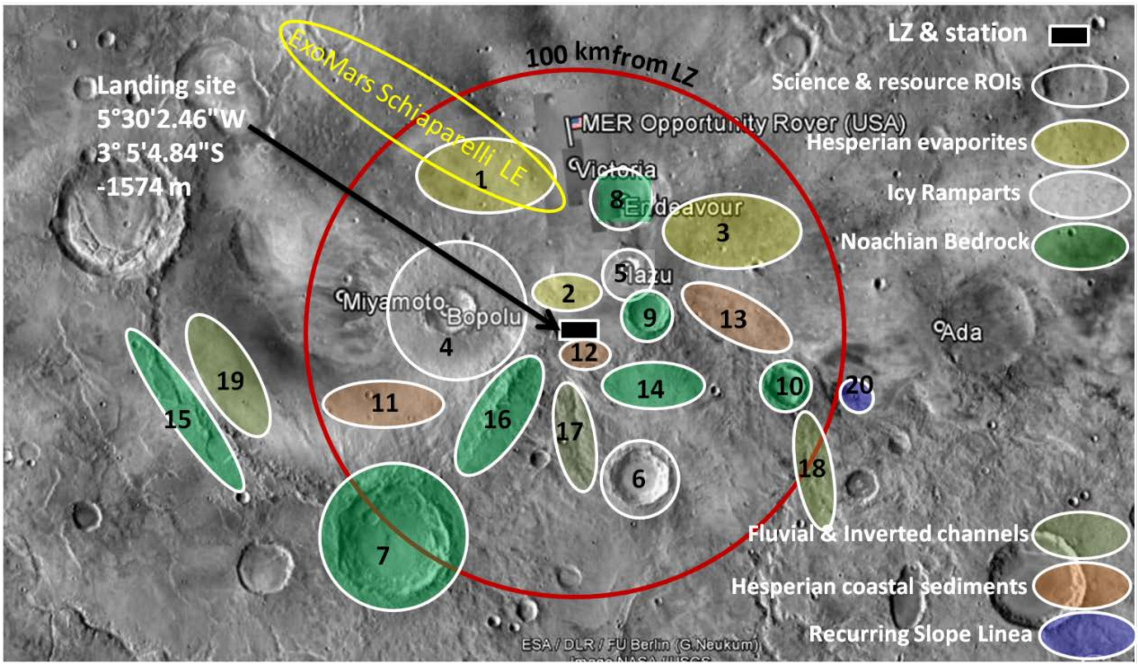

Figure 1: Characteristics of the proposed southern Meridiani exploration zone on Mars. From Clarke *et al*. (2015).

Similarly, the sites of potential resources (Allen and Zubrin 1999), especially water for propellants and life support, and regolith materials for field engineering works and construction, are of equal importance in landing site selection for crewed missions (Beaty and Niles 2015, LPI 2015). Water might be in the form of ice or hydrated minerals (Byrne *et al.* 2009, Gendrin *et al.* 2005) while regolith materials of interest include sand, gravel, aggregate, sulphates and basalt.

A regolith case study site on Mars – southern Meridiani Planum

One proposed landing site for a human mission to Mars is Meridiani Planum. It has many regions of interest for both resources and science (Figure 1) and we know that it is highly trafficable from more than 40 km of traverse by the *Opportunity* rover (Bell *et al*. 2004, Squyres *et al*. 2012). There are numerous scientific regions of interest (ROIs in Figure1), the Meridiani Planum site straddling the hemispheric dichotomy of Mars between the northern lowlands, mostly covered by relatively young (<3 Ga) volcanic and sedimentary material (Figure 2), and the ancient (mostly >4 Ga) southern highlands, composed of volcanic, sedimentary and intrusive rocks. The area includes exposures of older rocks and associated regolith surrounded by younger lowland material along uplifted crater rims (Figure 3). There are numerous resource regions of interest (ROIs in Figure1), including plains are rich in polyhdrated sulphate evaporites which are a potential water resource for crewed missions (Clarke *et al*. 2010) and diverse regolith materials (Clarke *et al.* 2015).

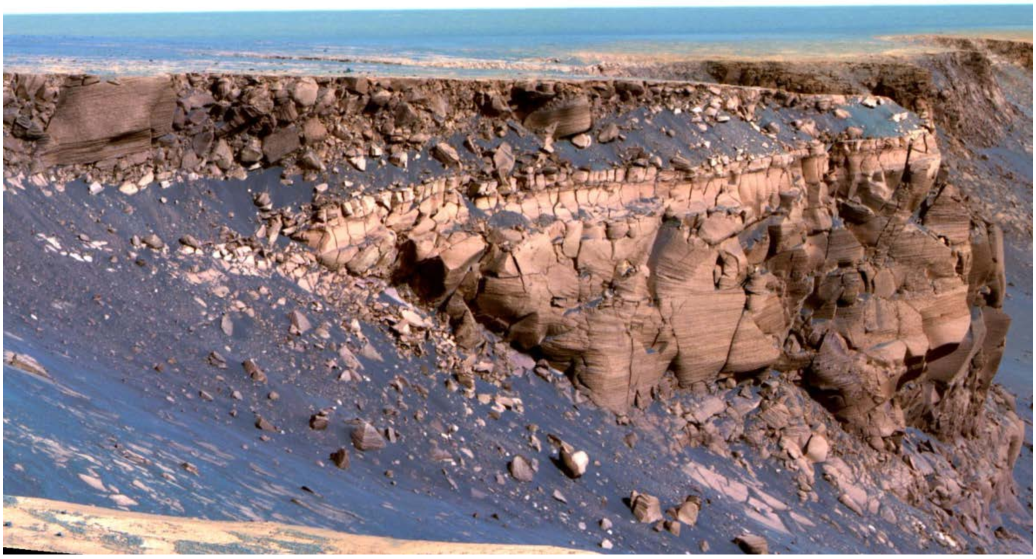

Figure 2: Regolith architecture of Meridiani Planum exposed in the wall of Victoria crater. Bedrock is rich in polyhydrated sulphate deposits. False-colour image from *Opportunity* rover (NASA image).

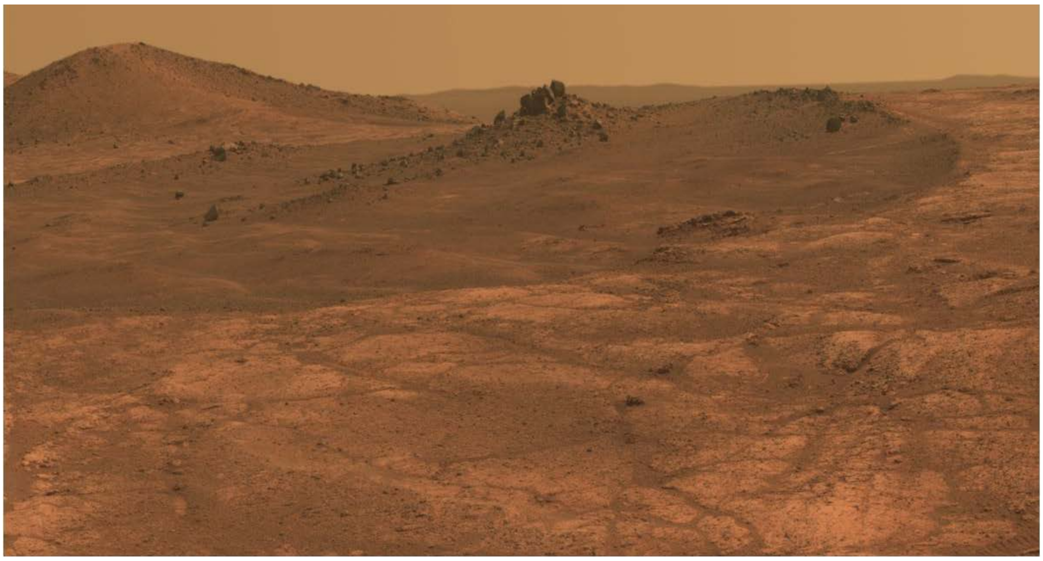

Figure 3: Diverse regolith developed on Noachian bedrock of the Endeavour crater rim, Meridiani Planum. True-colour image from *Opportunity* rover. NASA image.

Australian regolith research and Mars

Mars exploration objectives present many opportunities for Australian regolith research. First, data from NASA and ESA missions is publically available, especially imagery, which is often uploaded within hours of it being received. This allows Australian researchers to readily publish on Martian regolith (e.g. e.g. Thomas *et al.* 2005, Hobbs *et al*. 2011, Jones *et al*. 2014). Second, Australian researchers can contribute on a level of experience in regolith studies often lacking in many planetary scientists in the US and Europe (Rey 2013). Third, Australia has many analogues for Martian regolith Clarke and Bourke 2011, Hobbs *et al*. 2015). One unique example is the widespread presence of acidic weathering, sedimentation and diagenesis at the sub-continental scale (Rey 2013, Bowen *et al.* 2012,), a process thought to be relevant to Mars (Burns and Fisher 1990, Baldridge 2009) but rare elsewhere on Earth away from Australia, except for localised examples such as fumaroles and acid mine drainage. Regolith formed by such processes, such as the acid sediments of Lake Tyrrell, Victoria (Figure 4), are common in Australia, but rare elsewhere. Many analogues for bedrock features also exist (e.g. Thomas and Walter 2002, Brown *et al.* 2005). Fourthly, there is scope for the exploring the behaviour of Martian regolith simulants to better constrain engineering problems such as ISRU, for example water extraction from polyhydrated sulphates of Coober Pedy (Clarke *et al.* 2010). Such research could draw heavily on Australian experience in the mining and processing of regolith, in field robotics, and hyperspectral instruments.

Using Australian regolith geology as a key to understanding the martian surface and its exploration is also a potential tool for increasing student engagement at all levels. Many regolith features can be linked to those found on Mars (and other planets), broadening the scope and relevance of regolith science and student interest. First year geology students at Monash University have taken part in landing site selection projects for almost all NASA Mars surface missions over the past 20 years (Anderson undated). Mars Society Australia has carried expeditions to the Arkaroola Mars analogue area (Thomas *et al.* 2012) where engineering students have been instructed in geology and field robots have been tested in realistic field environments (Clarke *et al.* 2015, Mann *et al.* 2015). Lastly, Australians can contribute to workshops involving planetary science, site selection, and mission science goals, whether in person, through colleagues, and online, as shown by the recent Houston workshop (LPI 2015).

Figure 4: ironstone and halite deposition by acid springs along the shoreline of Lake Tyrrell, Victoria, a possible Mars analogue. Photo by P. English

Acknowledgements

We thank the ARGA committee for the opportunity to present this keynote address and paper. I am also indebted to my Mars colleagues, in particular the late Dave Cooper, along with Mary Bourke, Steve Hobbs, Eriita Jones, Colin Pain, Graham Mann, Ian Roach, Matilda Thomas, and Michael West.

References

ALLEN, C. C. AND ZUBRIN, R. 1999. In-situ Resources. *In* Larson, W. J. and Pranke, L. K. (eds.) *Human spaceflight: mission analysis and design*. McGraw-Hill, New York, 477-512.

ANDERSON, M. Undated. Selecting a Mars Landing Site – the 0.0003% solution. Web address when accessed 4/1/16 http://www.tesep.org.au/images/casestudy/TESEP_Case_Study_1.002-Selecting_a_Mars_Landing_Site.pdf

BALDRIDGE *et al*. 2009. Using Australian acidic saline lake deposits to describe geochemical variability on Mars. Geophysical Research Letters **36**, L19201.

BEATY, D. & NILES, P. 2015 Candidate Scientific Objectives for the Human Exploration of Mars, and Implications for the Identification of Martian Exploration Zones. Scientific Objectives for the Human Exploration of Mars Science Analysis Group. Web address when accessed 4/1/16 http://mepag.jpl.nasa.gov/reports/HSO%20summary%20presentation%20FINAL.pdf

BELL, J. F. *et al.* 2004. Pancam Multispectral Imaging Results from the Opportunity Rover at Meridiani Planum. *Science* **306**, 1703-1709.

BROWN, A. J., WALTER, M. R., AND CUDAHY, T. J. 2005. Hyperspectral imaging spectroscopy of a Mars analogue environment at the North Pole Dome, Pilbara Craton, Western Australia. *Australian Journal of Earth* Sciences **52**(3), 353-364

BOWEN, B. B., BENISON, K. C., AND STORY, S. 2012. Early diagenesis by modern acid brines in Western Australia and implications for the history of sedimentary modification on Mars. *SEPM Special Publication* **102**, 229-252.

BURNS, R. G., AND D. S. FISHER 1990. Iron-sulfur mineralogy of Mars: Magmatic evolution and chemical weathering products, J. Geophysical Research **95**, 14,169–14,173.

BYRNE, S. *et al*. 2009. Distribution of Mid-Latitude Ground Ice on Mars from New Impact Craters. *Science* **325**, 1674-1676

CLARKE, J. D. A. AND BOURKE, M. C. 2011. Travertine and tufa from Dalhousie Springs (Australia) - Implications for recognizing Martian Springs. *Geological Society of America Special Paper* **483**, 231-247.

CLARKE, J. D. A., WILLSON, D., AND COOPER, D. 2010. In-situ resource utilisation through water extraction from hydrated minerals – relevance to Mars missions and an Australian analogue. *Proceedings of the 6th Australians Mars Exploration Conference,* Melbourne 2006. Mars Society Australia. Web address when accessed 4/1/16 http://old.marssociety.org.au/library/coober_pedy_ISRU_AMEC.pdf

CLARKE, J. D. A., WILLSON, D., AND SMITH, H. D. 2015. First Landing: Southern edge of Meridiani Planum. Abstracts of the First Landing Site (LS)/Exploration Zone (EZ) Workshop for Human Missions to the Surface of Mars, Lunar and Planetary Institute, Houston, Abstract #**1057**. Web address when accessed 4/1/16 http://www.hou.usra.edu/meetings/explorationzone2015/pdf/1057.pdf

CLARKE *et al.* 2014. Field Robotics, Astrobiology and Mars Analogue Research on the Arkaroola Mars Robot Challenge Expedition. Proceedings of the 14th Australian Space Research Conference Sept 29-Oct 1st 2014, 237 -250.

CRAWFORD, I. 2012. Dispelling the myth of robotic efficiency. *Astronomy & Geophysics* **53**, 22-26.

GRANT, J. A., *et al*.,2010. The science process for selecting the landing site for the 2011 Mars Science Laboratory. *Planetary and Space Science* **59(11–12),** 1114-1127.

GENDRIN *et al.* 2005. Sulfates in Martian Layered Terrains: The OMEGA/Mars Express View. *Science* **307**, 1587-1591.

GOLOMBEK, M. P., *et al*. 2003. Selection of the Mars Exploration Rover landing sites, *Journal of Geophysical Research* **108(E12),** 8072.

HOBBS, S. W., PAIN, C. F., AND CLARKE, J. D. A. 2011. Slope Morphology of Hills at the Mars Pathfinder Landing Site. *Icarus* **214**, 258-264.

HOBBS S.W., PAULL D.J., CLARKE J.D.A. AND ROACH I.C. 2015. Multi-agent gully processes: Evidence from the Monaro volcanic Province, Australia and Noachis Terra, Mars. Geomorphology. http://dx.doi.org/10.1016/j.geomorph.2015.12.018.

HOBBS S.W., PAULL D.J., CLARKE J.D.A. AND ROACH I.C. 2016. Multi-agent gully processes: Evidence from the Monaro Volcanic Province, Australia and Noachis Terra, Mars. *Abstracts of the 4th Australian Regolith Conference* (This volume).

JONES, E., CAPRARELLI, G., MILLS, F., DORAN, B., AND CLARKE, J. 2014. An Alternative Approach to Mapping Thermophysical Units from Martian Thermal Inertia and Albedo Data Using a Combination of Unsupervised Classification Techniques. *Remote Sensing* **6**, 5184-5237.

LPI 2015. First Landing Site/Exploration Zone Workshop for Human Missions to the Surface of Mars Supplemental paper. Lunar and Planetary Institute, Houston. Web address when accessed 5/1/16 http://www.hou.usra.edu/meetings/explorationzone2015/program_presenter_info/Supplemental%20_Paper.pdf

MANN, G., SMALL, N., LEE, K., CLARKE, J. AND SHEH, R. 2015. Standardized Field Testing of Assistant Robots in a Mars-Like Environment. In C. Dixon and K. Tuyls (eds.). *Toward Autonomous Robotic Systems,* **LNAI 9287**, 167–179, Springer International Publishing.

REY, R. F. 2013. Opalisation of the Great Artesian Basin (central Australia): an Australian story with a Martian twist. *Australian Journal of Earth sciences* **60(3)**, 291-314.

SQUYRES, S. W. *et al*. 2012. Ancient Impact and Aqueous Processes at Endeavour Crater, Mars. *Science* **336**, 570-576.

THOMAS, M., CLARKE, J. D. A., GOSTIN, V. A., AND WILLIAMS, G. E. 2012. The Flinders ranges and surrounds, South Australia: a window into astrobiology and planetary geology. *Episodes* **35(1)**, 226-235.

THOMAS, M., CLARKE, J. D. A. AND PAIN, C. F. 2005. Weathering, erosion and landscape processes on Mars identified from recent rover imagery, and possible earth analogues. Australian Journal of Earth Sciences **52(3)**, 365-378.

THOMAS M. AND WALTER M. R. 2002. Application of hyperspectral infrared analysis of hydrothermal alteration on Earth and Mars. *Astrobiology* **2**, 335 – 351.

WEST, M. D., CLARKE, D. A., THOMAS, M., PAIN, C. F., AND WALTER, M. R. 2010. The geology of Australian Mars analogue sites. *Planetary and Space Science* **58(4)**, 447-458.

Multi-agent gully processes: Evidence from the Monaro Volcanic Province, Australia and Noachis Terra, Mars

S. W. Hobbs[1], D. J. Paull[1] J. D. A., Clarke[2] and Ian C. Roach[2]

[1] School of Physical, Environmental and Mathematical Sciences, University of New South Wales Canberra, Australian Defence Force Academy, Northcott Drive, Canberra, Australian Capital Territory 2600, Australia.
[2]Mars Society Australia. P.O. Box 327, Clifton Hill, VIC 3068, Australia.

Hillslope gullies occur on Earth in upland catchments and headwater settings and have a greater length than width. These types of gullies are also found on Mars (e.g., Malin and Edgett, 2000). On Earth, hillslope gullies have been well studied and can form by means of: concentrated surface runoff from topographic catchments (Selby, 1991); water seepage sourced from a subsurface aquifer (Soms, 2006); or, subsurface water transitioning from overland flow via subsurface piping (Wakelin-King and Webb, 2007). Liquid water within the hyper-arid, low temperature Amazonian Martian period has been postulated to have formed these features (Golombek *et al*., 2006), which has major implications for our understanding of liquid water-based processes operating on Mars at the current time.

In this paper we aim to test the validity of the aquifer hypothesis for gully formation by investigating an analogous gully site along Cooma Creek (Figure 1A, B, C) in the Monaro Volcanic Province near Cooma, New South Wales (e.g. Roach, 1999). As this site contains an abundance of porous layers constrained by impermeable material we conducted a detailed field survey in order to determine the likelihood of aquifer erosion occurring within the site's gullies, as well as identify the influences that local geological conditions, human activity and additional processes may have had on this site.

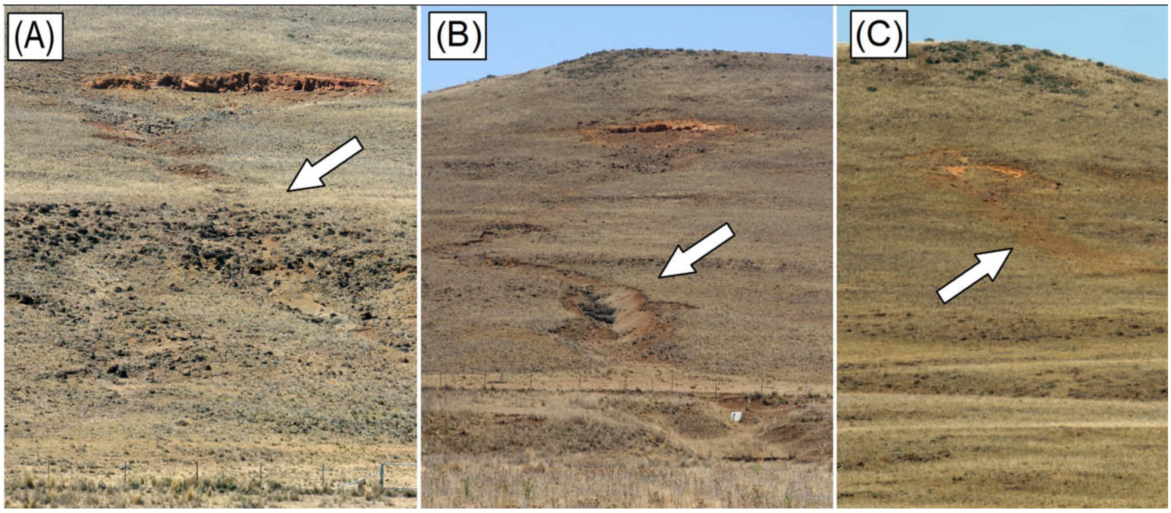

Figure 1: Location of studied gullies in Cooma Volcanic Province, New South Wales. (A) The largest gully studied showing an alcove eroded into a bauxite layer. White arrow indicates the location of a bedrock layer. (B) Additional gully with white arrow showing a V-shaped channel emerging below a bauxite alcove. (C) The smallest Cooma gully studied with white arrow indicating the location of the small gully channel.

We also conducted an analysis of Martian gullies located near Gasa Crater, whose morphology appeared structurally controlled and was similar to gullies postulated to be aquifer fed by Malin and Edgett (2000). We then compared results obtained from the two planets in order to gain a better understanding of how groundwater flow and multi-agent processes have operated on Earth and Mars.

The five studied Gasa Site gullies were located on a ~2 km stretch of south pole-facing escarpment (Figure 2) and were co-located with a rocky layer (white arrows, Figure 2) that transitioned downslope to material appearing smooth at HiRISE resolution. The heads of Gullies 1, 2 and 5 originated below this rocky layer, whereas Gullies 3–4 had eroded into the material above (black arrow, Figure 2). The gullies terminated at triangular depositional aprons downslope.

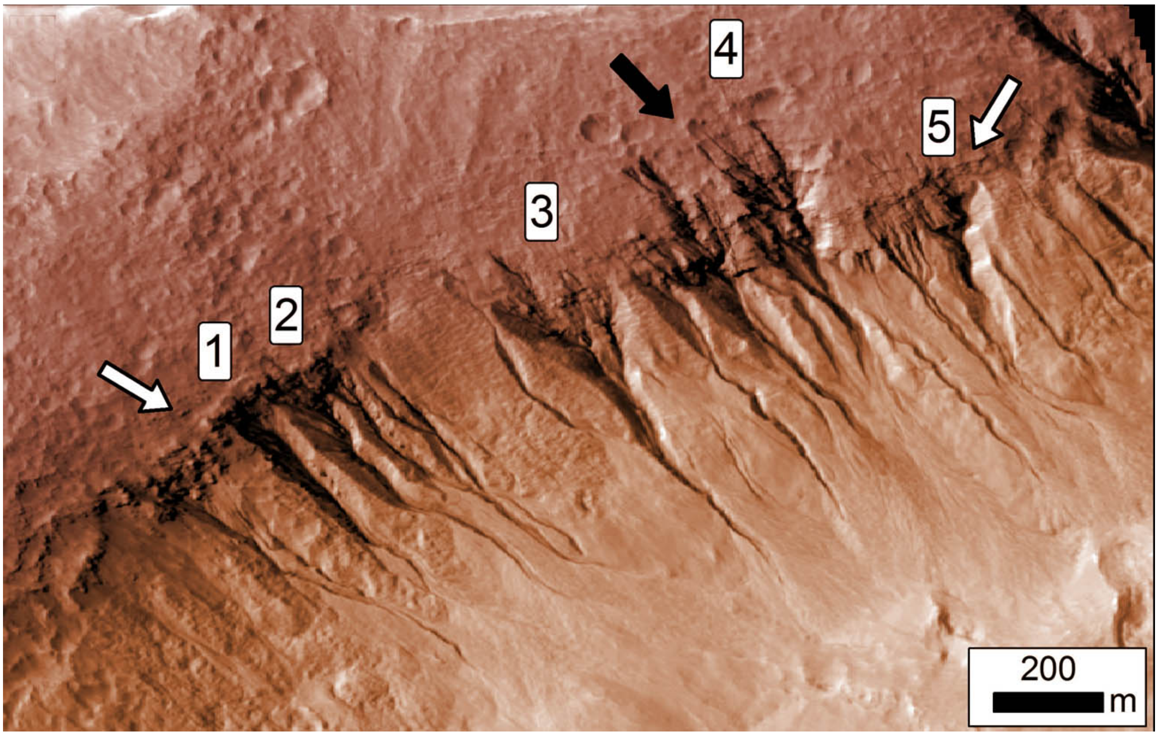

Figure 2: Location of studied craters near Gasa Crater, Mars. Studied gullies are numbered. Left white arrow points to a distinct regolith layer, black arrow indicates erosion past this layer, right white arrow indicates gully head originating below the layer.

Channel morphology also appeared to be strongly influenced by the regolith in which it had eroded for the Cooma Creek gullies. The presence of bedrock within the gully channels affected the shape of their longitudinal profiles. The Cooma Creek gully channels themselves were topographically constrained by the presence of bedrock. Layers of bedrock were expected in the Cooma Creek gullies, given the past volcanic nature of the site. The layers derived from these volcanic eruptions have served to provide differing resistances to erosion and may account for the significant variation in gully channel sizes at Cooma Creek. Additionally, the layered material constrained gully channel morphology and provided breaks in slope that have possibly triggered gully activity. In light of our field research we considered surface runoff and to a lesser extent, subsurface flow, to be the major process eroding the Cooma Creek gullies, with underlying geology providing structural control.

We found that despite the gullies at the Gasa Site being significantly larger than the Cooma Creek gullies, other morphology was remarkably similar. Alcoves, sinuous V-shaped channels, and depositional aprons were common to all studied gully sites. This concurred with previous research (Yue *et al*., 2014; Kumar *et al*., 2010), which pointed to a similarity in processes operating on the Martian and terrestrial gullies. Our ground-level observations revealed profound differences in erosive agents. These included rainfall and possible snowfall-induced runoff, not considered to be a viable process in Amazonian Mars (Carr, 2006), and animal grazing activity. Despite these differences we found that the presence of erodible material, slopes and concentration of fluvial agent through topography to be common factors for both gullies.

Our analysis of temperate gullies within the Cooma Creek catchment and gullies near Gasa Crater revealed a complex interaction between local geology, climate and erosive processes. We discovered the difficulty in obtaining conclusive evidence for aquifer activity using remote sensing techniques. Subsurface flow, if present at all, may be restricted to small scale activity. We found that despite significant differences in environmental settings our studied gullies were similar in morphometric parameters, sharing V-shaped, sinuous channels and depositional aprons. Martian channel and apron slopes were generally steeper than those for terrestrial gullies, suggesting reduced amounts of water available to erode them. We found that local geology was very important in influencing gully erosion, and changes in regolith type and breaks in slope heavily influenced gully morphology. Small scale geological changes in our studied terrestrial gullies had profound effects on local morphology and erosive agents, facilitating animal erosion at one site and inhibiting it at another. Local conditions thus play an important role in gully evolution, further highlighting that processes forming Martian gullies may be more heterogeneous than initially thought.

References

CARR, M.H., 2006, The Surface of Mars, Cambridge University Press, Cambridge, 307 pp.

GOLOMBEK, M.P., GRANT, J.A., CRUMPLER, L.S., GREELEY, R., ARVIDSON, R.E., BELL, J.F., WEITZ, C.M., SULLIVAN, R., CHRISTENSEN, P.R., SODERBLOM, AND L.A., SQUYRES, S.W.,2006. Erosion rates at the Mars Exploration Rover sites and long-term climate change on Mars. J. Geophys. Res. [Planets] 111(E12). doi: 10.1029/2006JE002754.

KUMAR, P.S., HEAD, AND J.W., KRING, D.A., 2010. Erosional modification and gully formation at Meteor Crater, Arizona: Insights into crater degradation processes on Mars. Icarus 208(2), 608-620. doi: 10.1016/j.icarus.2010.03.032

MALIN, M.C.,AND EDGETT, K.S., 2000. Evidence for recent groundwater seepage and surface runoff on Mars. Science 288(5475), 2330-2335. doi: 10.1126/science.288.5475.2330

ROACH, I.C., 1999. The setting, structural control, geochemistry and mantle source of the Monaro Volcanic Province, southeastern New South Wales. PhD Thesis University of Canberra, Australia.

SELBY, M.J., 1991, Earth's Changing Surface: An Introduction to Geomorphology, Clarendon Press; Oxford University Press, Oxford; New York.

SOMS, J., 2006. Regularities of gully erosion network development and spatial distribution in south-eastern Latvia. Baltica 19(2), 72-79.

WAKELIN-KING, G., AND WEBB, J.A., 2007. Threshold-dominated fluvial styles in an arid-zone mud-aggregate river: The uplands of Fowler’s Creek, Australia. Geomorphology 85(1-2). doi: 10.1016/j.geomorph.2006.03.011.

YUE, Z., HU, W., LIU, B., LIU, Y., SUN, X., ZHAO, Q., AND DI, K., 2014. Quantitative analysis of the morphology of Martian gullies and insights into their formation. Icarus 243, 208-221. doi: 10.1016/j.icarus.2014.08.028

Paleodrainage evolution and neotectonism in the western Murray Basin, southeast Australia

S.M. McLennan[1], D. Giles, & S.E. van der Wielen[2]

[1]University of Adelaide, Deep Technologies CRC, Geoscience Australia
[2]Deep Exploration Technologies CRC, Department of Earth Sciences, University of Adelaide

Sediments in the Murray Basin form a well-preserved record of Cenozoic marginal marine and continental depositional environments, covering some 300,000 km^2 of south eastern Australia. The Loxton-Parilla Sands are a regressive strandplain, consisting of predominantly marginal marine and lesser fluvial sediments, deposited during a retreat of sea level between 7.2 Ma and approximately 5.4 Ma (Miranda *et al.* 2009). Similar sequences exist in Brazil (Dominguez & Wanless 2009, Hein *et al.* 2013), Denmark (Tanner 1993), and the Gulf of Mexico (Tanner 1992). Isostatic subsidence from sediment loading has been minimal in the Murray Basin due to the relatively thin sedimentary sequence and low sedimentation rates (Brown & Stephenson 1991). As a result, neotectonism and eustasy are the dominant controls on the deposition of the Loxton-Parilla Sands and other Late Neogene units within the Murray Basin.

The depositional setting and sedimentary facies of the Loxton-Parilla Sands have been the subject of a number of publications (Brown & Stephenson 1991, Kotsonis 1995, Roy *et al.* 2000, Paine *et al.* 2004, Bowler *et al.* 2006, Miranda *et al.* 2009, Robson & Webb 2011). Such studies have looked at the marginal marine depositional environment of the Loxton-Parilla Sands and the preservation of neotectonism and eustatic change (Bowler *et al.* 2006, Miranda *et al.* 2009) as well as their significance for accumulation of heavy mineral sands (Roy *et al.* 2000, Paine 2005). Questions still arise, however, about the path of the ancient Murray River, the geography of the western Murray Basin and associated coastal and fluvial environments, and the extent of neotectonic influence. In this study we build on the current understanding of the Neogene stratigraphy and create a picture of the fluvial systems and associated sediment transport through time.

We compiled a database of over 8000 stratigraphic drillholes and field observations to produce the first 3D model of the entire Murray Basin. By modelling the large-scale geometry of sedimentary units we are able to infer likely rivers draining the Murray Basin and supplying clastic sediment to the ancient gulf, reworked into the Loxton-Parilla Sands. The results of the model reveal how paleodrainage systems interacted with reactivated faults and the significance of Pre-Cenozoic basement topography and structure in shaping Cenozoic sedimentary deposits. By developing a regional geological model we can better understand the structural and stratigraphic architecture of the Murray Basin, in particular the Neogene marginal marine and fluvial sediments.

The geometry of the Loxton-Parilla Sands shows that regional structures resulting from neotectonism are superimposed on sedimentary sequences deposited in response to long term sea level change and climatic fluctuations. The geological model results show the control that neotectonism has had on river courses throughout the history of the Murray Basin, influence that continues in the current landscape. This control is revealed at the basin-scale and is most apparent when we are able to visualise the geometry of sediments in 3D.

References

BOWLER J. M., KOTSONIS A. & LAWRENCE C. R. 2006. Environmental evolution of the Mallee region, western Murray basin. *Proceedings of the Royal Society of Victoria* **118**, 161-210.

BROWN C. M. & STEPHENSON A. E. 1991. Geology of the Murray Basin, southeastern Australia. *Bureau of Mineral Resources, Geology and Geophysics Australia Bulletin* **235**.

DOMINGUEZ J. M. L. & WANLESS H. R. 2009. Facies Architecture of a Falling Sea-Level Strandplain, Doce River Coast, Brazil. *In*, *Shelf Sand and Sandstone Bodies*, pp 257-281, Blackwell Publishing Ltd.

HEIN C. J., FITZGERALD D. M., CLEARY W. J., ALBERNAZ M. B., DE MENEZES J. T. & KLEIN A. H. D. F. 2013. Evidence for a transgressive barrier within a regressive strandplain system: Implications for complex coastal response to environmental change. *Sedimentology* **60**, 469-502.

KOTSONIS A. 1995. Late Cainozoic Climatic and Eustatic Record from the Loxton-Parilla Sands, Murray Basin, Southeastern Australia. Master of Science thesis, School of Earth Sciences, University of Melbourne, Melbourne (unpubl.).

MIRANDA J. A., WALLACE M. W. & MCLAREN S. 2009. Tectonism and eustacy across a Late Miocene strandplain: The Loxton-Parilla Sands, Murray Basin, southeastern Australia. *Sedimentary Geology* **219**, 24-43.

PAINE M. 2005. Sedimentology of the Bondi Main heavy mineral beach placer deposit, Murray Basin, southeastern Australia. *Sedimentary Geology* **174**, 177-195.

PAINE M. D., BENNETTS D. A., WEBB J. A. & MORAND V. J. 2004. Nature and extent of Pliocene strandlines in southwestern Victoria and their application to Late Neogene tectonics. *Australian Journal of Earth Sciences* **51**, 407-422.

ROBSON T. C. & WEBB J. A. 2011. Late Neogene tectonics in northwestern Victoria: Evidence from the Late Miocene-Pliocene Loxton Sand. *Australian Journal of Earth Sciences* **58**, 579-586.

ROY P. S., WHITEHOUSE J., COWELL P. J. & OAKES G. 2000. Mineral Sands Occurrences in the Murray Basin, Southeastern Australia. *Economic Geology* **95**, 1107-1128.

TANNER W. F. 1992. Late Holocene sea-level changes from grain-size data: evidence from the Gulf of Mexico. *The Holocene* **2**, 249-254.

TANNER W. F. 1993. An 8000-year record of sea-level change from grain-size parameters: data from beach ridges in Denmark. *The Holocene* **3**, 220-231.

The Trouble with Silcrete

G Taylor[1] and R.A. Eggleton[2]

[1] University of Canberra (graham.taylor@canberra.edu.au)
[2] Australian National University (tony.eggleton@anu.edu.au)

Silcrete

Silcrete is an enigmatic rock generally consisting of quartzose framework cemented by silica in one form or another. It mostly occurs in palaeochannels, often high in the landscape and on breakaway margins over a wide variety of bedrock types. Few true silcretes crop out low in the landscape but hardpans we would call proto-silcrete do occur in valley bottoms e.g. siliceous hard pans of Cape York) and replacing selected stratigraphic units (e.g. porcellanite near Darwin).

Silcrete major element geochemistry is relatively simple, comprising >90% SiO_2, <1% Al_2O_3, <3% Fe_2O_3 and <4% TiO_2. Alumina is well below most stream sediment or weathering profile averages and TiO_2 is well above them. Trace element contents are highly variable, but commonly include significant Zr, Ba, Sr, …………….

Silcrete mineralogy is, not surprisingly, dominated by quartz, other highly siliceous rock fragments, very fine-grained anatase and rutile, sometimes hematite/goethite with trace amounts of heavy minerals (e.g. zircon). The cement/plasma is most commonly microquartz with chalcedony, syntaxial quartz and opal overgrowth ar less common.

Some silcretes have distinctive pedogenetic fabrics (e.g. striotubules and cutans). Perhaps the most common fabric element in silcrete is geopetal accumulations of anatase/rutile atop framework grains (Figure 1) and associated with permeability boundaries in silcrete with pedogenetic fabrics. Most silcrete have a grain-supported framework fabric, but some pedogenetic and replacement silcrete have floating grain fabrics.

Troubles

Streams in most landscapes carry a load which reflects the geology of their catchment, in consequence in basaltic terrains they contain basalt fragments and weathered derivatives; in granitic regions granitic debris and so on. These aluminous rich components as well as quartzose detritus are derived locally or from farther upstream.

Despite the common presence of aluminous debris in most stream sediments, soils, and weathering profiles silcretes formed in them contain little Al_2O_3.

The high content of TiO_2 in by far the greater majority of silcretes, is in excess of that in the host material.

The common silcrete cements are quartz of one form or another, opal is relatively rare, but many argue that microquartz forms by the crystallisation of opal. We however see no indication of remnant opal in these silcretes. Opal tends to be more common in silcrete with pedogenetic fabrics but even there it is rare.

Some Thoughts

How can these troubles be resolved and what new insights can be gained to regolith processes?

The water (ground- or soil-water) forming silcrete must be rich with Al^{4+} being removed from the profile. Equally it must be saturated with Si^{4+} and Ti^{4+} as these are precipitated in a variety of forms as silcrete evolves. The source of the Ti and Si is unknown except to say it must be up water gradient (vertically or horizontally) from the silcrete or locally enriched by the removal of other material from the host material (see abstract Eggleton & Taylor, this volume). Both elements are very insoluble in natural waters except Si is readily soluble in high pH and Ti in very low pH. It is unlikely that pH can change so dramatically in natural waters, so we suggest that the mobility occurs in acid pH's (e.g. as associated with some soils and weathering profiles) and precipitation is induced by a an increase in pH, e.g. by the addition of higher or neutral pH water). Such low pH mobilisation would also explain the mobilisation of Al^{4+} but not how it is removed from the environs of the forming silcrete.

The geopetal Ti-caps atop framework and in pedogenetic materials suggest these waters were moving downward through the host materials, not laterally. So it is reasonable to assume that the host was relatively porous at the time silcrete began forming. Since Si, Ti and Al were, even when at saturation, in low quantities, large water volumes would be required to form a silcrete. This then relates to climate, so rainfalls must have been substantial, at least seasonally. Perhaps the pH changes required to precipitate Si and Ti occurred during a dryer season?

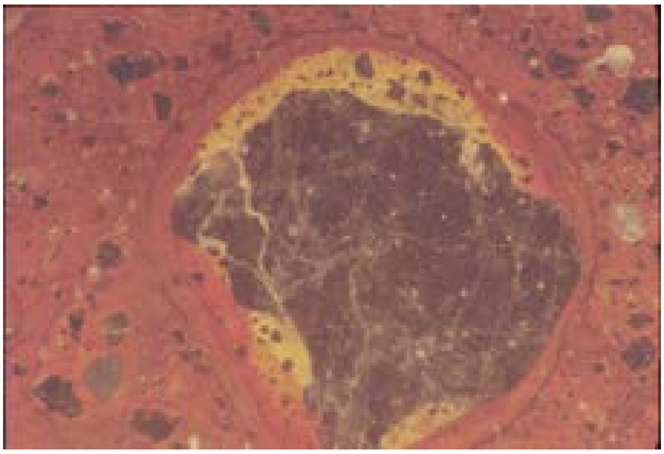

Figure 1: Typical anatase geopetal cap (yellow) on a quartz framework grain (grey) surrounded by ferruginous cutans (layered red) set in a plasma of ferruginous mud containing quartz silt grains.

Provenance of zircon in Miocene strandline heavy mineral deposits, south western Murray Basin - implications for paleo-coastal reconstructions

John Keeling[1], Anthony Reid[1], Baohong Hou[1] and Rick Pobjoy[2]

[1]Geological Survey of South Australia, Department of State Development, PO Box 320, Adelaide SA 5001
[2]Fish Hawk Resources Pty Ltd, Adelaide SA

Background

During Late Miocene to Early Pliocene time (~7.2-5 Ma) an extensive fluvial and coastal sandplain developed across the Murray Basin, in south-eastern Australia, in response to regional marine regression due to falling sea levels combined with gentle tectonic uplift. Sand ridges preserved across the sandplain record coastal shorelines formed at periods of highstand/stillstand during overall retreat of the sea towards the southwest. The paleo-coastal beach dunes and associated shallow offshore sands have been a focus of exploration for heavy mineral (HM) deposits since discovery, in 1983, of large resources of fine-grained heavy minerals at WIM 150, near Horsham, Victoria, followed in the mid-1990s by discovery of commercial grades of coarse-grained heavy mineral sands at Wemen, Woornack and Kulwin, near Mildura. In 1989, heavy mineral discoveries were made in the South Australian portion of the basin at Mindarie and Perponda. The Mindarie deposits were subsequently developed by Australian Zircon NL (2007-2009) and Murray Zircon Pty Ltd (2012-2015). Combined resources (measured, indicated and inferred), across 11 deposits reported by Murray Zircon to July 2014, totalled 249 Mt @ 3.1% (total HM), with valuable HM composition averaging 17.4% zircon, 4.9% rutile, 7.4% leucoxene and 44.7% ilmenite (Murray Zircon Pty Ltd. 2014). Mining operations at Mindarie were suspended in March 2015 as a consequence of lower prices for zircon and rutile, and depletion of heavy mineral resources within economic pumping distance of the primary concentration plant, located 1.5 km north of Mindarie township. Investigation of the provenance of zircon in HM deposits in the Mindarie area was initiated to identify the relative contribution of heavy minerals from possible source regions. The results provide data that can be used to evaluate reconstructions of the paleo-coastal environment and the influence of variation in source region as a factor affecting grade and quality of economic heavy minerals.

Samples, analyses and results

Ten samples from paleo-strandlines of Loxton Sand formed between Loxton and Karoonda were selected for analysis. Samples were taken mostly from anomalous heavy minerals intersections in company reverse circulation exploration drill holes. Zircons were separated using heavy liquid and magnetic techniques and quantitative analyses of contained U and Pb isotopes determined by laser ablation-inductively coupled plasma mass spectrometry (LA-ICPMS) at Adelaide Microscopy, University of Adelaide. Up to 100 individual grains were analysed from each sample. Full data on the analyses and age estimations are provided in Keeling *et al*. (2015). Using results of previous work on Murray Basin zircons (Sircombe, 1999) and reviews of zircon ages from likely source regions within the wider Murray Basin catchment (e.g. Veevers 1984, Champion, 2009), age ranges were selected that could be linked to possible source regions (Table 1). The relative proportion of zircons and the mix of age ranges were used to evaluate likely dispersion pathways and to identify changes of source inputs during progradation of the sandplain.

Zircon source and significance

All samples contained a high proportion of zircons younger than ca. 480 Ma; minimum contribution ranged from 31 to 54%. In this region of the Murray Basin, zircons younger than 480 Ma were unlikely to have been contributed from reworking offshore sediments or from the western headland of Adelaide Fold Belt rocks. Rather, they were delivered to the coastline by fluvial transport and subsequently reworked by wave action and longshore drift under westerly to south-westerly weather systems to concentrate as coastal residual deposits. Included in this Phanerozoic grouping was a significant population of zircons in the age range 350-440 Ma. The source of these zircons is attributed to the largely igneous second phase of the Lachlan Orogen, which produced granitoids over the period 360-440 Ma (Sircombe 1999). Zircons of this age dominate in the WIM 150 HM deposit and were sourced from southern central Victoria, accompanied by input of southern New England Orogen zircons with ages 440-480 Ma. The proportion of zircons from these two age groupings in the South Australian samples is higher than that reported for northerly and westerly Murray Basin samples from Spring Hill, Hispanola and Robinvale (Sircombe 1999). This provides the clearest evidence of fluvial transport from the southeast toward the western Murray Basin margin. Such a fluvial system was most likely the Miocene beginnings of an ancestral Murray River that developed as the sea retreated.

Table 1: Percentage zircon grains for various age ranges related to possible provenance region or intermediary sedimentary host.

Igneous / Metamorphic Provenance	**Miocene alkali basalts**	**Whitsunday Volcanic Province**	**Southern New England Orogen**	**New England Orogen**	**Lachlan Orogen granites**	**Southern New England Orogen**
Possible Intermediary Sedimentary Host	**Renmark Group, Murray Basin**	**Southeastern Queensland, Surat Basin, Eromanga Basin**	**Renmark Group, Murray Basin**	**Renmark Group, Murray Basin**	**Renmark Group, Murray Basin**	**Renmark Group, Murray Basin**
Age Range (Ma)	**12-25**	**100-175**	**175-225**	**225-350**	**350-440**	**440-480**
2017301	0	3	0	3	20	10
2017302	1	1	3	10	16	6
2017303	2	8	2	7	20	5
2017304	0	6	3	10	23	8
2017305	0	5	3	11	18	3
2017306	0	0	1	4	21	3
2017307	1	0	1	4	19	3
2017308	0	1	0	7	25	5
2017309	0	6	1	8	25	7
2017310	0	3	2	2	11	7

Igneous / Metamorphic Provenance	**Delamerian igneous activity**	**Pacific Gondwana, Antarctica**	**Undiff. source**	**Grenville-age Antarctica, Musgrave**	**Gawler Craton, Musgrave, Antarctica**	**Various possible sources**	**Gawler / Curnamona / Antarctica**
Possible Intermediary Sedimentary Host	**Cape Jervis Formation**	**Kanmantoo Group, Lachlan Ordovician turbidites, Hawkesbury Sandstone**		**Kanmantoo Group, Umberatana Group, Wilpena Group**	**Kanmantoo Group, Burra Group, GAB**		**Kanmantoo Group, Adelaidean Curnamona metasedim-ents**
Age Range (Ma)	**480-530**	**530-700**	**700-900**	**900-1200**	**1200-2100**	**1200-2700**	**>2700**
2017301	5	15	2	15	17	10	0
2017302	8	11	5	14	19	5	1
2017303	5	8	5	10	12	10	5
2017304	9	16	0	11	11	3	3
2017305	10	21	1	9	14	5	1
2017306	11	17	4	17	9	7	6
2017307	7	11	3	18	24	7	3
2017308	3	3	3	20	26	3	3
2017309	4	21	2	11	10	2	3
2017310	4	17	3	21	14	12	4

The population of Jurassic to Early Cretaceous (100 - 175 Ma) zircons is correlated with extensive volcanic arc activity of the Whitsunday Volcanic Province, mostly during the period 95 to 132 Ma along the eastern Queensland coast (Sircombe 1999, Bryant *et al*. 2012). Zircons in weathered detritus from volcanic deposits were extensively dispersed during the Cretaceous by westerly and south-westerly flowing rivers that deposited sediment in the Surat and Eromanga Basins (Veevers 1984, Bryant *et al*. 2012). The sediments were later reworked by early Cenozoic rivers, including southerly flows into the northern Murray Basin. During the Miocene, tributaries of the ancestral Darling River transported zircon directly from Queensland volcanics and also recycled zircon from earlier basin sediments. Early Cretaceous age zircons were not recorded in the WIM 150 Miocene sands, in the southern Murray Basin, but were present in northerly samples reported by Sircombe (1999). Using data from Sircombe (1999), the relative significance of northern fluvial inputs was estimated for each of the South Australian samples. The overall results suggest that an ancestral Murray River mostly dominated over the ancestral Darling River as a source of fluvial zircons in the Loxton-Karoonda strandlines. The exception was sample 217303, which recorded the highest percentage of 100-175 Ma zircons (10%), indicative of dominant northern fluvial input.

Zircon contribution from Neoproterozoic Adelaidean sedimentary rocks of the southern Adelaide Fold Belt were most probably fluvial inputs, principally from the northwest. Based on data from Ireland *et al*. (1998) the dominantly Umberatana Group sediments would contribute a zircon population centred on ~1140 Ma coupled with zircons from age groupings 1550-1900 Ma and 2100-2700 Ma. Some contribution from this combination of ages was evident in most of the strandline sample data but at a lower proportion than might be expected, given the proximity of these rocks to the western basin margin. The contribution of 1550-1900 Ma zircons ranged from 2 to 10% and 2100-2700 Ma zircons from 1 to 7%; the 1140 Ma population is present also in Kanmantoo Group and, in isolation, is not diagnostic of source. Overall, Neoproterozoic rocks contributed probably <30% of the strandline zircons.

Kanmantoo Group meta-sandstones are characterised by a main zircon population between 500-700 Ma, with a subordinate population between 900-1200 Ma and scattered older zircon ages of 2000-3500 Ma (Ireland *et al*. 1998). Additional contribution of zircon grains from coastal headlands of Kanmantoo Group and offshore Delamerian granite sources was indicated by an increase in the zircon population between 500-700 Ma coupled with an increase for 900-1200 Ma zircons, and a contribution from Delamerian granites at 480-530 Ma. Two samples possibly show this pattern, Mindarie A (217306) and Balmoral South strandline (217310); both samples recorded the lowest percentage of zircons younger than 480 Ma, at 31% and 32% respectively.

Conclusion

Zircon age populations indicate largely fluvial transport to the western Murray Basin Late Miocene - Early Pliocene coastline by a combination of paleo-drainage networks involving the ancestral Darling and Murray river systems. Sediment from the southeast mostly dominated over that from the north. It is likely, therefore, that an ancestral Murray River was established as a source of sediment supply by the time coastal progradation had extended to the south of Loxton. Significant but subordinate fluvial input is indicated for drainage from Adelaide Fold Belt rocks forming the western basin margin. In particular, samples from strandlines Mindarie A and Balmoral South contain a higher proportion of zircons from age populations consistent with additional inputs from Kanmantoo Group meta-sandstones eroded from coastal headlands or offshore islands. This may reflect periods of low river flows or reactivated fault activity on the western basin margin. Overall, the Loxton - Karoonda area of the Miocene Murray Basin received zircons from a wide range of source regions, with variable inputs as the coastline prograded. The mix of zircon sources and fluctuation in source inputs with time is expected to be reflected also in variation in the characteristics and quality of zircon product and associated heavy minerals.

References

BRYANT S.E., COOK A.G., ALLEN C.M., SIEGEL C., PURDY D.J., GREENTREE J.S. & UYSAL I.T. 2012. Early-mid Cretaceous tectonic evolution of eastern Gondwana: from silicic LIP magmatism to continental rupture. *Episodes* **35**, 142-152.

CHAMPION D.C., KOSITCIN N., HUSTON D.L., MATHEWS E. & BROWN C. 2009. Geodynamic synthesis of the Phanerozoic of eastern Australia and implications for metallogeny. *Geoscience Australia, Record* **2009/18**, 255p.

IRELAND T.R., FLOTTMANN T., FANNING C.M., GIBSON G.M. & PRIESS W.V. 1998. Development of the early Paleozoic Pacific margin of Gondwana from detrital-zircon ages across the Delamerian orogen. *Geology* **26** (3), 243-246.

KEELING J.L., REID A.J., HOU B. & POBJOY R. 2015. Provenance of zircon in heavy mineral sand deposits, western Murray Basin, **Report Book 2015/00031**. Department of State Development, South Australia, Adelaide.

MURRAY ZIRCON PTY LTD 2014. Mineral Resource Statement – JORC 2012 – effective 01 July 2014, viewed August 2015, <http://www.murrayzircon.com.au>.

SIRCOMBE K.N. 1999. Tracing provenance through the isotope ages of littoral and sedimentary detrital zircon, eastern Australia. *Sedimentary Geology* **124**, 47-67.

VEEVERS J.J. ed. 1984. *Phanerozoic Earth History of Australia*. Clarendon Press, Oxford, 418 pp.

Exploring for Heavy Minerals on Cape York Peninsula, Queensland, Australia

Lisa Worrall

Protean Geoscience, PO Box 125, Canberra ACT 2601

This presentation describes the results of a preliminary analysis of the heavy minerals potential of the northwest coast of Cape York Peninsula in far north Queensland. The analysis was funded by the Queensland Government's Future Resources Program Industry Priorities Initiative. It was commissioned following the 2013 discovery of heavy minerals on the northwest coast of Cape York by Oresome Australia Pty Ltd (a wholly owned subsidiary of Metallica Minerals Pty Ltd). The evolution of the coastline in this rugged and remote region is poorly understood and the age and geomorphological context of the 2013 discovery was unknown.

The analysis that was carried out placed the discovery in context and established that the northwest coast of Cape York Peninsula has the potential to host world class heavy minerals deposits. All the essential ingredients in a HM Mineral System are present: fertile source rocks, effective transport mechanisms and abundant trap sites, particularly along the Pleistocene coastline. It was recommended that ongoing exploration focus on potential trap sites on the Pleistocene coast and that two sites, where structural traps could have been formed by coastal promontories, should be targeted in the first instance.

Identifying sources of acidity and acid sulfate soil characterisation in the Anglesea River catchment

Vanessa Wong[1], Chin Cheng Yau[1], David Kennedy[2]

[1]School of Earth, Atmosphere and Environment, Monash University, Wellington Rd, Clayton VIC 3800
[2]School of Geography. The University of Melbourne. Parkville VIC 3010

Globally, coastal and estuarine floodplains are frequently underlain by sulfidic sediments. When exposed to oxygen, sulfidic sediments oxidise to form acid sulfate soils, adversely impacting on floodplain health and adjacent aquatic ecoystems. In eastern Australia, our understanding of the formation of these coastal and estuarine floodplains, and hence, spatial distribution of acid sulfate soils, is relatively well established. These soils have largely formed as a result of sedimentation of coastal river valleys approximately 6000 years BP when sea levels were one to two metres higher. However, our understanding of the evolution of estuarine systems and acid sulfate soil formation, and hence, distribution, in southern Australia remains limited.

The Anglesea River, in southern Australia, is subjected to frequent episodes of poor water quality and low pH resulting in closure of the river and, in extreme cases, large fish kill events. Poor water quality has been linked to acid leakage from mining activities and Tertiary-aged coal seams, peat swamps and acid sulfate soils in the region. However, our understanding of the sources of acidity and distribution of acid sulfate soils in this region remains poor. In this study, four sites on the Anglesea River floodplain were sampled, representative of the main vegetation communities. Peat swamps and intertidal marshes were both significant sources of acidity on the floodplain in the lower catchment. However, acid neutralising capacity provided by carbonate sands suggests that there are additional sources of acidity higher in the catchment.

Regional Biogeochemistry in the Capricorn Orogen: Prairie Downs Project

N. Reid[1], S. Spinks[1] and R. Thorne[1]

[1]CSIRO Mineral Resources, ARRC, Kensington, Western Australia

Biogeochemical sampling was done at and around (to 40 km) the Prairie Downs Project, in the Capricorn Orogen of Western Australia. Both mulga (*Acacia aneura*) and spinifex (*Triodia basedowii*) were sampled along four transects over the fault hosting the Prairie and Wolf deposits, and where possible, coincident with the groundwater sample locations to the north of the fault.

Background

This work was carried out as a direct comparison to research in the north Yilgarn Craton (Reid *et al*. 2010), where mulga was also sampled coincident to groundwater and mulga chemistry could be used to distinguish lithological boundaries and shallow ore deposits at that scale. Sampling spinifex follows on from previous work in the Tanami Desert (Reid *et al*. 2009, 2010), where spinifex showed very good point source detection of ore bodies and some potential to detect lateral enrichment of ore bodies.

Methods

Spinifex and mulga leaf samples were collected while wearing leather gloves. Sampling contamination risk was reduced by removing all watches, jewellery and other metallic objects. Field sampling error was reduced by using the methodology adapted from Hill (2002). Plants in good health were chosen and those growing in or near drill spoil were avoided.

Results

The geochemical composition for both species reflect similar patterns to the previous studies. Both species show tight anomalism in Pb over the deposits with very little lateral footprint (Figure 1 and 2). Spinifex also shows the same effect in Zn (Figure 4) and quite a few other important elements. Mulga shows much lower concentrations for both Pb and Zn, with the Zn (Figure 3) not related to the mineralisation, but most likely to individual plant health.

Many elements are strongly elevated in both species along the fault associated with Prairie Downs (such as Sb in Figure 5, Ag, As, Bi, Fe, Li, Na, Pt, Se, and Th). Further information would be required to determine if all are directly associated with mineralisation or the increased fluid flow along fault zones.

Contamination

There was a minor contamination issue with both species sampled, and it was different in both cases. With spinifex, the contamination was most likely derived from drilling activity, which can be seen in Fe and Hf concentrations being higher over the transects but this did not correspond directly with the anomalous elements of interest. The mulga showed contamination from dust associated with cattle. Fe and Hf contents were much higher around the pumping water sites where more cattle were present and hoof traffic increased aeolian material.

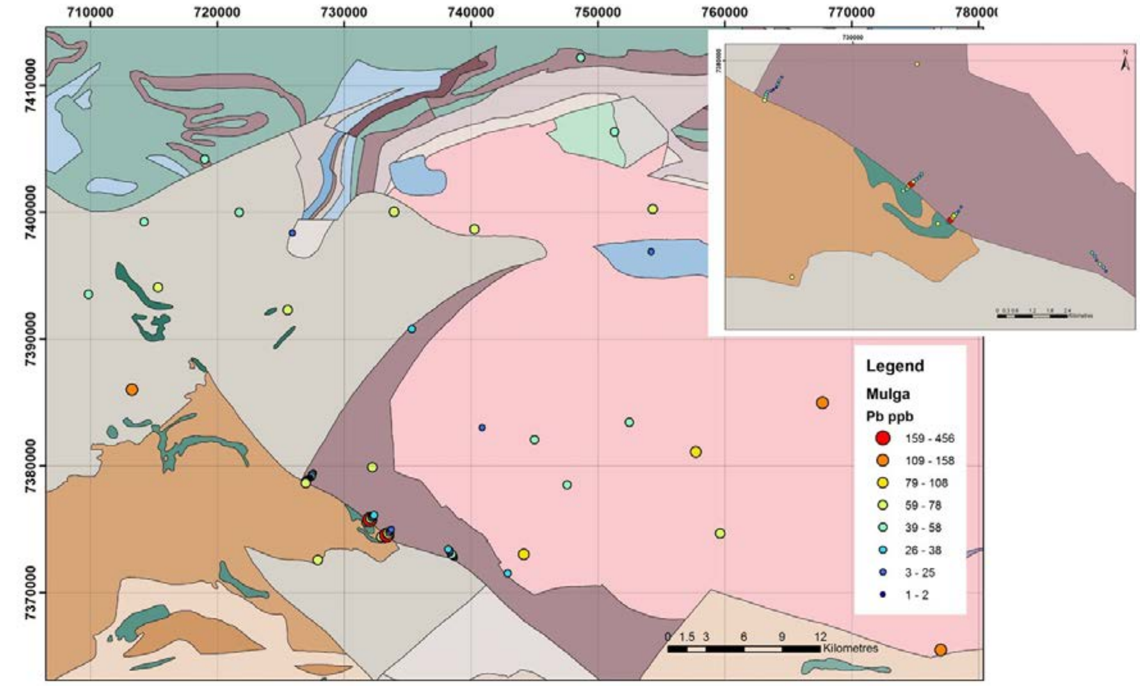

Figure 1: Lead concentrations in mulga in the regional sampling, with the inset showing a close up over the Prairie Downs deposits and fault.

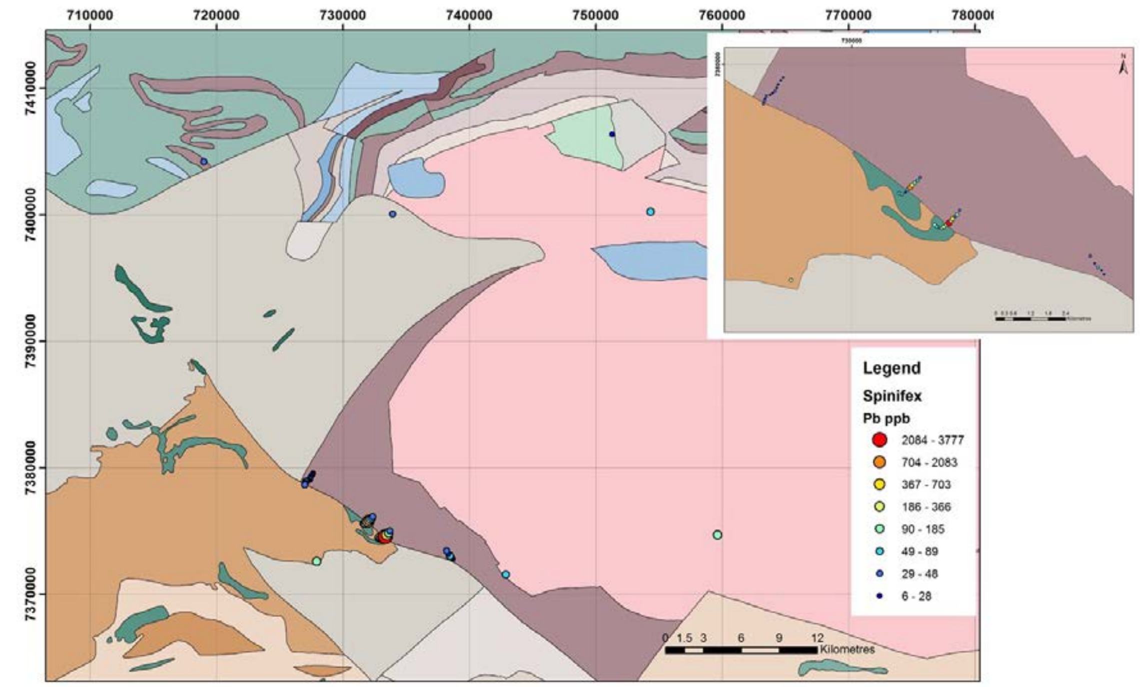

Figure 2: Lead concentrations in spinifex in the regional sampling, with the inset showing a close up over the Prairie Downs deposits and fault.

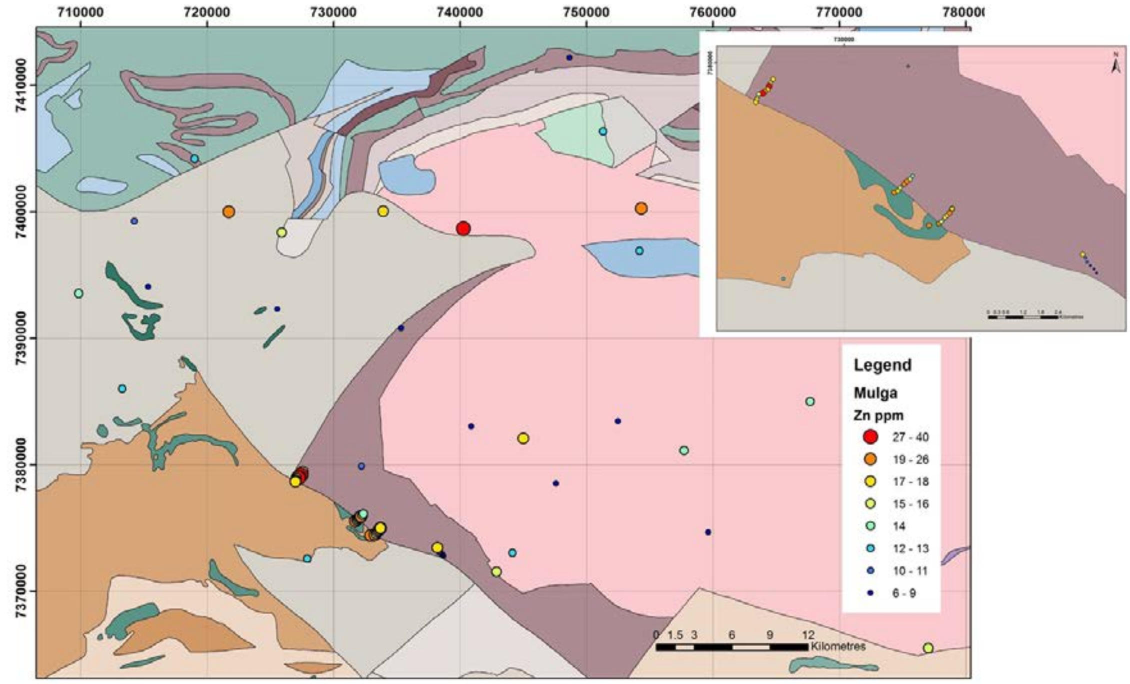

Figure 3: Zinc concentrations in mulga in the regional sampling, with the inset showing a close up over the Prairie Downs deposits and fault.

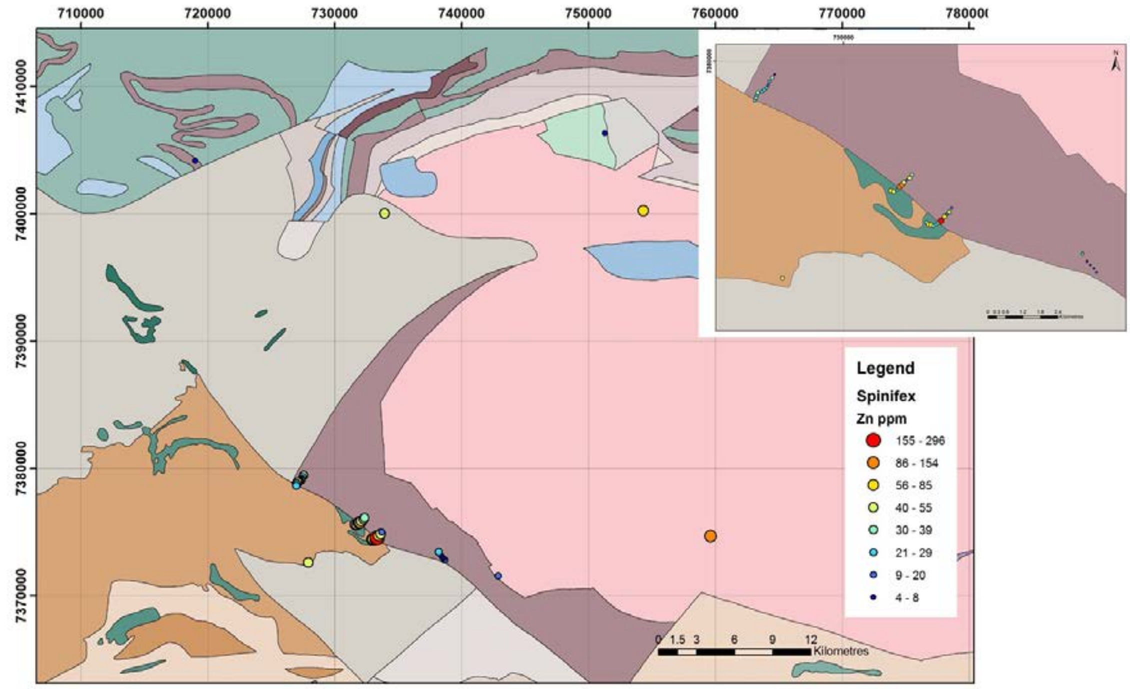

Figure 4: Zinc concentrations in spinifex in the regional sampling, with the inset showing a close up over the Prairie Downs deposits and fault.

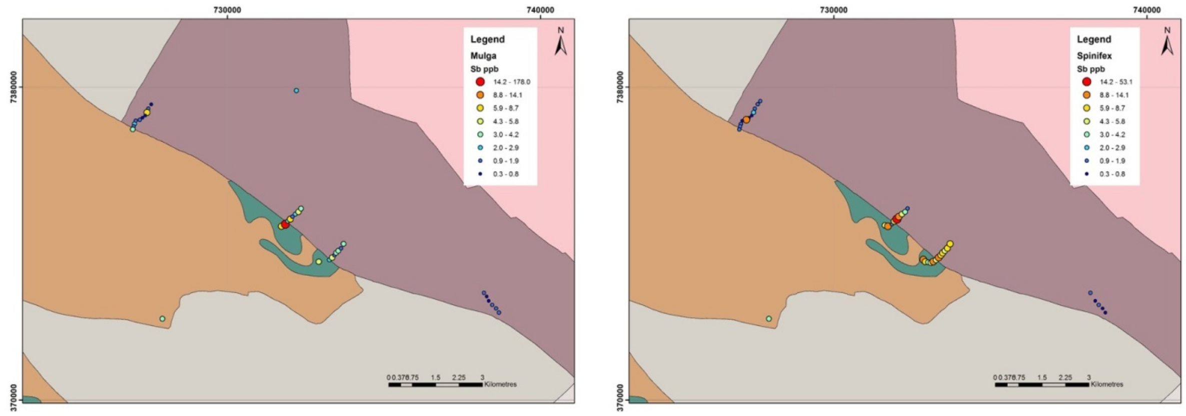

Figure 5: Antimony in mulga (left) and spinifex (right) over the Prairie Downs deposits and fault.

Acknowledgements

The authors thank Marindi Metals for site access and logistical support, and LabWest for analyical support. This project was funded as part of the SIEF Capricorn Distal Footprints Project.

References

HILL, L. J., 2002. Branching out into biogeochemical surveys: A guide to vegetation sampling, in, Roach I.C. (ED), Regolith and Landscapes of Eastern Australia 2002, pp.50-53.

REID N, HILL SM, LEWIS DM. 2009. Biogeochemical expression of buried gold mineralization in semi-arid northern Australia: penetration of transported cover at the Titania Gold Prospect, Tanami Desert, Australia. Geochemistry: Exploration, Environment, Analysis 9: 267–273.

REID N, HILL SM. 2010. Biogeochemical sampling for mineral exploration in arid terrains: Tanami Gold Province, Australia. Journal of Geochemical Exploration 104: 105–117.

SPINKS, S. C., UVAROVA, Y., THORNE, R., ANAND, R., REID, N., WHITE, A., LEY-COOPER, Y., BARDWELL, N., GRAY, D., MEADOWS, H., LEGRAS, M., 2016. Detection of zinc deposits using surface ferromanganese crusts in a semi-arid environment. Ore Geology Reviews, *In Press*.

Dolerite weathering in the saline landscapes of north-east Tasmania.

Margaret Sweeney[1] and Leah Moore[2]

[1]Institute for Applied Ecology, University of Canberra, ACT 2600
[2]Dryland salinity Hazard mitigation program, University of Canberra, ACT 2600

Researchers into salinity hazards in the Launceston area (Moore *et al*. 2014) identified that land salinisation, salt load and elevated electrical conductivity levels in nearby streams were associated with weathered paleo-estuarine sediments and terrace deposits along the Tamar and Esk Rivers, some Holocene estuarine sediments, and significantly, on deeply weathered Jurassic quartz dolerite. Previous studies did not consider quartz dolerite to be a significant salt store meaning that the volume of salt stored in the landscapes may have been underestimated. Understanding what forms and what is released as dolerite weathers will lead to a better understanding of where salt is stored in the landscapes.

The geochemistry and mineralogy of dolerite corestones and regolith including weathered rinds and soils, has been examined at five sites in north-east Tasmania (Figure 1) in order to understand the association between salinity and weathered dolerite. Samples were analysed for geochemistry using XRF and mineralogy using thin sections, ion microprobe and XRD. Regolith waters (1:5 soil to water suspensions) were analysed using ICPMS.

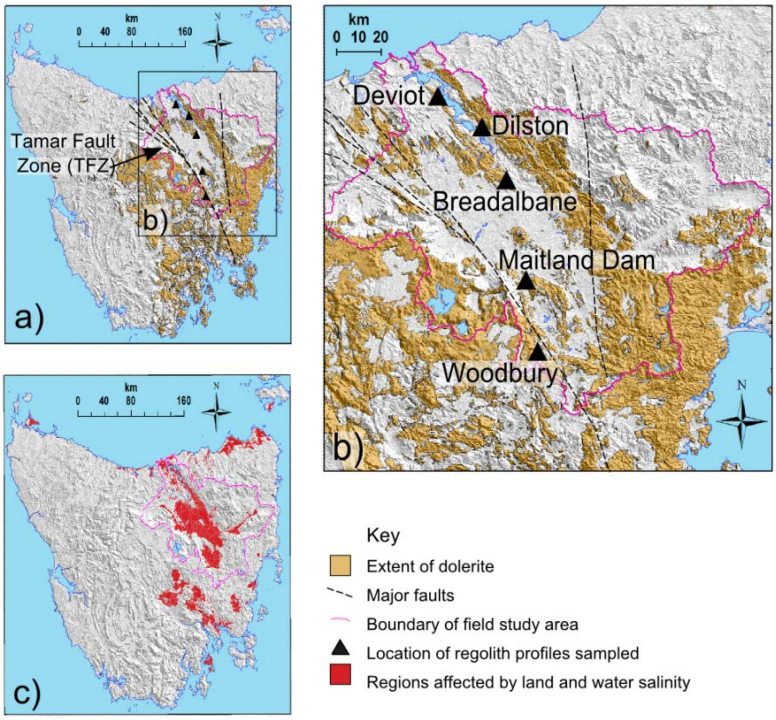

Figure 1: a) Map of Tasmania, showing dolerite terrain in orange (Mineral Resources Tasmania 2011) location of the Tamar Fracture Zone (Stacey and Berry 2004) and b) location of regolith profiles sampled (indicated by triangles). Regions affected by land and water salinity are shown in red in c) (Bastick and Lynch 2003).

Dolerite breaks down to form smectite (mostly montmorillonite) and kaolinite clays and Fe-bearing sesquioxides, goethite and hematite (Figure 2). Quartz increases in the A and B horizons of the profiles because it is a physically resistant phase. Weathered dolerites store salt in pore spaces, by adsorption (kaolinite, smectite, iron oxides and oxyhydroxides) and in interlayer spaces (smectite).

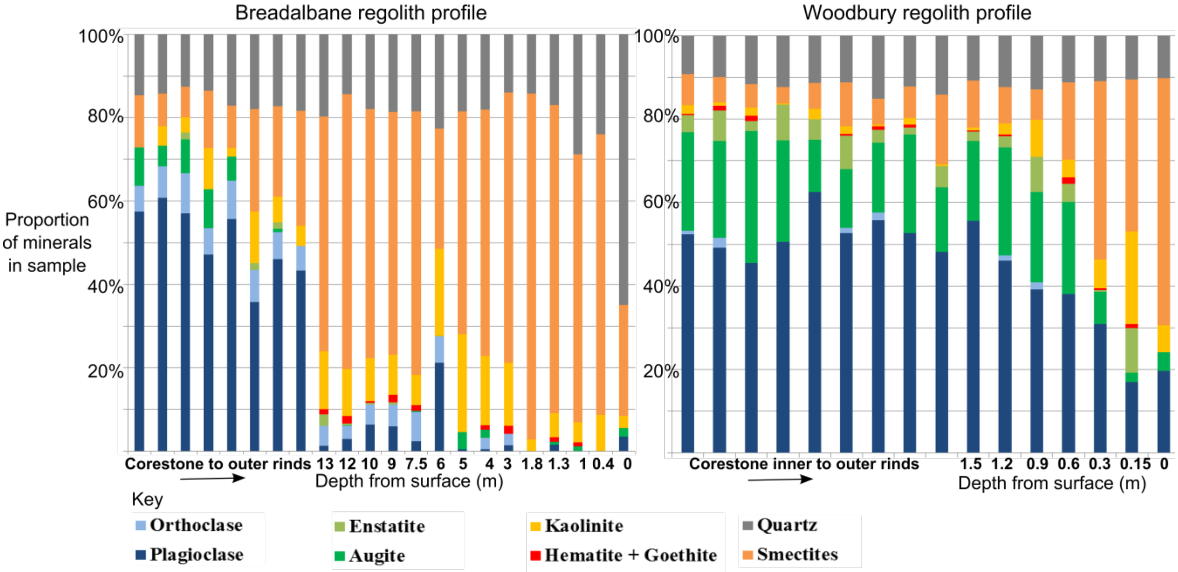

Figure 2: Quantitative XRD analysis of primary and secondary mineralogy from two of the five regolith profiles, Breadalbane and Woodbury. On the diagrams, the samples are in order of decreasing depth from left to right with the freshest rock analyses on the left and the A-horizon soil samples on the far right. The primary minerals, pyroxene and plagioclase, weather to form secondary minerals dominated by hematite, goethite, kaolinite and smectite.

The electrical conductivity (EC) of 1:5 soil to water suspensions (Figure 3) increases with weathering (maximum 4900 µS/cm in the Breadalbane profile). This confirms field observations that deeply weathered dolerite can serve as a significant store for salt in the landscape. However, the clay content and salinity of the dolerite regolith profiles varies, depending on the local geomorphic context (Figure 4).

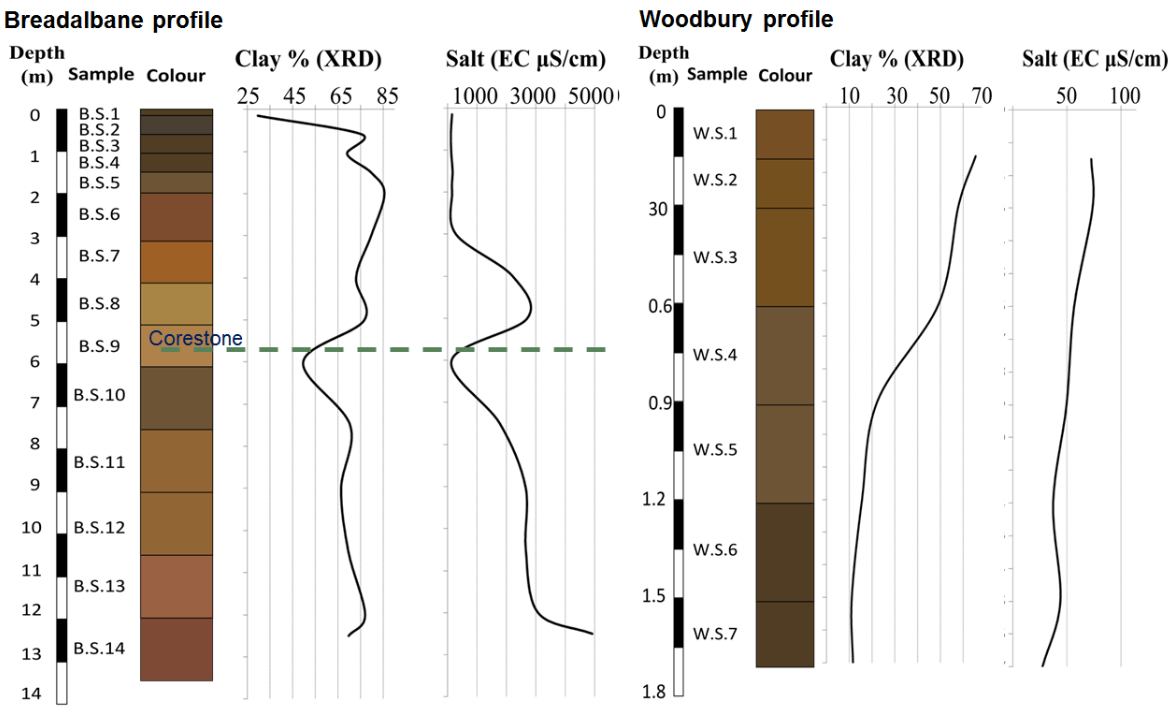

Figure 3: Breadalbane **and** Woodbury regolith profiles, showing changes in clay proportion and salinity (EC) with depth. Secondary mineralisation (clays and Fe-oxides) are controlled by structures in the profile (corestones). Materials above are enriched in clays (and generally salt). The volume of smectite and EC (salt concentration) is higher in the Breadalbane profile compared to the Woodbury profile.

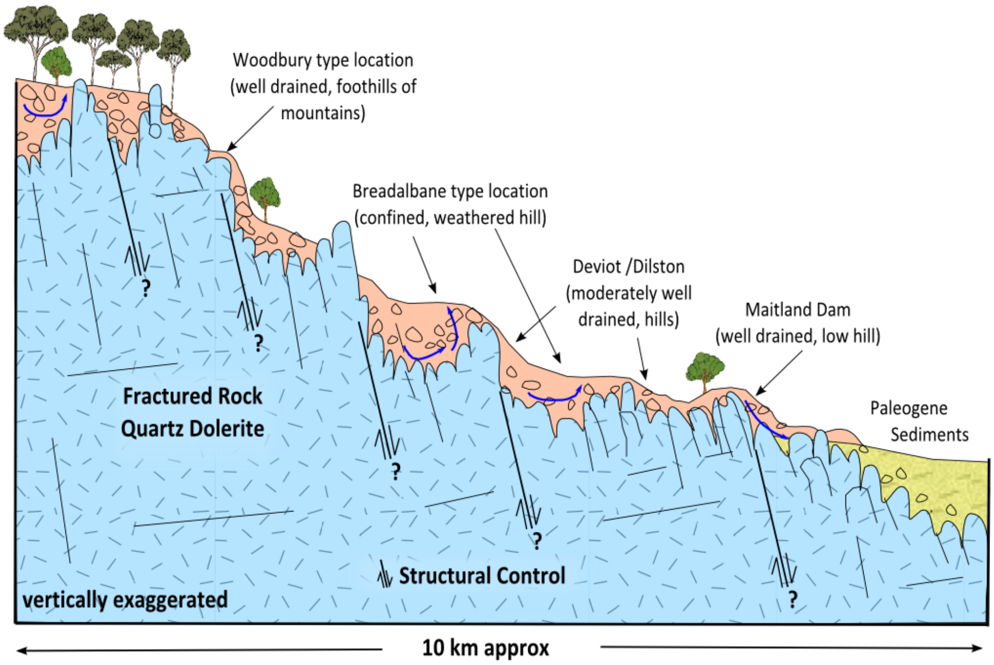

Figure 4: Conceptual diagram of how the geomorphology controls the nature of weathering and salt store of materials, Woodbury and Maitland Dam are in positions in the landscape that are well drained, Deviot and Dilston are moderately well drained and lower in the landscape than Woodbury, and Breadalbane is situated in intensely weathered hills where there is a structural impediment preventing erosion of *in situ* weathered regolith and colluvium.

Weathering to form regolith, on the well-drained slopes of the Great Western Tiers (Woodbury) and other dolerite mountains has favoured the formation of 1:1 kaolinite clays, (with more intensive weathering leading to bauxite formation in some areas). However, there are fault-bounded pockets of colluvium and highly-weathered, *in-situ* dolerite material, (Breadalbane) where 2:1 clay minerals dominate, (mostly montmorillonite). These regions have the capacity to store large volumes of salts.

To assist in understanding why salt is found in certain parts of the landscape but not in others, it is essential to model how water moves through the regolith and geological structures. By exploring the complex interactions of geomorphology and other biophysical parameters the study area has been divided into Hydrogeological Landscape (HGL) units.

The HGLs have a range of structural and geomorphic controls. Each HGL unit is linked to a conceptual hydrological model which describes water movement and regolith distribution, as well as management approaches for specific parts of the landscape. The geomorphology affects the configuration of the regolith (salt store) and where there are impediments to flow. Describing the association of dolerite with salinity and this multidisciplinary analysis will enable evaluation of land management in other landscapes dominated by dolerite (or basalt or andesite).

References

BASTICK C. & LYNCH S. 2003 Extent and Impacts of Dryland Salinity in Tasmania.: Department of Primary Industries, Water and Environment, Tasmania.

MINERAL RESOURCES TASMANIA 2011 Digital Geological Atlas 1:250,000 Scale Series. Digital Geology Data. Mineral Resources Tasmania.

MOORE C. L., et al. 2014 Greater Launceston Area Hydrogeological Landscapes Stage 2 Project Report. Canberra: Dryland Salinity Hazard Mitigation Program.

STACEY A. R. & BERRY R. F. 2004 The structural history of Tasmania: a review for petroleum explorers., PESA Eastern Australasian Basins Symposium II, pp. 151-162.

Regolith of the Capricorn region of Western Australia; geomorphic provinces and mineral exploration

R. L. Thorne[1], R. Anand[1], S. Spinks[1], N. Reid[1]

[1]CSIRO Mineral Resources, ARRC, Kensington, Western Australia

The Capricorn Orogen of Western Australia represents a relatively underexplored area for mineral exploration. Little work has been undertaken to determine regolith evolution and its impact upon mineral exploration. Large scale sample transects across the region (Fig. 1) combined with detailed case studies have resulted in the recognition of 4 major regolith geomorphic provinces. The west of the region is comprised of exposed crystalline basement, thin litho-soils dominate and granitic tors are common in a dissected landscape. In contrast the south west of the region is deeply weathered, with thick saprolite developed over both sediments and volcanics. Ferruginous nodules and pisoliths are present at surface and weathering profiles capped by duricrust are common. Thick (>100 m) paleochannel sequences are found throughout the area, these are represented by mottled clays and sands. The lithologies in the north of the area are dominated by Mesoproterozoic basin sediments and can be split into two geomorphic provinces. The upland basin regions are highly dissected and possess different generations of ferruginous pisoliths and nodules, commonly located on the flanks of hills, various forms of calcrete are common and silcrete is present, delineating paleodrainage systems. The lowland basins are dominated by hardpan, calcrete and colluvial/alluvial planes below low hills on which basin sediments are exposed.

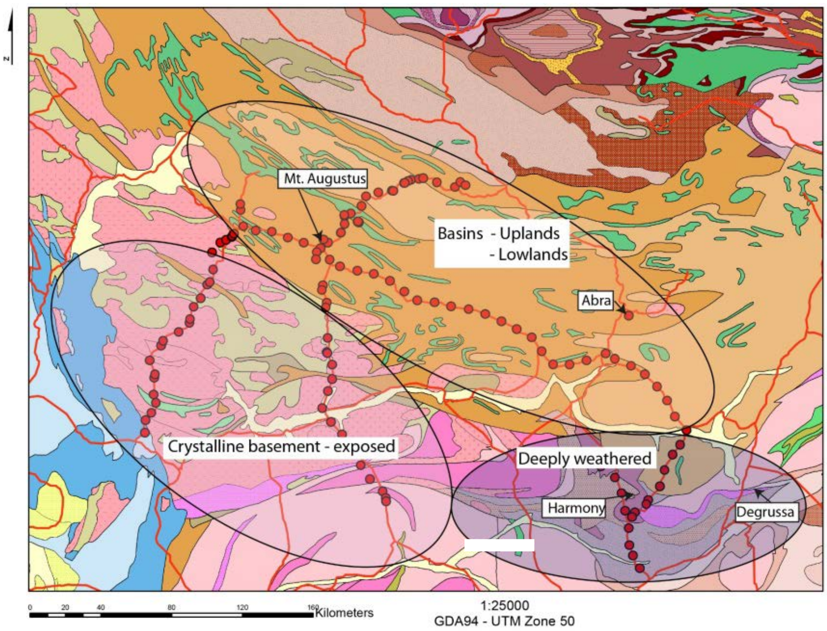

Figure 1. Map of the Capricorn Orogen showing the broad outline of the geomorphic provinces. Red dots represent soil sampling points.

Soil sampling has been undertaken across the four geomorphic provinces in order to establish the relationship to the soil geochemistry. Chromium and V concentrations can differentiate between the different provinces though this is due mostly to the association of these elements with iron oxides which are more abundant in the deeply weathered terrains. The soil samples were split into four different size fractions, with different elements concentrated in the different size fractions (Fig. 2, Fig. 3). Concentrations of V, As and Cr and Fe are higher in the coarser (>2000 µm) size fraction, this is due to iron oxides being found within pisoliths and nodules, these iron oxides adsorb elements such as V, As and Cr leading to the observed elevated concentrations. The fine grained fraction possess higher concentrations of Zn, W, Ni and Bi (Fig. 3).

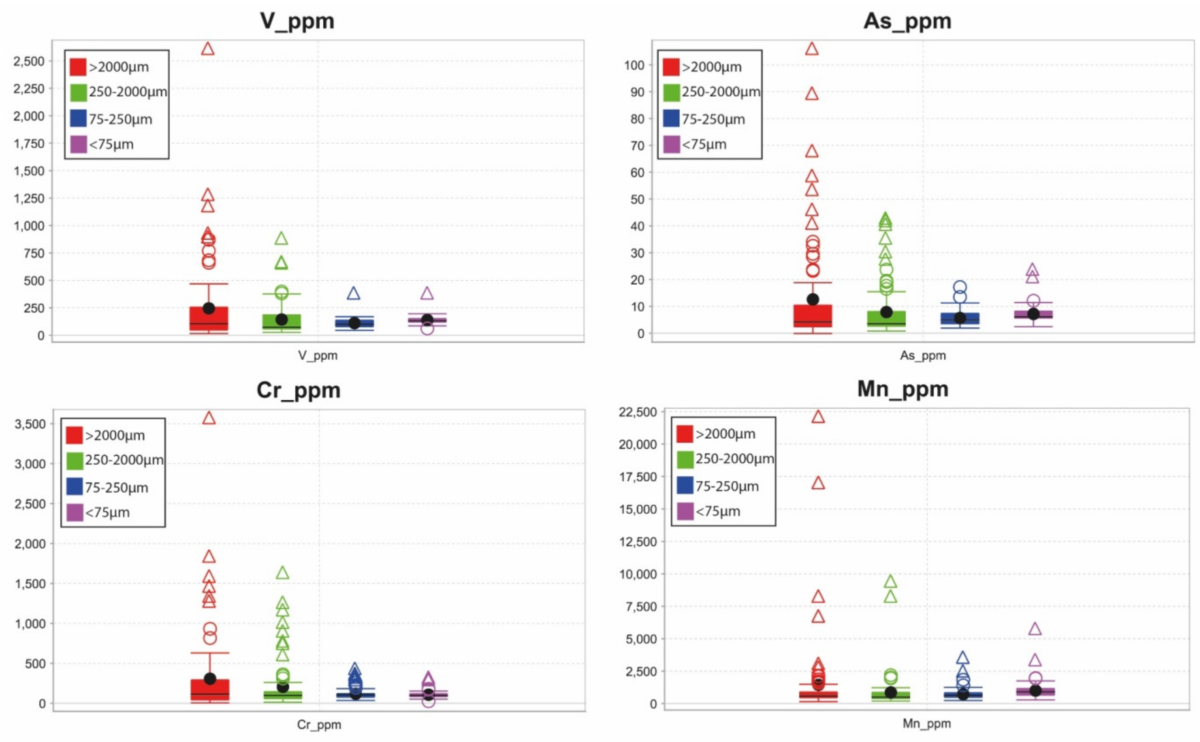

Figure 2. Element concentrations are greater in the coarse (>2000 µm) size fraction. Median value = line, mean = black circle, central box = 50% of the data.

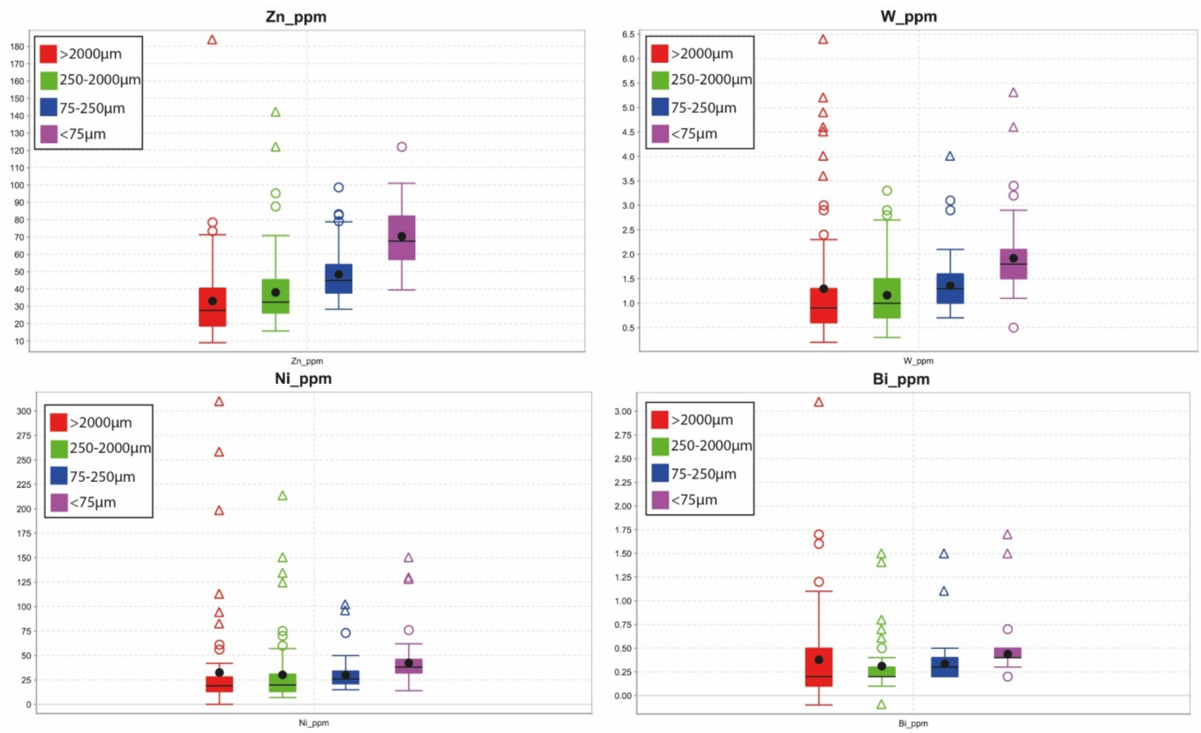

Figure 3. Element concentrations are higher within the fine (< 75 µm) size fractions. Median value = line, mean = black circle, central box = 50% of the data.

This ongoing study of the regolith evolution of the Capricorn region has resulted in the recognition of four major geomorphic provinces, combined with variations in soil geochemistry a template for regolith mapping and mineral exploration in the region can be developed.

Regolith studies and the UNCOVER Initiative at Geoscience Australia

Ian C. Roach, Richard S. Blewett, Karol Czarnota, Patrice de Caritat, Andrew A. McPherson, Anthony J. Meixner, Narelle Neumann, Anthony Schofield, Matilda Thomas and John Wilford

Geoscience Australia, GPO Box 378, Canberra ACT 2601

The UNCOVER Initiative and Geoscience Australia

In 2012 the Australian Academy of Science released the document *Searching the Deep Earth: A vision for exploration geoscience* (Australian Academy of Science, 2012), which summarised the Academy's 2010 Theo Murphy Think Tank discussions on the future of the Australian minerals industry. This was released by the Academy as the UNCOVER Initiative and was adopted as part of the National Mineral Exploration Strategy by the Council Of Australian Governments in 2012 (COAG, 2012), and is now part of Geoscience Australia's work program. This strategy has been endorsed by AMIRA under *P1162 Unlocking Australia's hidden potential: An Industry Roadmap – Stage 1* (AMIRA, 2015).

The UNCOVER Initiative recognises that it is becoming increasingly difficult to discover near-surface mineral resources in Australia, and our continuing prosperity requires effective exploration that leads to new discoveries to provide an ongoing 'pipeline' of resource development. One factor for the decline in exploration expenditure in Australia is the perception that Australia is 'mature', with limited prospects for big new discoveries. The decline in exploration success is in large part due to the difficulty in exploring beneath the highly weathered bedrock (the *regolith*) and sedimentary basins that cover approximately 80 per cent of Australia's landmass.

The ultimate goal of the UNCOVER Initiative is to achieve a step change in knowledge and methodologies in Earth sciences which is relevant to mineral exploration within or beneath the cover, building on earlier work by cooperative research centres (e.g. CRC LEME, pmd*CRC, CRC AMET, AGCRC), Geoscience Australia, CSIRO, State and Territory geological surveys and universities. This will be achieved through the four themes of the Initiative:

1. Characterising Australia's cover
2. Investigating Australia's lithospheric architecture
3. Resolving the 4D geodynamic and metallogenic evolution of Australia
4. Characterising and detecting distal footprints of mineralisation.

The AMIRA *P1162 Unlocking Australia's hidden potential: An Industry Roadmap – Stage 1* document rates understanding the type, age and depth of cover as the number 1 national priority of all its focus Area Themes (AMIRA, 2015).

Geoscience Australia capabilities for UNCOVER regolith-related activities

The Resources Division at Geoscience Australia is at the forefront of research and development aligned with the UNCOVER Initiative and is currently working with partners from the State and Territory geological surveys, universities and the DET CRC to uncover potential new minerals provinces under regolith and basin cover across the continent. This program includes a range of geological, geochemical and geophysical acquisition and modelling activities, underpinning the long association with CRC LEME and the pmd*CRC, both of which expired in 2008.

Low density geochemical mapping

Geoscience Australia continues to work on low density geochemical mapping, building on the National Geochemical Survey of Australia (NGSA) project (Caritat and Cooper, 2011), which itself was founded on pilot projects by CRC LEME (e.g. Caritat and Lech, 2007). Under the NGSA project, catchment outlet sediment samples were collected across Australia to provide pre-competitive data and knowledge to support exploration for energy and mineral resources. The resulting continental-scale geochemical patterns have the potential to identify areas of elevated background or components of large mineral systems. NGSA data and methodologies have also led to more detailed surveys by State Government geological surveys, e.g. the Geological Survey of Queensland Cape York study (Tang, 2015). Most recently higher density, NGSA-compatible low density sampling was carried out to infill the NGSA data in the Southern Thomson Project study area straddling the New South Wales-Queensland border near Hungerford to improve knowledge of the distal footprints of potential mineral systems under regolith and basin cover in that area (Main and Caritat, in prep) and Caritat *et al*. (this volume).

Neotectonics
Identification and characterisation of neotectonic structures is significant as they have potential impacts on current- and palaeo-groundwater and surface water systems. These are important for understanding potential secondary dispersion pathways, both geochemical (e.g. groundwater dispersion) and mechanical (e.g. placer deposits). In addition, neotectonic structures may also impact the distribution and thickness of regolith or sediments overlying basement, contributing to variability in cover thickness (e.g. folding resulting in stripping and redistribution of overlying sediments) and again influencing potential dispersion pathways by controlling lateral variability in cover characteristics (e.g. permeability, porosity).

Multi-component regolith modelling
Geoscience Australia is developing new modelling algorithms to join disparate point estimates of thickness of regolith cover, and depth to geological surfaces, using machine learning. These data may be point estimates from geological and geophysical data, and modelled regolith thickness developed using multivariate statistical analysis. The aim of this project is to develop new nation-wide maps of regolith and basin cover thickness, and depths to stratigraphic interfaces, using available data.

Active seismic methods
Geoscience Australia has a high-resolution seismic reflection and refraction capability using an in-house 48-channel seismic acquisition system. This system uses either a sledge hammer or 40 kg accelerated weight drop as an energy source and recent testing shows that the accelerated weight drop energy source can be detected at far offsets of up to 1.2 km for seismic refraction acquisition, making it possible to detect the density contrast between basin cover and igneous or metamorphic basement up to ~500 m below the ground surface. The weight drop source is also used for high-resolution seismic reflection work. More powerful vibroseis energy sources are available through the Australian National Seismic Imaging Resource (ANSIR), allowing high-resolution mapping of regolith and basin cover to depths of over 1 km.

Passive seismic methods
Geoscience Australia has an in-house, near-surface passive seismic capability and is able to access the passive seismic acquisition resources of ANSIR. Passive seismic seismometers may be deployed as spiral arm arrays, or as single stations, and the results are modelled to produce weathering thickness, depth to lithostratigraphic interface and depth to basement soundings.

Airborne electromagnetics
Geoscience Australia provides leadership of airborne electromagnetic (AEM) data acquisition, processing, modelling and interpretation using data collected by a panel of commercial AEM contractors. Geoscience Australia supervises the AEM data acquisition in a quality assurance and quality control (QA/QC) process and inverts the AEM data using its own algorithms on the National Computational Infrastructure (NCI) supercomputer at the Australian National University. Interpretation products from the inversions are used for a variety of purposes including near-surface under-cover geological mapping, identifying the critical elements of mineral systems, hydrostratigraphic mapping and groundwater advice.

Hyperspectral logging and remote sensing
Geoscience Australia works with CSIRO, State and Territory government partners and the National Virtual Core Library node hyperspectral logging facilities. The HyLogger™ hyperspectral drill core scanning system allows geoscientists to use fast spectroscopic scanning of drill core, chips and other material to identify mineralogy, particularly that which cannot be seen by the human eye. This helps to map and understand mineral systems and distal mineralogical footprints, e.g. Thomas *et al.* (2015) and Laukamp *et al.* (2011).

Geoscience Australia also works with its partners to develop new multispectral and hyperspectral image products to map the mineralogy of Australia's surface (for example the ASTER satellite image products, see http://www.ga.gov.au/scientific-topics/earth-obs/satellites-and-sensors/aster-radiometer/national-aster-maps). Both of these methods are used to develop 2- and 3-dimensional mineralogical models of Australia to detect at- or near-surface weathered bedrock and alteration mineralogy, and to look for distal alteration indicator minerals at the Earth's surface, and in cover.

Magnetotelluric methods

Geoscience Australia works with its State, Territory and university partners to acquire, process and interpret magnetotelluric data, using Geoscience Australia equipment, commercial contractors, ANSIR and AuScope resources. Magnetotelluric data complement resistivity and AEM data by providing a model of the electrical structure of the Earth. Magnetotelluric data are normally used to map the 2- and 3-dimensional electrical conductivity structure of the crust and upper mantle. However; these data are increasingly being used to map near-surface basin features and the basement-cover interface in sedimentary basins that are too deep for adequate electrical resistivity soundings and airborne electromagnetic signal penetration. The technique is also being applied to electrical mapping in areas where there is thick conductive cover which inhibits resistivity and AEM techniques.

Rock properties measurements

Geoscience Australia is providing national leadership for the archiving and delivery of fundamental rock properties data (e.g. density, magnetic susceptibility, porosity, permeability, remanent magnetisation). Rock properties data from surface and drill hole samples are delivered in a machine-readable format via the Rock Properties Explorer website. These data can be explored, selected and downloaded for use in geophysical modelling algorithms to model the 3-dimensional structure of the regolith, basin cover and bedrock. Geoscience Australia is engaged in a program of legacy data discovery and archiving with its State and Territory geological survey partners, the universities and industry, to make these fundamental data available to the public.

Potential fields geophysical modelling

Geoscience Australia is working to develop more accurate geophysical modelling routines to take advantage of the geophysical differences in potential fields (gravity, magnetics) between the generally geophysically bland sedimentary basin cover and more geophysically variable basement rocks. Work is progressing on the benchmarking of geophysical models, especially of magnetic data, against drilling information to test the application of geophysical models to cover thickness mapping.

Point elevation estimates of geological and geophysics surfaces

Geoscience Australia is constructing a new database to store point "Estimates of Geological and Geophysical Surfaces" (EGGS). This database will house point elevation estimates of borehole intersections as well as point elevation estimates of surfaces derived by geophysical observations and modelling. The database will contain metadata to enable points to be linked as a chronostratigraphic surface. The dataset will be used to unify disparate surface elevation estimates with the aim of developing national cover thickness maps.

Stratigraphic drilling

Geoscience Australia is engaged with its State partners in a new program of stratigraphic drilling to learn more about cover and basement sequences in key regional greenfields areas. Drill holes are purpose-designed for each area and may be fully-cored to help characterise the cover sequences, or partially cored to characterise the basement sequences. Samples are taken to describe the distal footprints of mineral systems, learn about element dispersion from the basement through the cover and for mineralogical, geochemical and geochronological analysis to better define basement and cover stratigraphy. Examples of this are in the Stavely and Southern Thomson Projects described below.

Collaborative regional projects

Geoscience Australia is engaged with its state partners in two research projects to encourage mineral exploration in underexplored regions by providing new data on under-cover, potentially mineralised terrains. The research aims to discover a new minerals province under cover of regolith and/or sedimentary basins.

1. Stavely Project

The Stavely Project is a collaborative project between Geoscience Australia and the Geological Survey of Victoria in the Stavely region of western Victoria (Figure 1).

The project seeks to address the challenges of greenfield exploration under areas of younger cover in Australia through the provision of pre-competitive geoscience data and concepts in a Cambrian volcanic arc setting under cover of the Murray Basin and Cenozoic basaltic volcanic rocks. The Stavely Project aims to reduce exploration risk and increase mineral discovery in the Stavely region through the objectives of: characterising the under-cover geology and recognising where major mineral systems may have been active; identifying key elements that demonstrate mineral systems potential; understanding the depth and nature of cover; and, delivering new pre-competitive data and concepts for industry. See Thomas (this volume) for more information on hyperspectral logging results from the Stavely Project drill core.

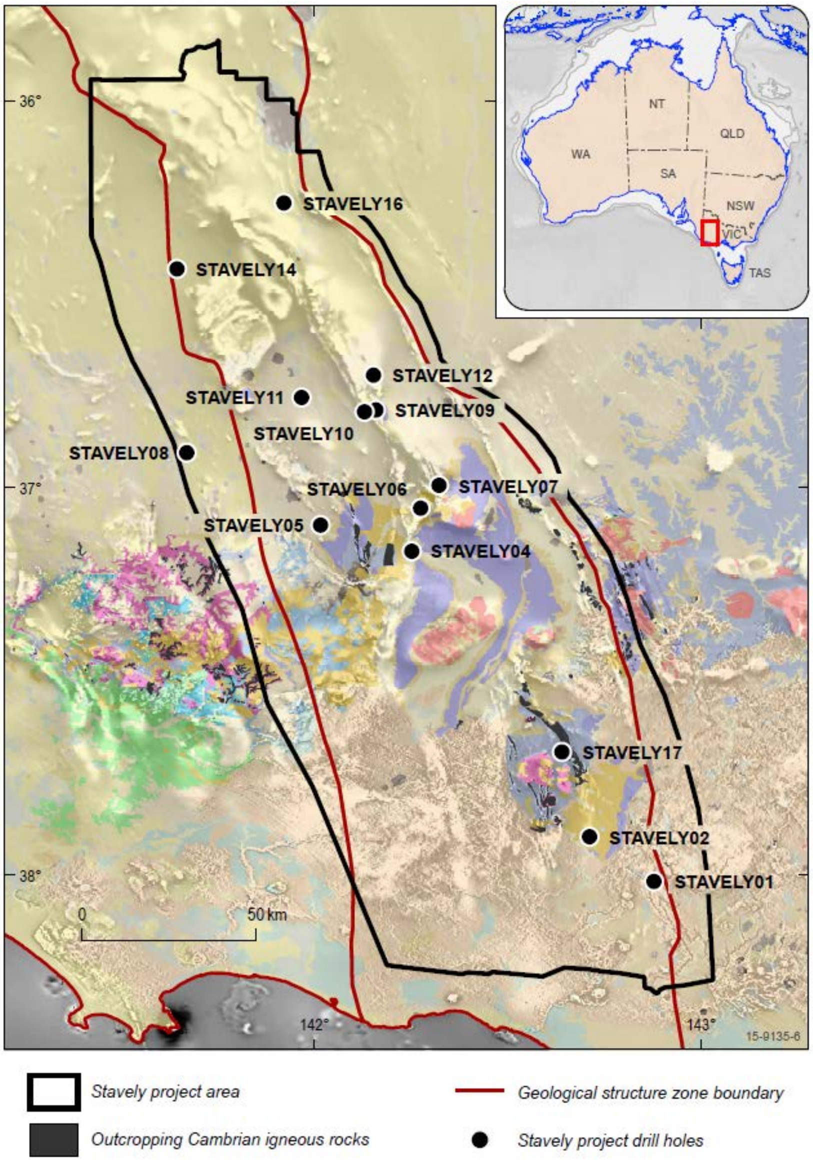

Figure 1: Location map of the Stavely Project showing the locations of new holes drilled for the project. Background: 1:1 million scale Geological Map of Australia (Raymond, 2010) overlain on a first vertical derivative total magnetic intensity greyscale image.

2. Southern Thomson Project

The Southern Thomson Project (Figure 2) is a collaborative project between Geoscience Australia and its partners the Geological Survey of New South Wales and the Geological Survey of Queensland.

The project aims to understand the geology and mineral systems potential beneath the regolith and sedimentary basin cover of the Eromanga and Lake Eyre basins in the border region between New South Wales and Queensland.

The research encompasses new pre-competitive geophysical data acquisition including gravity, magnetotelluric (Broad Band and AMT) and AEM data (see Roach & McPherson, this volume). This complements new geochemical and geochronological data acquisition including low density surface geochemical sampling (see Caritat and Main, this volume) and sampling available drill core.

The Southern Thomson Project will also engage in a stratigraphic drilling program targeting information-poor areas to gain new knowledge of the geology, structural history and mineral potential of the region. The aim is to encourage new mineral exploration into the region by reducing exploration risk and answer the fundamental science question of whether the Thomson Orogen is different from the Lachlan Orogen.

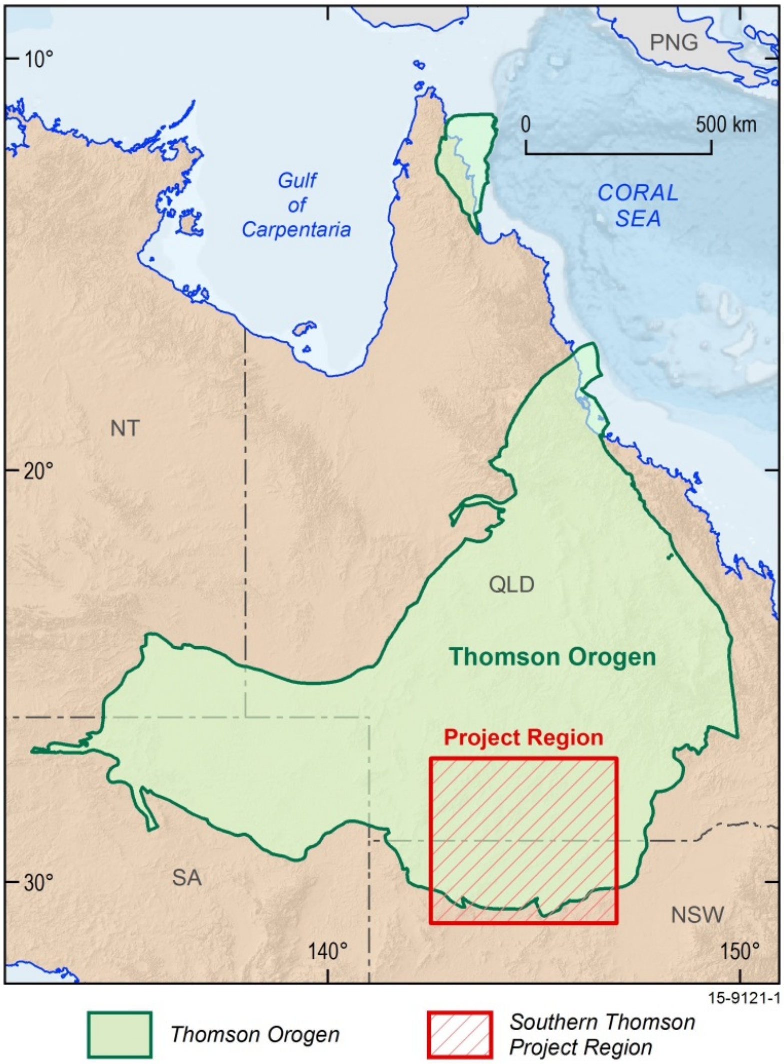

Figure 2: Location map of the Southern Thomson Project area.

Conclusion

Geoscience Australia aims to maintains its leadership of regolith research in Australia, continuing the initial work of the Bureau of Mineral Resources' Regolith Group, and later, the CRC LEME, in applying regolith research to science questions that are important to Australia's social and economic development.

Research at Geoscience Australia is multidisciplinary, including hazard and environmental assessments, geology, geophysics, geochemistry, geochronology, and attempts to answer national-scale problems in characterising the nature and thickness of cover. The work program at Geoscience Australia is closely aligned with the national priorities outlined by AMIRA (2015), most particularly with understanding the type, age and depth of cover.

Acknowledgements

This paper is published with the permission of the CEO, Geoscience Australia. The authors thank reviewer Tim Barton for his constructive comments.

References

AGCRC. Australian Geodynamics Cooperative Research Centre. Online: http://trove.nla.gov.au/people/523526?c=people.

AMIRA, 2015. Unlocking Australia's hidden mineral potential - Stage 1: The Roadmap. Online: http://www.amira.com.au/web/site.asp?section=projects&page=projectdetails&ProjectLink=3065&Source_ID=1.

ANSIR. Australian National Seismic Imaging Resource. Online: http://ansir.org.au/index.php.

AuScope. Online: http://auscope.org.au/site/index.php.

AUSTRALIAN ACADEMY OF SCIENCE, 2012. Searching the Deep Earth. Online: http://www.science.org.au/sites/default/files/user-content/searchingthedeepearth.pdf.

CARITAT, P. D. AND LECH, M. E., 2007. Thomson Region Geochemical Survey, Northwestern New South Wales. Cooperative Research Centre for Landscape Environments and Mineral Exploration. Open File Report 145, 1021 pp. Online: http://crcleme.org.au/Pubs/OPEN%20FILE%20REPORTS/OFR%20145/OFR%20145.pdf.

CARITAT, P. D. AND COOPER, M., 2011. National Geochemical Survey of Australia: The Geochemical Atlas of Australia. Geoscience Australia, Canberra. Record 2011/020, 557 pp. Online: https://www.ga.gov.au/products/servlet/controller?event=GEOCAT_DETAILS&catno=71973.

COAG, 2012. Council of Australian Governments National Mineral Exploration Strategy. Online: https://scer.govspace.gov.au/files/2012/12/National-Mineral-Exploration-Strategy.pdf.

CRC AMET. Cooperative Research Centre for Australian Mineral Exploration Technologies. Online: http://www.eoas.info/biogs/A001920b.htm.

CRC LEME. Cooperative Research Centre for Landscape Environments and Mineral Exploration. Online: http://crcleme.org.au.

LAUKAMP, C., CUDAHY, T., THOMAS, M., JONES, M., CLEVERLEY, J. S. AND OLIVER, N. H. S., 2011. Hydrothermal mineral alteration patterns in the Mount Isa Inlier revealed by airborne hyperspectral data. Australian Journal of Earth Sciences 58(8), 917-936.

MAIN, P. T. AND CARITAT, P. d., in prep. Geochemical survey of the southern Thomson Orogen, southwestern Queensland and northwestern New South Wales: The chemical composition of surface and near-surface catchment outlet sediments. Geoscience Australia, Canberra.

NGSA. NATIONAL GEOCHEMICAL SURVEY OF AUSTRALIA. ONLINE: http://www.ga.gov.au/about/what-we-do/projects/minerals/concluded/national-geochemical-survey.

PMD*CRC. PREDICTIVE MINERAL DISCOVERY COOPERATIVE RESEARCH CENTRE. ONLINE: HTTP://WWW.PMDCRC.COM.AU/.

RAYMOND, O. L., 2010. Surface geology of Australia 1:1 000 000 scale. Geoscience Australia, Canberra. 2010. Online: http://www.ga.gov.au/mapconnect/.

ROCK PROPERTIES EXPLORER. GEOSCIENCE AUSTRALIA ROCK PROPERTIES DATA DELIVERY WEBSITE. Online: http://www.ga.gov.au/explorer-web/rock-properties.html.

SOUTHERN THOMSON PROJECT. Online: http://www.ga.gov.au/scientific-topics/minerals/unlocking-resource-potential/southern-thomson.

STAVELY PROJECT. ONLINE: http://www.ga.gov.au/scientific-topics/minerals/unlocking-resource-potential/stavely-project.

TANG, J., 2015. Geochemistry of the Cape York Peninsula - a revived exploration frontier. In: Digging Deeper 2015, Brisbane. Geological Survey of Queensland.

THOMAS, M., SCHOFIELD, A., GORDON, G., DUNCAN, R. AND HAYDON, S., 2015. Regional geology and mineral systems of the Stavely region, western Victoria: data release 2 – HyLogger data and catalogue. Geoscience Australia, Canberra. Record 2015/27. Online: http://www.ga.gov.au/metadata-gateway/metadata/record/gcat_84572.

Detection of zinc deposits using surface ferromanganese crusts in a semi-arid environment

Sam Spinks[1]*, Yulia Uvarova[1], Robert Thorne[1], Ravinder Anand[1], Nathan Reid[1]

[1] CSIRO Mineral Resources, Australian Resources Research Centre, 26 Dick Perry Avenue, Kensington, WA 6151, Australia.

Abstract

Ferromanganese (FM) crusts, coatings of manganese and iron oxide minerals, occur in various forms on a broad range of surface materials in the subaerial environment (Figure 1). Manganese oxide minerals in particular, have very high adsorption capacities for heavy metals and trace elements (Chao and Theobald 1976; Manceau *et al*. 2007). Thus in the scenario whereby metals from ore deposits are liberated and mobilized to the surface and interact with ferromanganese crusts, there is potential for such crusts to adsorb anomalous concentrations of target and pathfinder elements, thereby offering a potential sampling medium during geochemical exploration.

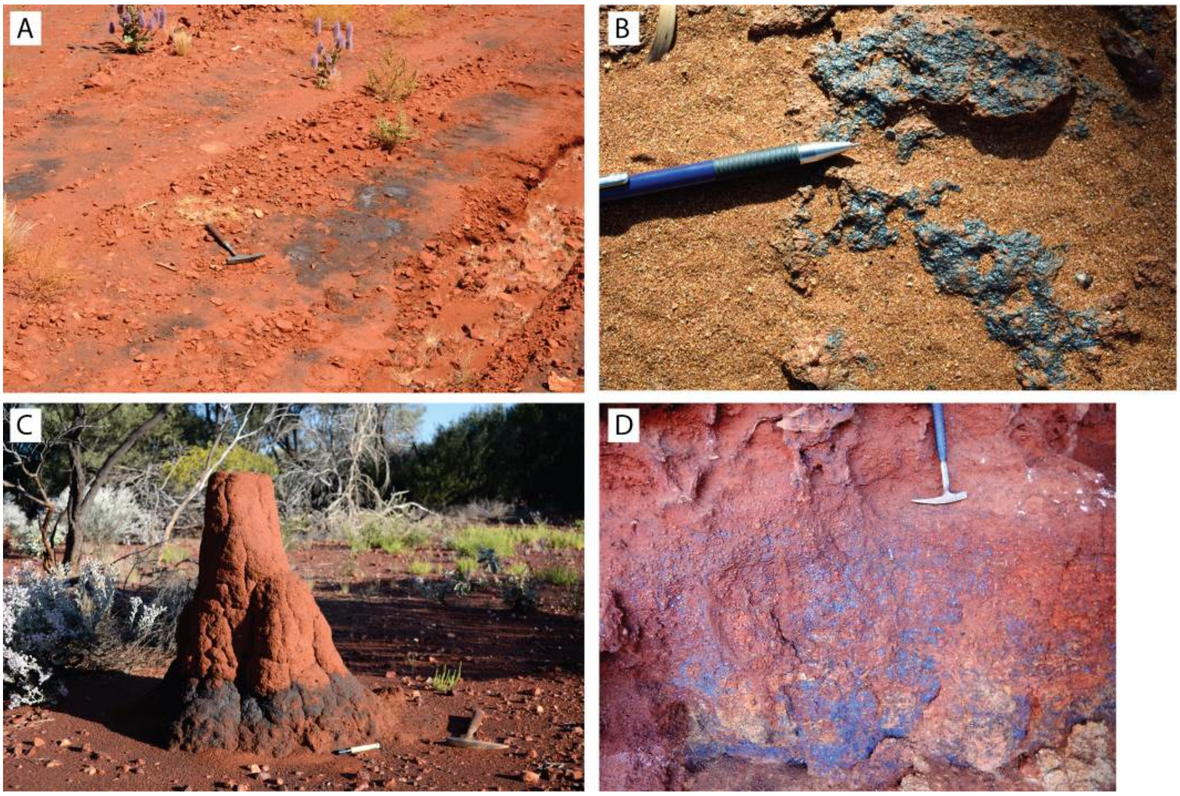

Figure 1. Typical occurrences of ferromanganese crusts on surface media in the Capricorn Orogen of WA. A: FM crust on recently graded road surface. B: Subcropping sandstone with FM crust exposed at surface. C: Termite mound with FM crust at base. D: Hardpanised alluvium with widespread FM crust on exposed surfaces.

Demand for mineral resources growing, the rate of giant discoveries is falling, but the depth at which discoveries are being made is increasing. In Australia, a major producer of mineral resources, ~80% of the surface is covered by regolith and most/all outcropping mineralization has been discovered. For new discoveries to be made, new methods and technologies are required to facilitate exploration through cover. Here we present results on the use of ferromanganese crusts as a potential exploration medium in areas of variable cover.

Two case studies were undertaken at known Zn-bearing base metal deposits, Abra and Prairie-Wolf (Figure 2) in the Capricorn Orogen terrane in Western Australia, where ferromanganese crusts are abundant at surface. Elemental mapping and microprobe analysis identified alternating laminae of Fe and Mn oxide minerals in the crusts, and confirm the presence of Zn preferentially in

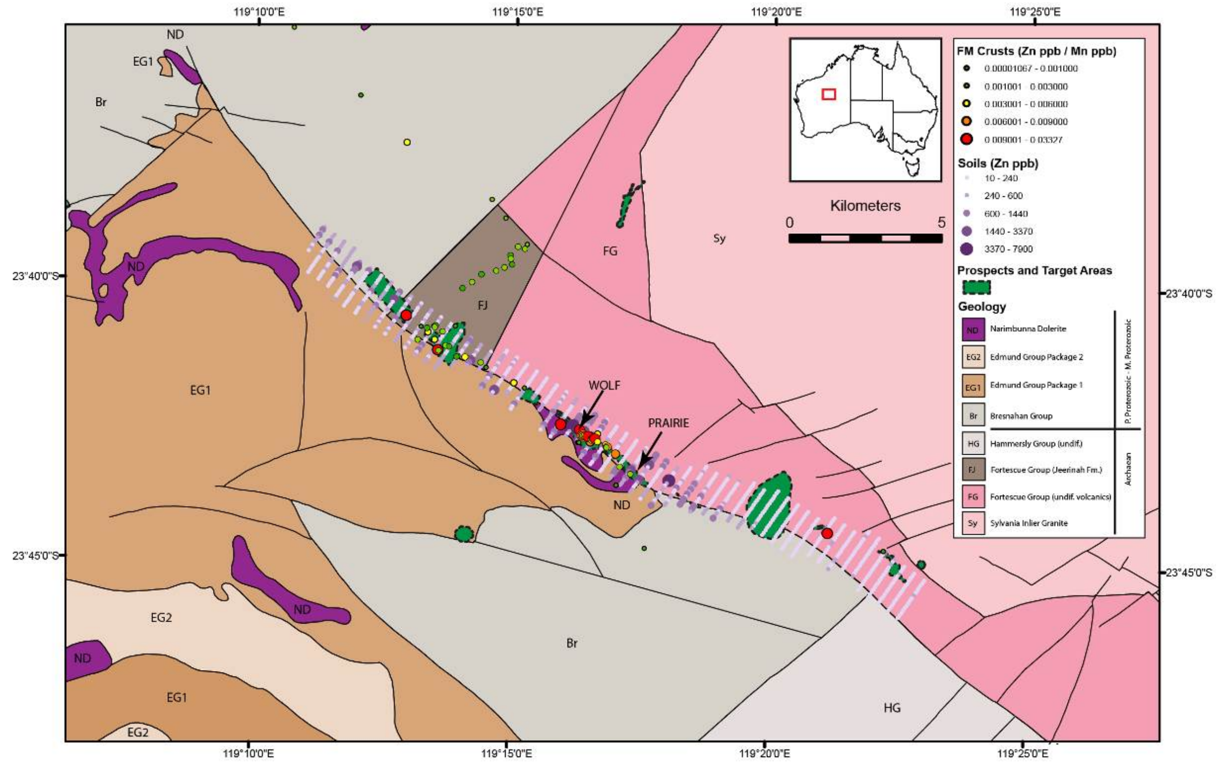

Figure 2. Results from Abra showing Zn anomalism in soils, and Zn/Mn ratios in FM Crusts.

Mn oxide layers. Selective leaching of Mn oxides (Chao 1972) within ferromanganese crusts followed by ICP-MS analysis yielded a broad range of results. High Zn/Mn ratios (>6*10-3) were returned from crusts proximal to the Prairie-Wolf deposits (Figure 2, 3, 4), and ratios in crusts decreased to as low as <1*10-3 with decreasing proximity to the mineralization.

Ferromanganese crusts directly overlying mineralization at Abra, however, yielded low Zn/Mn ratios. This is interpreted be a function of limited vertical mobilization of metals and preferential Mn scavenging in soils (Figure 3 next page). Our results suggest deep geochemically-blind deposits remain difficult to detect, but the analysis of ferromanganese crusts from semi-arid environments can be used to detect relatively shallow base metal mineralization (Figure 4, on page 102).

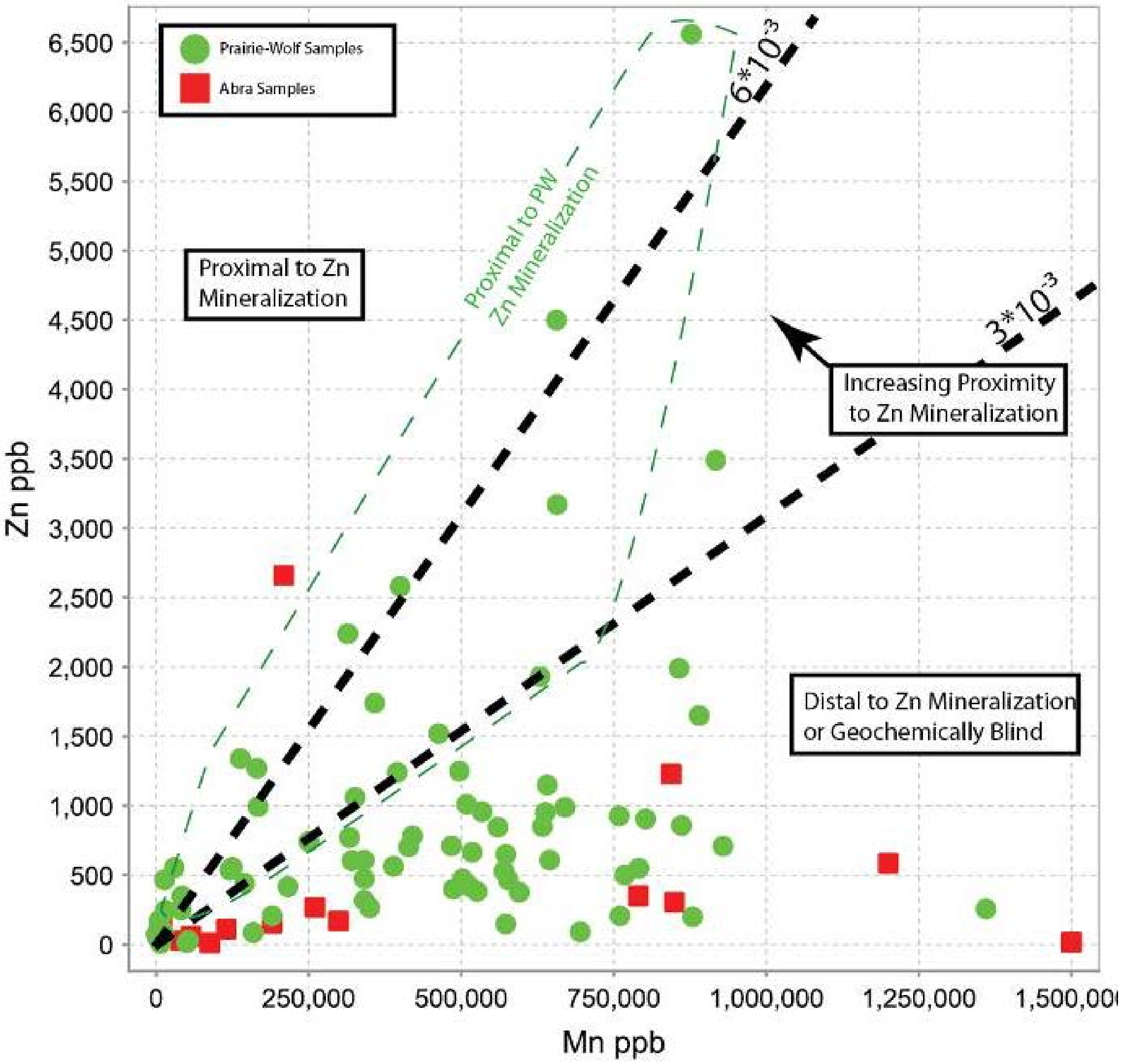

Figure 3. Crossplot of Zn and Mn in FM crusts showing positive correlation in samples proximal to known mineralization. Ratios can offer a baseline for proximity to Zn anomalies at surface during geochemical exploration.

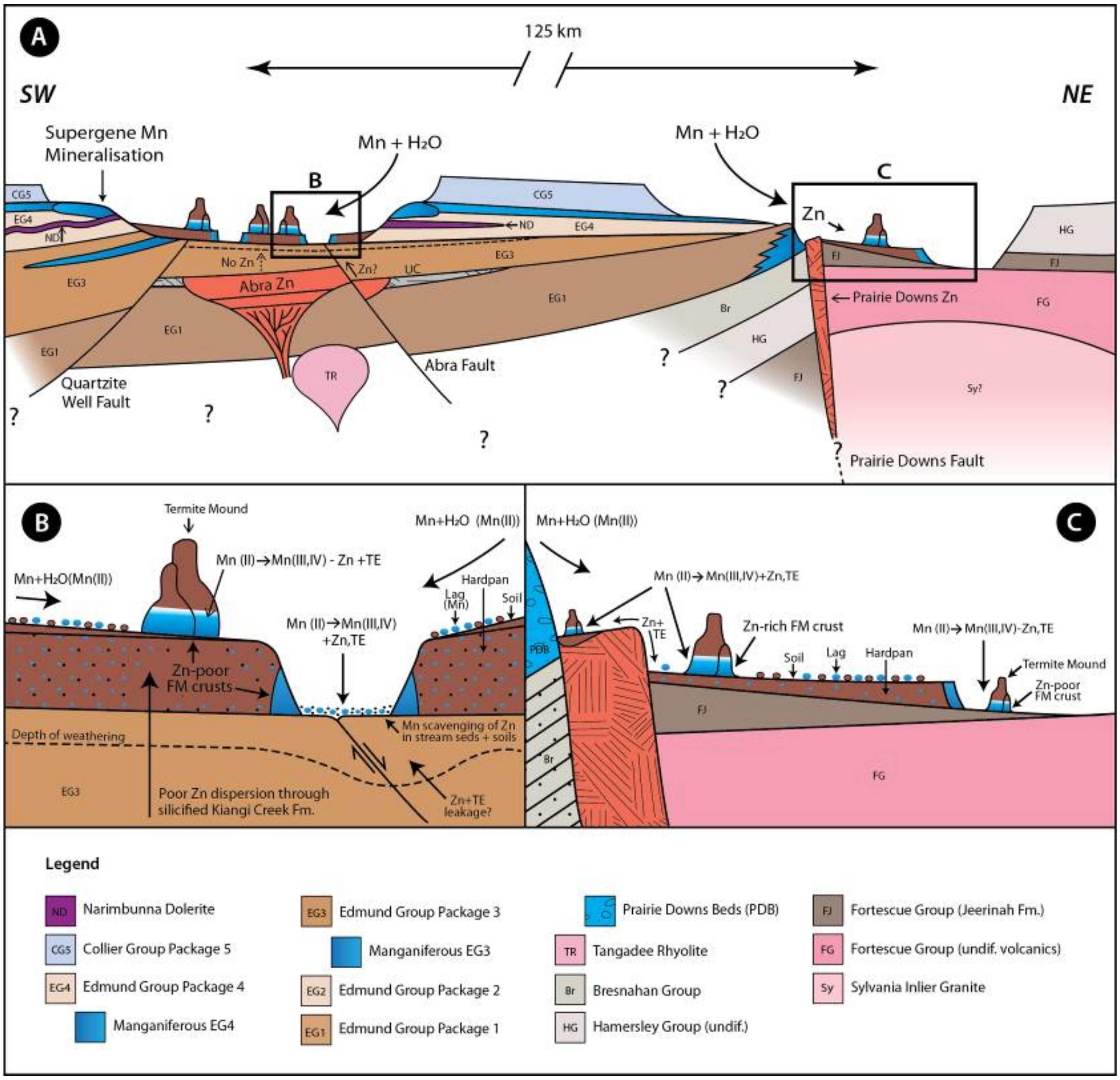

Figure 4. Proposed model of Mn cycling in the Capricorn Orogen and Zn adsorption onto Mn oxide minerals. A: Summary cross section of the geological framework with Abra and Prairie-Wolf Zn deposits. B: Schematic of Mn cycling at surface at Abra showing preferential Mn scavenging of Zn in soils. C: Schematic of Mn cycling at Prairie-Wolf showing Zn adsorption onto FM crusts proximal to the known deposits.

References

Chao, T. T., and Theobald Jnr., P. K. 1976. The significance of secondary iron and manganese oxides in geochemical exploration. Economic Geology, 71, 1560-1569.

Chao, T. T. 1972. Selective dissolution of manganese oxides from soils and sediments with acidified hydrochloride. Soil Science Society of America Proceedings, 36, 764-768.

Manceau, A., Lanson, M. & Geoffroy, N. 2007. Natural speciation of Ni, Zn, Ba, and As in ferromanganese coatings on quartz using X-ray fluorescence, absorption, and diffraction. Geochimica et Cosmochimica Acta 71, 95-128.

Mars analogues of the Monaro Volcanic Province

Ian C. Roach[1], Jonathan D. A. Clarke[1] and Steven W. Hobbs[1,2]

[1]Mars Society Australia, PO Box 327, Clifton Hill, Victoria 3068
[2]School of Physical, Environmental and Mathematical Sciences, University of New South Wales Canberra, Australian Defence Force Academy, Northcott Drive, Canberra, Australian Capital Territory 2600

Introduction

The landscapes of planet Mars are tantalizing to Earth-bound geologists and geomorphologists who are constantly seeking Earthly analogues for objects they see on the *Red Planet*. The surface of Mars, by the fact that it is not covered by water bodies, is better mapped than the surface of the Earth! The numerous complex robots now traversing the surface of Mars (one for over a decade), and satellites orbiting it, offer clues to the composition of Mars, but lack the ability to bend over, pick up a rock, look at it and think about it like a human can.

Planetary scientists are always on the lookout for features on the Earth that can be used to explain surface features that are seen on the other terrestrial (rocky) planets and moons (Mercury, Venus and Mars, the Earth's Moon), but also the features of the icy moons of the gas giant planets, dwarf planets, the larger asteroids, comets and Kuiper Belt objects. The Monaro Volcanic Province (MVP) is an ideal Mars analogue because it contains many geological and geomorphological features and processes that are known to occur on Mars, and it is also essentially treeless making it appear even more Martian. This paper describes a planetary science day trip to the MVP where relatively easily accessible sites are used as analogues to illustrate for processes occurring on Mars and other terrestrial planets, and to generate discussion on extra-terrestrial geology.

The Monaro Volcanic Province

The MVP is one of a large number of Cenozoic intraplate volcanic provinces located along the eastern margin of Australia and is more approachably described by Brown *et al*. (1992, 1993), Lewis *et al*. (1994), Roach *et al*. (1994), Roach (1996, 1999) and Taylor and Roach (2003). These volcanic provinces occur in an zone stretching along the highlands from Mount Gambier in South Australia through Victoria (including northern Tasmania), eastern and central New South Wales, Queensland and the Torres Strait. Volcanism is thought to be related to post-Gondwanan passive margin continental rifting and tectonic plate motion (refer to Johnson 1989 for a synthesis of ideas). The MVP lies in the NSW Southern Highlands roughly between Cooma, Nimmitabel, Bombala, Dalgety and Berridale, approximately 120 km south of Canberra. Potassium-Argon ages on basalts indicate a maximum age of *ca*. 54.4 Ma (Taylor et al. 1990) and a minimum age of *ca*. 34 Ma (Wellman and McDougall 1974). Palynological ages on sub-basaltic sediments indicate a maximum depositional age of volcanism of *ca*. 58-60 Ma (Taylor et al. 1990). Volcanic eruptions occurred in a variety of styles creating fissure-fed lava shields and scoria cones, and tuff rings or maars in water-logged areas (Brown *et al.* 1993; Roach *et al*. 1994). Extensive intra-basaltic weathering profiles occur throughout the MVP, including thick bauxitic weathering horizons on flow tops (Brown et al. 1992, Taylor *et al.* 1992).

The MVP is now an eroded landscape dominated principally by grasslands, typical of many intraplate basaltic lava fields in the temperate and semi-arid zones world-wide. Native trees (principally *Eucalyptus pauciflora* or snow gum; Costin 1954), where they occur at all, tend to be restricted to the southern or southeastern facing sides of basaltic hills and valleys as sparse savannah woodlands, rooted into solid bedrock on the basalt. Elsewhere, the landscape is dominated by *Stipa sp*. grasslands, except where inliers of Ordovician-Silurian country rock appear through the basalt; these tend to more heavily vegetated as savannah woodland or dry sclerophyll forest (Costin 1954). The exact cause of this relative treelessness is the subject of much debate, although it is not due to land clearing, given that the first European to visit the area (Captain Mark Currie RN) reported on the extensive grassy "traps" (Currie 1825). The paucity of vegetation lends an other-worldly appearance to the MVP, making it all the more useful as a Mars analogue and natural teaching laboratory.

The landscape is now one of a trap or steppe, with numerous sub-horizontal lava flow remnants forming a terraced landscape incised by gullies (see Hobbs *et al*. this volume), creeks and rivers (Taylor and Roach 2003). The terraces are composed of individual weathering profiles on one or more lava flow tops (Roach 1999) and are also marked by numerous shallow deflation lakes

(Pillans and Walker 1987). Within the lava pile the landscape is punctuated by hills, many of which are the remains of eroded volcanoes now seen as volcanic plugs lying above major crustal-scale fault systems that have controlled the magmatic plumbing (Roach 1996, 1999, Roach *et al*. 1993). The volcanic plugs frequently contain crustal and upper mantle inclusions including Paleozoic country rocks, granulites and peridotites, as well as copious amounts of kaersutite amphibole (Roach 2004). Rarely, remnants of scoria cones and tuff beds are preserved in the sides of volcanic plugs and even rarer are hyaloclastite and pillow lava deposits, formed when lavas flowed into lakes perhaps formed by lava dams during the eruptive life of the MVP (Brown *et al*. 1993).

Examples of Mars analogues

The MVP contains many sites that can be used as analogues to demonstrate surface processes occurring on Mars and other terrestrial bodies including Mercury, Venus and the Earth's Moon. A number of well-known field sites are used to illustrate volcanic and weathering processes and engender discussion on planetary geology, plate tectonics, the driving forces of volcanism on Earth and other bodies, the rock cycle, weathering processes and landscape evolution processes (Roach and Clarke 2013a, b). Some of the sites and concepts are described below.

Hudsons Peak area, Coonerang

The Hudsons Peak area (Figure 1) is a great introduction to the MVP and natural teaching laboratory for learning about intraplate volcanism, weathering and erosion. Here we describe the historical and geological setting of the MVP in the southern Highlands of New South Wales and as part of the larger system of volcanism in eastern Australia. Using the examples on site, discussion centres on the causes of volcanism on terrestrial planets and their satellites, what other kinds of volcanism occurs throughout the solar system, what controls where volcanoes occur, how magma composition controls what style of volcanism occurs and how rock weathering shapes a volcanic landscape. A short drive back down the road stops at an exposure of intra-flow bauxite, where we discuss rock weathering and the process of bauxitisation in detail, but also how we might use surface materials on other planets to build complex infrastructure—does Mars have bauxite? Numerous small volcanic plugs dot the landscape around Hudsons Peak; here we discuss the processes of building volcanic edifices and how satellite vents form in association with major eruption sites, how weathering and erosion create the landscape we see today and how similar landforms on Mars could evolve. Some of the smaller volcanic plugs contain mantle and crustal inclusions, engendering discussion on how it is possible to sample the interior of a planet or satellite and learn about its three-dimensional structure. A brief stop at a well-formed deflation lake completes this site, where the processes of weathering and wind erosion are discussed, processes that are all too common on Mars.

Myalla Road area, The Brothers

The Myalla Road site (Figure 1) provides a cross-section through the lava pile of the MVP and is a useful site to discuss the volcanic stratigraphy of lava fields, how intraplate volcanic piles are constructed and how their chemistry changes as volcanism progresses, how marker horizons are used to map stratigraphy, and rock weathering and the development of mineral pseudomorphs (also described by Taylor and Roach 2003). The site sits underneath South Brother, one of the three volcanic plugs of The Brothers hills that dominate the local landscape south of Cooma. At this site the Cooma Creek valley hosts spectacular gully erosion features that have been compared to gully erosion features on Mars (see Hobbs *et al*., this volume). The site also has a spectacular view northwards along Cooma Creek towards Cooma.

Hazeldean Plug, Arable

The Hazeldean Plug (Figure 1) is a volcanic plug first described by Lambert and White (1965) and is the first known eruption point of the ankaramite (coarse pyroxene-rich) lavas that form a distinctive marker horizon within the lava pile of the MVP. The plug erupted through the local granite country rock (Berridale Batholith; White *et al*. 1977), and lavas from this vent, or others in the local area, buried the ancient weathered granitic landscape under thin lava flows. The ancient landscape is now being exhumed by weathering and erosion, revealing the torfields of the Berridale Batholith from underneath terraced lava flow remnants on the hillsides, and also small lava buttes on the plains. The site contains a number of features that provoke discussion about the landscape evolution of lava fields including the remnants of small sub-basaltic streams, now preserved as silcreted quartz sand and gravel, and "bole" which is interpreted as baked soil (Taylor and Smith

1975), perhaps developed on muddy overbank sediments. The site is useful for demonstrating landscape evolution and regolith induration as well as relief inversion in volcanic terrains.

Wambrook Hill, Rhine Falls

To complete the day the tour ends at Wambrook Hill near Rhine Falls, where ankaramite lava is interpreted to have flowed down an ancient gully with well-developed fanglomerate deposits. The site is a great demonstration of relief inversion, where what was once in the bottom of the landscape (the lava flow) is now at the top. Topographically-inverted landscapes are common on Mars, where indurated fluvial sediments may be seen as ridge tops and lava flows have created their own relief, as is commonly seen around volcanoes on the Earth. Fanglomerates have been documented on the surface of Mars, for example in imagery from the floor of Gale crater (Williams *et al.* 2013). Similar examples of interaction between fluvial and volcanic facies are likely on Mars.

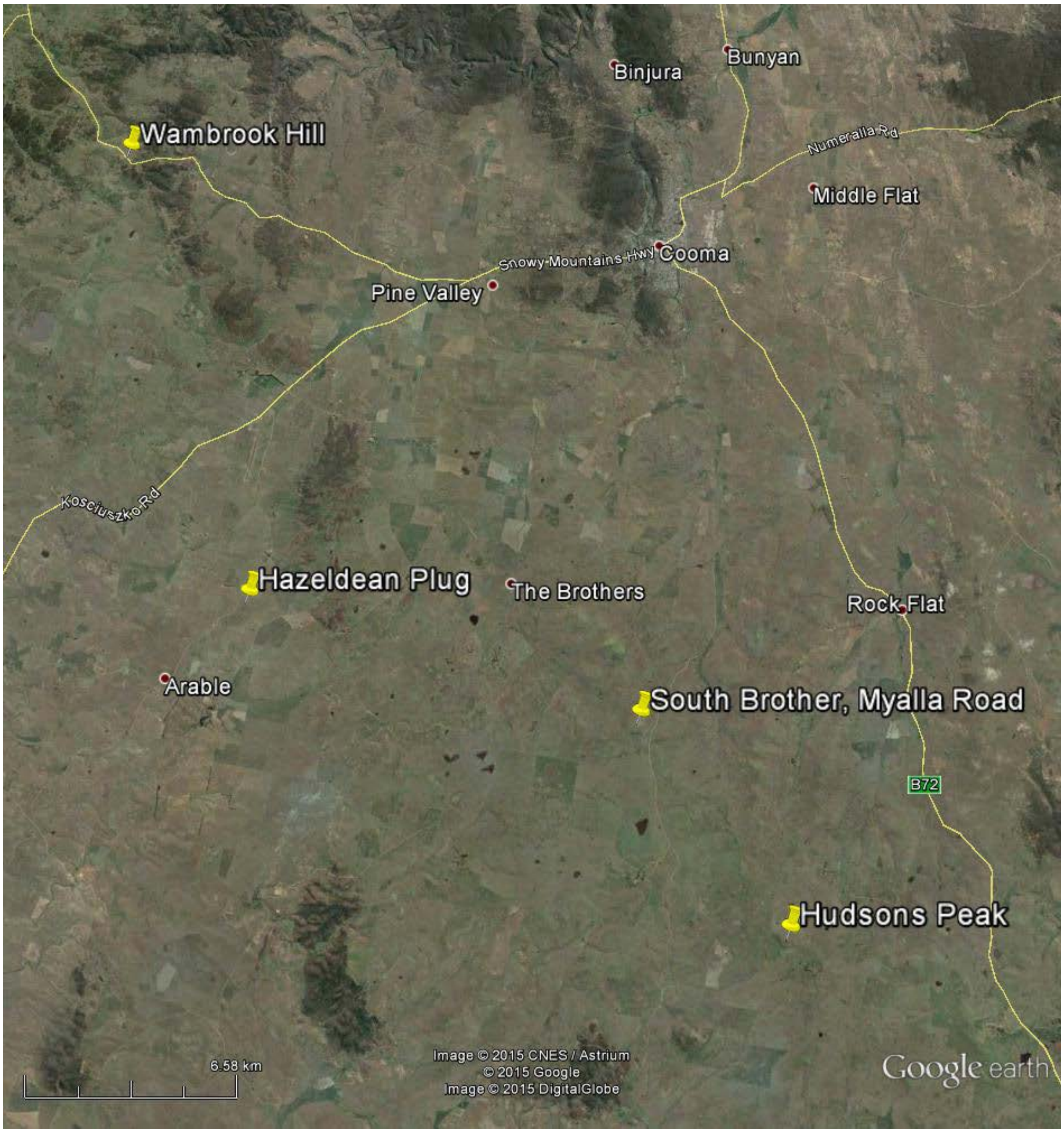

Figure 1: Location map of the Cooma area showing the field sites discussed in this paper. Many of the sites are on private property and landholder permission must be sought before entry. Source: Google Earth.

Conclusions

The MVP is a wonderful natural teaching laboratory where many sites demonstrating different volcanic and regolith processes are publicly accessible, or are available to groups on consultation with the friendly landholders. All are within easy reach of day trips from Canberra. The landscapes bear many similarities to eroded landscapes on Mars and help set the context for landscapes on Mars that may not be visited for some decades or centuries into the future. The advent of higher-resolution remote sensing technology on spacecraft forces us to look more closely at the Earth to understand the processes that are occurring on other planets and their satellites. While the materials may be different on some of the planets and their satellites (for example, cryovolcanism on Pluto and Triton powered by liquid methane or ammonia creating scoria cones of water ice; Cook *et al.* 2010, Witze 2015), the processes remain similar, and Earthly analogues can be used to explain them.

Acknowledgements

We are grateful for the knowledge so graciously imparted over many years by researchers at the University of Canberra and the Australian National University including Graham Taylor, Max Brown, Tony Eggleton, Brad Pillans, John Field and Ken McQueen. The authors gratefully acknowledge the support of the local landholders including the Litchfield family and the Tozer family for continually, over many years, allowing access to various sites.

References

BROWN M.C., MCQUEEN K.G. TAYLOR G. 1992. A core through the Monaro basalt: Bega (BMR) No. 7. *Australian Journal of Earth Sciences* **39**, 555-559.

BROWN M.C., MCQUEEN K.G., ROACH I.C. & TAYLOR G. 1993. *IAVCEI Canberra 1993 Excursion Guide: Monaro Volcanic Province*. Australian Geological Survey Organisation **Record 1993/61**.

COOK J-R.C., BROWN D.C. AND LAUSTSEN P. 2010. Cassini Spots Potential Ice Volcano on Saturn Moon. NASA-Jet Propulsion Laboratory California Institute of Technology, Cassini Solstice Mission. Online: http://saturn.jpl.nasa.gov/news/newsreleases/newsrelease20101214/.

COSTIN A.B. 1954. *A study of the ecosystems of the Monaro region of New South Wales*. Soil Conservation Service of New South Wales, Sydney.

CURRIE M.J. (Capt. R.N.) 1825. Journal of an excursion to the southward of Lake George. In: Field, B. ed. *Geographical Memoirs of New South Wales*. Sydney.

JOHNSON R.W. ed. 1989. *Intraplate Volcanism in Eastern Australia and New Zealand*. Cambridge University Press.

LAMBERT I.B. AND WHITE A.J.R. 1965. The Berridale Wrench Fault: an major structure in the Snowy Mountains of New South Wales. *Journal of the Geological Society of Australia* **12(1)**, 25-33.

LEWIS P.C., GLEN R.A., PRATT G.W. AND CLARKE I. 1994. *Bega-Mallacoota 1:250,000 geological sheet explanatory notes*. Geological Survey of New South Wales, Sydney.

PILLANS B.J. AND WALKER P.H. 1987. Lake shadows: aeolian clay sheets associated with ephemeral lakes in basalt terrain, southern New South Wales. *Search* **18**, 313-315.

ROACH I.C. 1996. The formation of the Monaro Volcanic Province, southeastern NSW, Australia. *Chapman Conference on Long Lava Flows, Townsville, Australia.* 60-61.

ROACH I.C. 1999. *The Setting, Structural Control, Geochemistry and Mantle Source of the Monaro Volcanic Province, southeastern New South Wales, Australia*. University of Canberra PhD Thesis, unpublished.

ROACH I.C. 2004. Mineralogy, Textures and P-T Relationships of a Suite of Xenoliths from the Monaro Volcanic Province, New South Wales, Australia. *Journal of Petrology* **45(4)**, 739-758.

ROACH I.C. AND CLARKE J.D.A. 2013a. *Analogues for terrestrial volcanism: the Monaro Volcanic Province*. Notes for a Mars Society Australia field trip for the American Institute of Aeronautics and Astronautics, unpublished.

ROACH I.C. AND CLARKE J.D.A. 2013b. The Monaro volcanics as Mars analogues. *LAVA News: Newsletter of the Learned Australasian Volcanology Association, Geological Society of Australia* **25(February 27)**, 9-11.

ROACH I.C., MCQUEEN K.G. AND BROWN M.C. 1994. Physical and petrological characteristics of basaltic eruption sites in the Monaro Volcanic Province, southeastern New South Wales, Australia. *AGSO Journal of Australian Geology and Geophysics* **15(3)**, 381-394.

TAYLOR G., EGGLETON R.A., HOLZHAUER C.C., MACCHONACHIE L.A., GORDON M., BROWN M.C. AND MCQUEEN K.G. 1992. Cool climate lateritic and bauxitic weathering. *The Journal of Geology* **100**, 669-677.

TAYLOR G. AND ROACH I.C. 2003. Monaro Region, New South Wales. *In:* Anand R.R. and De Broekert eds. Regolith landscape evolution across Australia. Cooperative Research Centre for Landscape Environments and Mineral Exploration, Perth. Online: http://crcleme.org.au/RegLandEvol/Monaro.pdf.

TAYLOR G. AND SMITH I.E. 1975. The genesis of sub-basaltic silcretes from the Monaro, New South Wales. Journal of the Geological Society of Australia **22**, 377-385.

TAYLOR G., TRUSWELL E.M., MCQUEEN K.G. & BROWN M.C. 1990. Early Tertiary palaeogeography, landform evolution, and palaeoclimates of the Southern Monaro, N.S.W., Australia. *Palaeogeography, Palaeoclimatology, Palaeoecology* **78**, 109-134.

WELLMAN P. AND MCDOUGALL I. 1974. Potassium-argon ages on the Cainozoic rocks of New South Wales. *Journal of the Geological Society of Australia* **21(3)**, 247-272.

WHITE A.J.R, WILLIAMS I.S. AND CHAPPELL B.W. 1977. *Explanatory Notes: Geology of the Berridale 1:100 000 Sheet*. Geological Survey of New South Wales, Sydney.

WILLIAMS R. M. E., GROTZINGER J. P., DIETRICH W. E., GUPTA S., SUMNER D. Y., WIENS R. C., MANGOLD N., MALIN M. C., EDGETT K. S., MAURICE S., FORNI O., GASNAULT O., OLLILA A., NEWSOM H. E., DROMART G., PALUCIS M. C., YINGST R. A., ANDERSON R. B., HERKENHOFF K. E., MOUÉLIC S. LE, GOETZ W., MADSEN M. B., KOEFOED A., JENSEN J. K., BRIDGES J. C., SCHWENZER S. P., LEWIS K. W., STACK K. M., RUBIN D., KAH L. C., BELL III J. F., FARMER J. D., SULLIVAN R., VAN BEEK T., BLANEY D. L., PARISER O., DEEN R. G., AND MSL SCIENCE TEAM *ET AL.* 2013. Martian Fluvial Conglomerates at Gale Crater. *Science* **340**, 1068-1072.

WITZE A. 2015. Icy volcanoes may dot Pluto's surface. *Nature*. Online: http://www.nature.com/news/icy-volcanoes-may-dot-pluto-s-surface-1.18756.

Author Index

Anand	R.	82, 90
Blewett	R.	84
Clark	D.J.	40
Clarke	J.D.A.	59, 63, 94
Cowood	A.L.	17
Cracknell	M.J.	17
Czarnota	K.G.	84
de Caritat	P.	33, 84
de Souza Kovacs	N.	38
Eggleton	T.	50, 68
English	P.	10, 27
Gallant	J.	9
Giles	D.	66
Gordon	G.	27, 56
Gore	O.	34
Grunsky	E.	33
Hobbs	S.W.	63, 94
Hou	B.	70
Jowitt	S.	34
Keeling	J.	70
Kennedy	D.	74
Krapf	C.B.E.	57
Laukamp	C.	48
Leitch	H	15
Main	P.	33
Mann	A.	33
McLennan	S.M.	66
McPherson	A.A.	21, 40, 84
McQueen	K.G.	51
Meixner	T.	27, 84
Moore	L.	17, 79
Morris	B.J.	56
Neumann	N.	84
Paul	D.J.	63
Pillans	B.	15
Pobjoy	R.	70
Reid	A.	70
Reid	N.	75, 82, 90
Roach	I.C	21, 63, 84, 94
Schofield	A.	27, 84
Smith	H.	59
Spinks	S.	75, 82, 90
Sweeney	M.	79
Talbot	J.	56
Taylor	G.	50, 68
Thomas	M.	27, 84
Thorne	R.	75, 82, 90
Uvarova	Y.	90
van der Wielen	S.E.	66
Werner	M.X.	57
Wilford	J.	84
Wilson	S.	34
Wilson	D.	59
Wong	V.	34, 74
Worrall	L.	73
Yau	C.C.	74